The Cytotoxic Effects of Methylmercury on Cardiomyocytes: A Possible Implication for Heart Diseases?

Jocelyn Truong

Thesis submitted to the

Faculty of Graduate and Postdoctoral Studies, University of Ottawa

In partial fulfillment of the requirements for a Masters degree in Biology

with specialization in Chemical and Environmental Toxicology

Department of Biology, Faculty of Science,

University of Ottawa, Canada

Abstract

Methylmercury (MeHg) is known predominantly as a neurotoxicant, however emerging experimental and epidemiological evidence has shown associations between MeHg exposure and the potential for increased risks of cardiovascular diseases. This thesis investigated the *in vitro* cytotoxic effects of MeHg in two cardiomyocyte cell lines, H9C2 rat neonatal cell line and AC16 adult human cell line. We observed significant increases in cell death at concentrations from 1 – 10 μM. ROS production and intracellular calcium concentrations increased dose-dependantly with MeHgCl exposure. Furthermore, while assessing mitochondrial function, a decline in maximal respiration at 1 μM was seen. However, these observations may in turn be a direct consequence of decreased cell numbers following exposures. These observations suggest that MeHgCl is toxic at high concentration to cardiomyocytes. Additionally, this study highlighted the differences in cellular bioenergetics which may impact how certain cells respond to contaminant stressors. The distribution of MeHg and total Hg in rat heart tissues was also examined and we observed increasing concentrations of MeHg in high and low dosed rat groups as compared to the vehicle controls. No difference was observed in Hg levels between the normal and high fat and sugar diet groups. The urinary isoprostane levels, which are indicative of systemic oxidative stress, showed significant increases in lean rats exposed to the high dose treatment. It was also observed that a high fat and sugar diet in lean and obese rats can contribute to increasing oxidative stress regardless of the level of contaminants they were dosed with. This thesis demonstrated several *in vitro* effects of MeHg on heart cells as well as determine the distribution of Hg levels in heart tissues and oxidative stress markers from an *in vivo* study.

Résumé

Bien que le méthylmercure (MeHg) soit principalement un neurotoxique, de nouvelles études expérimentales et épidémiologiques semblent faire un rapprochement entre l'exposition à ce contaminant et l'augmentation du risque de maladies cardiovasculaires. L'existence de données probantes pour confirmer la présence d'une relation de causalité entre l'exposition au MeHg et les maladies cardiovasculaires étant insuffisantes, nous proposons d'étudier l'effet de concentrations sous-létales sur les cellules cardiaques in vitro. Pour ce faire, nous aurons recours à deux lignées cellulaires : H9C2, cellules néonatal du rat et AC16, une lignée cellulaire d'humain adulte. Nous avons observé une recrudescence importante dans le taux de mortalité, la production de radicaux libres et la concentration intracellulaire de calcium à la suite d'une exposition au méthylmercure et ce d'une manière tributaire de la dose. Par ailleurs, l'évaluation de la fonction mitochondriale a démontré un abaissement dans la capacité respiratoire maximale à une dose de 1 μM. Ces résultats suggère une toxicité du méthylmercure à fortes doses sur les cellules cardiaques. De plus, cette étude souligne les différences dans les mécanismes bioénergétiques au niveau cellulaire, ce qui pourrait aider à comprendre l'effet des perturbateurs environnementaux sur différents types cellulaires. Un examen de la distribution du MeHg et du mercure total (THg) dans les cellules cardiaques du rat fut aussi effectué. Celui-ci a indiqué une présence accrue du MeHg dans les rats exposés à des faibles doses et à des doses élevés de méthylmercure relativement au groupe non exposé. Aucune différence n'a été observée entre le groupe control et le groupe ayant une diète riche en gras et sucre pour ce qui est du taux de mercure mesuré. Par contre, le niveau urinaire d'isoprostane, un indicateur systémique du stress oxydatif, a montré une importante hausse dans les rats minces exposés à de fortes doses de

contaminants. Nous avons aussi remarqué que les régimes riches en gras et sucre consommés par les rats obèses et minces, augmentent les marqueurs du stress oxydatif nonobstant les niveaux de contaminants auxquels les animaux furent exposés. Dans l'ensemble, la présente étude confirme les effets toxiques in vitro du MeHg sur les cellules cardiaques. Elle révèle aussi la distribution du mercure ainsi que les indicateurs du stress oxydatif dans le cœur suite à des essais in vivo.

Acknowledgements

First and foremost I would like to thank my supervisor, Dr. Laurie Chan, who I am greatly indebted to for accepting me as a graduate student in his lab and his support throughout my MSc studies. I appreciate your openness for being able to explore novel methods during my research. Through your guidance and encouragement, I have learned how to become a better and more conscientious researcher. I would next like to thank my committee members, Dr. Dawn Jin, your expertise and input was invaluable to this thesis. I thank you for always being available for our enriching discussions. I would also like to thank Dr. Sean Kennedy and Dr. Frances Pick for their valuable input during and outside of meetings which contributed immensely to this project.

Numerous people have graciously shared their assistance and knowledge, without which, this thesis would not have been possible. I would like to express my gratitude to Dr. Ryan Mailloux for his insights and bioenergetics expertise. Thank you to Dr. Mary-Ellen Harper for generously allowing me to conduct these experiments in her laboratory and for your help along the way. Thank you to Dr. Lionel Fillion for your expertise and input with flow cytometry experiments. I am grateful for the assistance provided by Dr. Emmanuel Yumvihoze with mercury quantifications and extractions. Special thanks to undergraduate students who contributed to this project, Paula Ou and Shilpa Arora.

Thank you to the Chan lab members, in particular, Yueting Shao, Natalia Ziencuk, Sonja Campbell, Paulin Junior Vanié, Tiff-Annie Kenny, Susie Huang, Aline Philibert, Myriam Fillion and Judy Mitchell for their great friendship, optimism, and humour which enhanced this whole experience.

Finally, I want to thank my family and friends for their unwavering love, support and encouragement, without whom, I could not have gotten this far.

I would like to acknowledge the financial support from the University of Ottawa in the form of an admission scholarship and the Ontario Graduate Scholarship (OGS) program. Funding for this research was provided by National Science and Engineering Council (NSERC) to Dr. Laurie Chan.

Table of Contents

List of Tables

List of Figures

List of Abbreviations

ADP: adenosine diphosphate

AMI: acute myocardial infarction

ANOVA: Analysis of variance

ANT: adenine nucleotide translocator

ATP: adenosine triphosphate

BMI: body mass index

CHD: coronary heart disease

CM-H2DCFDA: chloromethyl derivative of dichlorodihydrofluorescein diacetate

CNS: central nervous system

CVD: cardiovascular disease

DCF: dichlorodihydrofluorescein

DCM: dichloromethane

DHA: docosahexanoic acid

DMEM: Dulbecco's Modified Eagle Medium

DMSO: dimethyl sulfoxide

DPA: docosapentanoic acid

EC: excitation-contraction coupling

EGTA: ethylene glycol tetraacetic acid

eNOS: endothelial nitric oxide synthase

US EPA: US Environmental Protection Agency

EPA: eicosapentanoic acid

ETC: electron transport chain

FADH2: flavin adenine dinucleotide

FBS: fetal bovine serum

FCCP: Carbonyl cyanide 4-(trifluoromethoxy)phenylhydrazone

GI: gastrointestinal tract

GP_X: glutathione peroxidase

GSH: glutathione

H_2O_2: hydrogen peroxide

HBSS: Hank's balanced salt solution

HC: Health Canada

HCAEC: human coronary endothelial cells

HCl: hydrogen chloride

HFSD: high fat and sugar diet

Hg: mercury

$HgCl_2$: mercury chloride

HRP: horseradish peroxidise

ICAM-1: intercellular adhesion molecule 1

K_d: dissociation constant

KOH: potassium hydroxide

LAT: large neutral amino acid transporter

MeHg: methylmercury

MeHgCl: methylmercury chloride

MI: myocardial infarction

MRA: mesenteric resistance arteries

MTT: 3-(4,5-dimethylthiazol-2-yl)-2,5-diphenyltetrazolium bromide

n-3 PUFA: omega-3 polyunsaturated fatty acids

Na2S2O: sodium thiosulfate

NAC: N-acetylcysteine

NADH: nicotinamide adenine dinucleotide

NCM: northern contaminants mixture

NCP: Northern Contaminants Program

ND: normal diet

NO: nitric oxide

NRCC: National Research Council of Canada

OCR: oxygen consumption rate

PBS: phosphate buffered saline

PCB: polychlorinated biphenyls

PON1: paraoxonase 1

ROS: reactive oxygen species

Se: selenium

SERCA: sarcoplasmic reticulum within muscle cells

SH: sulfhydryl group or thiol group

SRM: standard reference materials

THg: total mercury

UCP3: mitochondrial uncoupling protein 3

UI: urinary isoprostane

WHO: World Health Organization

Statement of Contributions

Chapter 3: Jocelyn Truong performed all experiments in this chapter. Paula Ou, undergraduate CO-OP student, assisted in cell culture and performed some MTT assays.

Chapter 4: Animal study was conducted at Health Canada in the laboratory of Dr. Dawn Xiaolei Jin. Jocelyn Truong performed methylmercury quantification on rat heart tissues and urinary isoprostane ELISA on rat urine samples. Paula Ou performed total mercury quantifications on rat heart tissues.

Chapter 1 - General Introduction

1.1 General Overview

Mercury is a toxic, global pollutant that is considered an important public health concern. It is a heavy metal that is present naturally in the environment; it can be released through such processes as forest fires, volcanoes and degradation of minerals (Diez, 2009). Anthropogenic Hg emissions contributes to the majority of worldwide emissions, sources of these emissions include the burning of fossil fuels, waste incineration, and smelting of base metals (Clarkson *et al*., 2003). Methylmercury (MeHg), an organic form of elemental mercury (Hg), is the most toxic form as it biomagnifies along aquatic food chains and bioaccumulates in humans. Exposure through fish consumption at acute high concentrations has been shown to cause severe neurodevelopmental damage (Clarkson, *et al.*, 2003; Mergler *et al., 2007)*. It is now widely recognized that chronic low dose exposures are associated with adverse effects on the cardiovascular, reproductive and immune system functions (Mergler *et al*., 2007). This thesis focuses specifically on cardiovascular diseases (CVD). CVD are a group of diseases that cause injuries to the cardiovascular system comprising the heart and blood vessels (veins and arteries) (Heart & Stroke Foundation of Canada, 2013). This group of diseases remains one of the leading causes of death worldwide and in 2008 an estimated 17.3 million people died from CVD, representing 30% of all global deaths (WHO, 2013). Although the etiology of many CVD is multi-factorial, exposure to environmental contaminants has been associated with the increased progression of CVD. MeHg has been found to affect the functioning of the cardiovascular system and aid the progression of CVD (Karagas *et al*., 2012). A growing number of epidemiological studies have shown correlations between MeHg exposures and the risks of

developing CVD such as, myocardial infarctions, hypertension, arrhythmia and atherosclerosis in diverse populations worldwide (Egeland and Chan, 2004; Houston, 2011). Currently, the toxic mechanism by which MeHg causes these cardiovascular outcomes are unknown. There is experimental evidence showing the adverse effects on endothelial cells (cells lining the lumen of the blood vessels) which can lead to the progression of atherosclerosis and myocardial infarctions. However, effects of MeHg on the heart have yet to be fully investigated.

This thesis aims to elucidate the toxic mechanisms by which MeHg causes potential cardiac insults using an *in vitro* cell culture model to determine cytotoxic effects. Moreover, cell culture data were correlated with results from an ongoing *in vivo* rat feeding study conducted in Health Canada.

1.2 Thesis Ratonale

MeHg mediated toxicity in cell types such as neuronal cells, T lymphocytes and neuroblastoma cells is associated with the loss of Ca^{2+} homeostasis triggering potential cell death pathways. The mitochondrion is also reliant on Ca^{2+} concentrations as it is a powerful regulator of metabolic activity by promoting ATP synthesis (Brookes *et al.,* 2004). ATP synthesis failure can result in mitochondrial dysfunction causing swelling and eventual cell death (Alissa & Ferns, 2011). MeHg has been demonstrated to accumulate rapidly in mitochondria and in this way can cause increased reactive oxygen species (ROS) production and alteration in Ca^{2+} levels (Farina *et al.,* 2011; Roos *et al*., 2011). Cardioymcoytes are highly oxygenated cells containing large numbers of mitochondria as ATP synthesis and calcium intracellular stores are needed for contraction (Walker & Spinale, 1999). Therefore, MeHg has the potential to cause adverse

effects and affect the function of cardiomyocytes.

Currently, much of the research related to MeHg and CVD is focused on dysfunction of the endothelial cells. This has been the focus because environmental contaminants can remain in the blood for long periods of time where these cells are subjected to constant exposure, leading to speculation that exposures can cause inflammation and plaque formation in the arteries (Jin et al., 2011). However, few studies have examined the effect of MeHg exposure on cells of the heart. It is known that Hg can accumulate in heart tissues and about 80% of this Hg is in the form of MeHg (Matsuo *et al., 1989*.). I hypothesize that through the production of ROS, downstream effects of MeHg exposure on cells include disruption of Ca^{2+}, mitochondrial dysfunction, increased production of LDL through lipid peroxidation and finally inflammation. Together, these processes lead to the progression of various CVD (Figure 1.1). Previous research has focused primarily on the adverse effects in endothelial cells; by examining the effects of this contaminant specifically on cardiomyocyte cells and the heart we can better determine the effects of MeHg on the whole cardiovascular system and its implications for heart diseases.

1.3 Objective and Hypotheses

1.3.1 Objectives

1. To investigate the cytotoxic effect of MeHg on cardiomyocyte cells *in vitro* examining specific endpoints which may contribute to dysfunction of the cell including, cell viability, intracellular Ca^{2+} concentrations, mitochondrial function profiles and

production of ROS**.**

2. Currently, there is very little information on the Hg levels that can accumulate in the heart therefore, in collaboration with Health Canada, we will determine the levels of total Hg and methylmercury in rat hearts from an ongoing *in vivo* study and compare these results with oxidative stress markers.

1.3.2 Hypotheses

1. Exposure to MeHg will contribute to the cytotoxic impairment of cardiomyocyte cells by:

   a. Decreased cell viability with increasing concentrations of MeHg exposures
   b. Oxidative stress through increased ROS production.
   c. Increased intracellular calcium concentrations.
   d. Mitochondrial dysfunction leading to a disruption of ATP synthesis.

2. I hypothesize that MeHg in rat hearts will accumulate dose-dependently and these levels will compare with oxidative stress markers

   a. Higher concentrations of MeHg levels will be found in high dose treatment group as compared to low dose or control treatment groups.
   b. High dose groups will have higher urinary isoprostane levels (a marker of oxidative stress) as compared to those in the low dose and control groups.

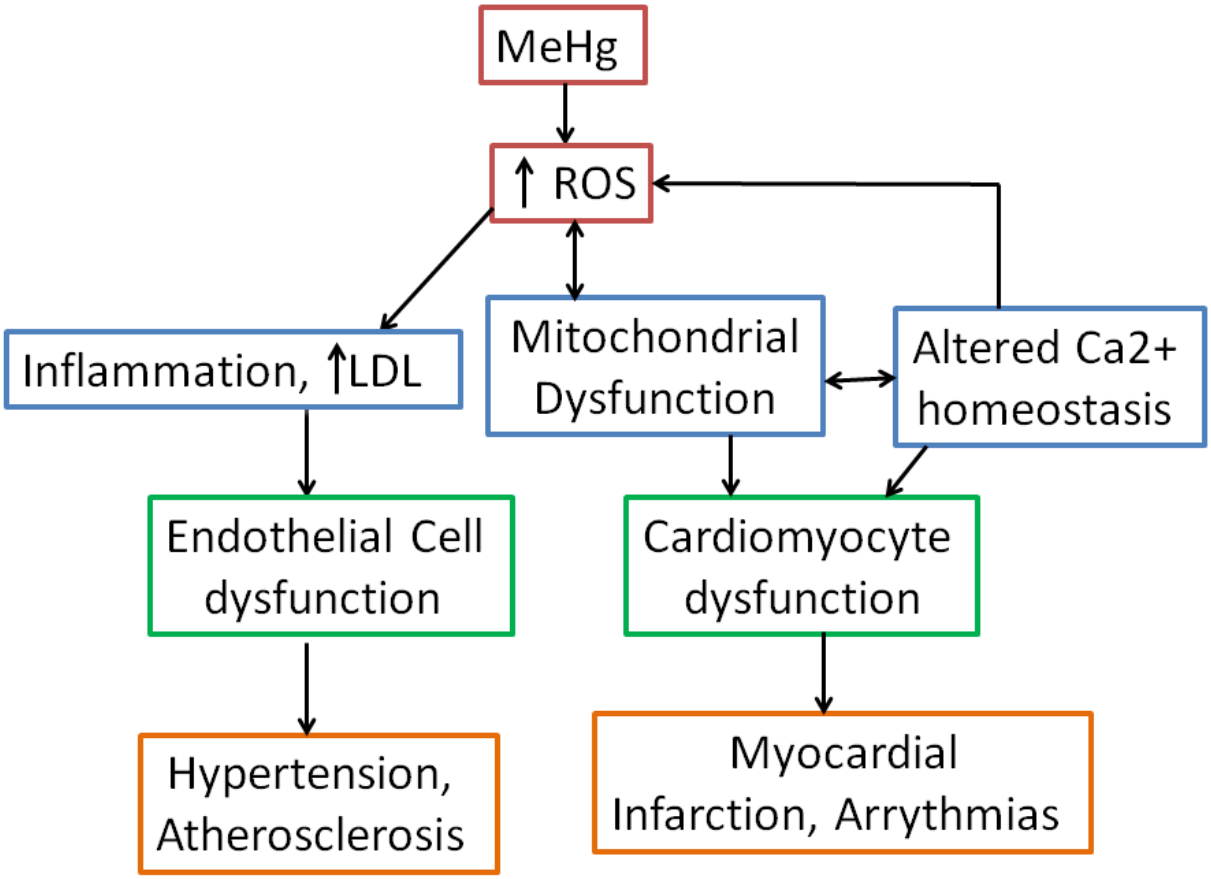

Figure 1.1 Hypothesized mechanism by which MeHg causes downstream adverse effects in the heart and blood vessels. Increased production of MeHg mediated ROS can lead to dysfunctions of the mitochondria leading to altered intracellular Ca^{2+} homeostasis leading to physiological changes in cardiomyocytes and downstream heart effects. ROS can lead to increased production of LDL through lipid peroxidation and inflammation and can lead to hypertension and atherosclerosis.

Chapter 2 - Literature Review: Introduction to Methylmercuy and Cardiovascular Effects

2.1 Mercury – Physical and Chemical Properties

Mercury (Hg) is a heavy metal which is found naturally in the earth's crust and the environment. It can be released through such processes as forest fires, volcanoes and degradation of minerals (Clarkson, 2006; Díez, 2008). Hg is released into the environment through anthropogenic processes and the majority of which are industrial activities. Emissions from intentional industrial uses of Hg include artisanal and small scale gold mining, dental amalgams, and the chlor-alkali industry (UNEP, 2013). Unintentional release of Hg into the environment includes by-products from the burning of fossil fuels, incineration of waste, and smelting of base metals (Clarkson et al., 2003). Hg is a toxicant associated with adverse health effects to both humans and organisms. These toxic effects, however, are dependent on the chemical form, the concentration and the exposure pathway (Clarkson, 2006; Díez, 2008; Grandjean et al.,2010) .

Hg is found in three basic forms: elemental mercury, inorganic mercury, and organic mercury. Elemental mercury (Hg^0) is the most volatile form. It exists as a silver liquid at ambient temperatures and can vaporize into a stable monoatomic vapor which,can stay up in the atmosphere for up to 1 year (Boening, 2000). Inorganic mercury (Hg^{2+}), such as mercuric chloride ($HgCl_2$), exists as salts and is found in divalent and monovalent cationic forms. These compounds are formed when Hg combines with non-carbon elements such as chlorine or sulphur. It is the form which can be found naturally in the environment and is the toxic species found in human tissue after it is converted from other species of Hg (Clarkson *et al.,* 2006).

Lastly, organic mercury, such as methylmercury (MeHg or CH3Hg+), is the form considered to be the most toxic to humans and wildlife as it bioaccumulates in tissues and top consumers in the food chain through the consumption of fish and marine mammals (Clarkson *et al*., 2003; Clarkson, 2006).

2.2 MeHg in the environment

Once released into the atmosphere, Hg enters a biogeochemical pathway that transports it across various environmental compartments (Boening, 2000; Clarkson, 2006). Long-range atmospheric transport is one of the primary ways in which Hg is distributed throughout the global environment.

The cycle begins when Hg^0 vapour from anthropogenic or natural sources rises from the earth's surface and circulates into the atmosphere. It is then picked up by local winds and circulating prevailing air currents to be dispersed and transported globally. In the upper atmosphere, Hg^0 oxidizes into the more soluble form of Hg^{2+} and is deposited into lakes, rivers and soil through rainwater. Hg^{2+} may be converted back to Hg^0 in the soil and water by microorganisms, which leads to re-emission back into the atmosphere allowing mercury to re-circulate for extended periods of time (Clarkson et al., 2003). Hg^{2+} deposited into aquatic sediments in fresh and ocean water undergoes methylation by microorganisms, such as sulphate-reducing bacteria, into MeHg. This methylation is thought to be a protective mechanism as Hg^{2+} is more toxic to these microorganisms (Clarkson, 2006). MeHg bioaccumulates in biota through dietary absorption and then biomagnifies in the aquatic food web leading to top consumers accumulating higher concentrations. Top consumers, mainly large predatory fish such as

northern pike (*Esox lucius*), walleye (*Sander vitreus*), mackerel (*Scomberomorus cavalla*) and various marine mammals, accumulates the highest concentrations of MeHg. Humans, birds and mammals are solely exposed to MeHg through the consumption of contaminated fish and marine mammals. Depending on abiotic factors such as pH and redox potential of the water, as well as size, age and species of the fish, MeHg concentrations are reported in the range from 0.01 and 4 mg/kg (Díez, 2008).

2.3 Toxicity of MeHg

Mercury toxicity is of particular concern because of its ability to bioaccumulate and induce adverse effects on the central nervous system (CNS). The first two widely reported cases of acute environmental mercury poisoning occurred in the 1950's in Minamata and in 1965 in Niigata, Japan. In both cases, the contaminant was released as wastewater into nearby bodies of water by an acetaldehyde plant that used MeHg as a catalyst. Those who ingested contaminated seafood developed a range of neurological symptoms into a condition later called Minimata Disease. MeHg levels in fish found in Minimata during this period were up to 20 ppm (Clarkson, 2006). Exposed adults developed ataxia (loss of coordinated muscle movements), muscle tremors, parasthesia (numbness in the extremities), blindness, deafness and in severe cases mental deterioration and death (Igata, 1993). Developing fetuses were also discovered to be susceptible to MeHg toxicity. Children born to mothers who showed little to no clinical symptoms developed severe neuro-developmental symptoms including mental retardation, cerebral palsy, microencephaly and seizures (Myers & Davidson, 1998). In 1971, acute mercury poisoning in Iraq from the consumption of bread baked with MeHg treated grains led to wide-spread intoxication with symptoms and pathologies very similar to those seen in Japan,

confirming the acute toxicity of MeHg (Bakir *et al*., 1973).

Acute Hg exposures have decreased due to wide-spread efforts to improve industrial activities and minimize the release of mercury into the environment (Clarkson, 2006; UNEP, 2013). However, it remains a pervasive global pollutant, due to the persistence and ease with which it transports throughout different environmental compartments. Fish and marine mammal-eating populations are the most at risk for MeHg exposures, and chronic low concentration exposures in the human diet are an increasing cause for concern. Epidemiological cohort studies conducted in the Seychelles Island, Faroe Islands, and Brazilian Amazon have demonstrated the adverse neurological effects of chronic MeHg exposure (Mahaffey, 2000). These and other emerging studies highlight a range of toxic effects on organ systems other than the CNS most notably the liver, kidney, immune system and cardiovascular system (Clarkson *et al*., 2003; Mergler *et al*., 2007; Zahir *et al., 2005)*. In light of these findings, the US Environmental Protection Agency (EPA) has set the reference dose for MeHg consumption at 0.1 µg/kg body weight per day (US EPA, 2014) and the World Health Organization lowered the provisional tolerable weekly dose from 3.3 µg/kg/week to 1.6 µg/kg/week (WHO, 2014). Canada and many other countries have also set fish consumption advisories for certain species of fish.

In light of the environmental and health effects of this pollutant, the Minamata Convention on Mercury, an international treaty requiring governments to regulate and address the use and emissions of mercury, was agreed upon by over 140 nations in January 2013.

2.4 MeHg Toxicokinetics

MeHg is highly absorbed by humans and accumulates readily in tissues of organisms. MeHg binds strongly to the sulfur atoms of thiol (-SH) ligands on proteins resulting in a water-soluble complex with the ability to transport across cell membranes (Díez, 2008). Mercuric ions have a high binding affinity to various molecules including, glutathione (GSH), cysteine, homocysteine, N-acetylcysteine (NAC) and albumin (Bridges & Zalups, 2010). Because Hg binds to these molecules, cooking and cleaning of contaminated fish will not remove the MeHg and once consumed can accumulate in the body of organisms throughout life (Canuel *et al*., 2006; Mergler *et al*., 2007).

In humans there is no mechanism to actively excrete Hg from the body as it is not essential for living cells and has no physiological role (Houston, 2011). Experimental and animal studies have demonstrated that once MeHg in fish is ingested, 95% is absorbed by the gastrointestinal (GI) tract. Further animal and human studies suggest that absorption can vary with age and sex of the individual (Clarkson, 1997; Mergler *et al*., 2007). Once absorbed, MeHg travels through the bloodstream and accumulates mainly in the liver and kidneys but is also distributed to other tissues and crosses the blood-brain and placental barriers (Clarkson, 2006). After a single exposure, MeHg absorption and disposition throughout the body is complete within 3 days. In the bloodstream, MeHg is bound to the amino acid cysteine in the hemoglobin of red blood cells. The ability of MeHg to readily transport across cell membranes is in due part to the structural resemblance between the MeHg-cysteine complex and the large neutral amino acid, methionine (Clarkson *et al.*, 2007). As a result, MeHg-cysteine complexes can be transported through the cell membranes on neutral amino acid transporters, such as LAT1 and LAT2 (Clarkson *et al*., 2007; Simmons-willis, *et al.*, 2002). Once MeHg-cysteine enters the

cells, a large portion of the MeHg binds to the antioxidant peptide glutathione (GSH) where it can be transported back into the extracellular space and the blood stream as a MeHg-GSH complex (Rooney, 2007). It may be these two processes Hg entering the cell as an Hg-cysteine complex and exiting through the glutathione pathway, that facilitates the mobility of Hg throughout the body (Bridges & Zalups, 2010; Clarkson, 2006).

MeHg leaves the body quite slowly, with a half-life of about 50 days (Clarkson *et al.*, 2003). It is mainly excreted from the fecal route and to a lesser extent in the urine (about 10% or less from the total body burden) (Ballatori & Clarkson, 1985), however this does not occur before extensive enterohepatic circulation. MeHg-GSH complexes may enter the liver of which a portion is secreted into the bile. The biliary secretions are transported to the small intenstine and intestinal microflora comes into contact with MeHg which demethylates it into inorganic Hg^{2+}(Rowland, 1988). The biochemical mechanism of this demethylation is still currently unknown. Hg^{2+} is poorly absorbed and therefore can be secreted in feces, however MeHg that has not been demethylated can be re-absorbed into the bloodstream and bind to GSH thus completing the enterohepatic cycle (Clarkson *et al*., 2007).

The large neutral amino acid transporters also transports the MeHg-cysteine complexes to the hair follicles as there is a high demand for amino acids to synthesize keratin. MeHg incorporated into hair follicles serves as an elimination method, albeit an inefficient one as the half-life in the hair averages at 65 days. The concentration of MeHg in hair is about 250 times that of the concentration in the bloodstream, serving as a useful biomarker for MeHg exposures in epidemiological studies (Clarkson *et al*., 2007). Furthermore, based on the growth rate of hair, it is estimated that each 1 cm segment represents about 1 month of MeHg exposure (Grandjean *et al.,* 1999*;* Matsumoto *et al*., 1975).

2.5 MeHg and Cardiovascular disease

Recently, more attention has been given to the potential for MeHg exposures to affect the functioning of the cardiovascular system and risks of developing cardiovascular diseases (CVD). It is important to note that exposures associated with CVD are to lower concentrations and more long term dose exposures of MeHg than those associated with neurological deficits (Karagas *et al*., 2012). The toxicity of MeHg at high levels of exposures is well investigated; however the current concern is continual exposures to low levels which may lead to chronic health effects. The most vulnerable populations are those who are more sensitive to the effects of Hg, such as the developing fetus, newborn and children and populations that regularly consume seafood containing high levels of mercury (WHO, 2014).

The human body derives many important nutrients from fish, including proteins, Vitamin D, selenium and *omega-3* polyunsaturated fatty acids (n-3 PUFA), especially eicosapenatnoic acid (EPA) and docosahexanoic acid (DHA). The beneficial effects of fish are well documented and is associated with the prevention of CVD, however some species may contain contaminants which have the potential to off-set these benefits (Mergler *et al*., 2007; Van Oostdam *et al*., 2005). This seemingly contrasting advice has led to public uncertainty about the risks and benefits of fish consumption.

Despite a number of advancements in CVD treatment, it remains the number one cause of death worldwide. The mortality rate for CVD, mainly from heart disease and stroke, is expected to reach 23.3 million by the year 2030 (WHO, 2014). Environment, diet and lifestyle factors appear to be the most determinant in the development and progression of CVD. The correlation between environmental contaminants and CVD has only recently been investigated. A growing

number of epidemiological studies have shown correlations between MeHg exposures and the risks of developing CVD such as, myocardial infarctions (heart attacks), hypertension, arrhythmia (irregular heart beat) and atherosclerosis in diverse populations worldwide (Fillion *et al.,* 2006; Houston, 2011; Salonen *et al., 1995;* Stern, *2005;* Valera *et al., 2008)*.

Interestingly, the correlation between CVD and MeHg exposures may also incur potential economic impacts. Rice *et al.* (2010) generated a probabilistic model assessing Hg exposures and the distribution of health and economic benefits to the U.S. populations. They estimate that by reducing Hg exposure by 10% could save the U.S. more than $860 million in health costs each year, 80% of these health costs are associated with reduction of fatal heart attacks (Rice, *et al.*, 2010).

2.5.1 Epidemiological Evidence

As this thesis is not epidemiology-based; I will only outline a selection of studies showing the correlations between MeHg and CVD. The evidence thus far shows some positive correlations however the data still remains inconclusive. Salonen *et al.* (1995) was the first study examining MeHg exposures and CVD. Hair Hg concentrations and dietary history of 1833 middle aged men in Northern Finland possessing no history of coronary heart diseases or stroke were taken for baseline measurements. Following which acute myocardial infarction (AMI) and fatal coronary events were recorded for a period of 6 years. Values were adjusted for confounders such as smoking, socio-economic status, residence and major coronary risk factors. Men with the highest tertile of hair Hg concentration (>2.0 μg/g) had a 2.0 fold increased risk for developing coronary heart disease (CHD) and 2.9 fold increased risk in developing cardiovascular disease compared to those with lower hair Hg concentrations (Salonen *et al.*,

1995). The study was extended for an additional 4 years during which fatty acids from fish, DHA and docosapentanoic acid (DPA) were measured in the serum of cohort subjects. The groups in the lowest quintile of hair Hg concentrations (below 2 μg/g) had the highest DHA + DPA levels showed a 52% reduction in the risk of coronary events than compared to those in the lowest DHA+ DPA levels. Moreover, groups with hair Hg concentrations above 2 μg/g and lower DHA + DPA had only 24% reduction in risks and no reduction in risk of those in the upper three quintiles of Hg concentrations suggesting that risk protection may be a balance between fatty acid concentration and MeHg (Rissanen, *et al.*, 2000).

Guallar *et al*. (2002) conducted a case-control study on men aged 70 years or younger in 8 European countries and Israel. They correlated Hg concentrations in toenails and DHA in adipose tissue of men hospitalized with risks of AMI with matched controls representative of the sample populations. After adjusting for confounders, mercury was 15% higher in the patients than compared to the controls and the odds ratio (OR), the measure of the association of a variable with an outcome, for the association of Hg in the highest quintile and AMI was 2.16. Additionally, after adjusting for Hg levels, the DHA levels were inversely associated with risk of myocardial infarctions suggesting that, similarly to the Finnish study, MeHg may decrease the cardioprotective effects of DHA in fish (Guallar *et al*., 2002).

In contrast, Yoshizawa *et al.* (2002) conducted a prospective cohort study of male health professionals (ages 40-75 years old) with no history of cardiovascular disease. After collecting toenail Hg concentrations and recording cases of CHD over a period of 5 years, they found no statistically significant association between Hg and risks of CHD. In the highest and lowest quintile of mercury, the relative risk was 0.97 (Yoshizawa *et al*., 2002). Two Swedish studies also found no associations between mercury and cardiovascular endpoints; Hallgren *et al.* (2001)

found no statistically significant correlations between mercury-erythrocyte concentrations from individuals in Northern Sweden and first myocardial infarction (MI) cases (Hallgren *et al*., 2001). The second study found no correlation between total serum Hg concentrations and risk of MI in middle-aged women (Ahlqwist *et al*., 1999).

Many studies have also examined hypertension or high blood pressure following MeHg exposures. Hypertension can enhance the progression of arteriosclerosis and myocardial infarction and as such is a good indicator of CVD (Lawes, *et al.*, 2008). Fillion *et al.* (2006) conducted a study in the Brazilian Amazon wherein communities did not possess the usual risk factors of CVD (i.e. obesity, sedentary lifestyle etc.). In the study, hair Hg concentrations were correlated with blood pressure. Blood pressure in this community was found to be relatively low with 8% of the participants displaying hypertension; however there was a significant dose-response relationship between Hg exposure and blood pressure with age and BMI (Fillion *et al.*, 2006). Valera *et al.* (2008) measured diastolic blood pressure and pulse pressure in adults in Nunavik, Quebec. They observed that higher diastolic blood pressure and pulse pressure were positively correlated with increased MeHg concentrations in blood (Valera *et al.,* 2008).

Although several studies show a positive correlation between MeHg and CVD, other studies do not show any association between the two. It is important to note that there are still limitations. For one, numerous studies recorded CVD events years after the initial baseline Hg measurements; therefore changes in dietary patterns during this period of time can skew observed relationships. Another limitation is the varying MeHg and nutrient contents of fish in various geographic regions, as certain fish have lower levels of n-3 PUFAs compared to other fish (Roman *et al*., 2011; Stern, 2005).

Despite these discrepancies, in 2010 the U.S. EPA held a workshop in Washington D.C.

to examine the current science and generate recommendations to potentially include these cardiovascular effects in future MeHg risk-benefit assessments. Although studies have examined many cardiovascular endpoints the panel concluded that currently there is sufficient evidence to generate a MeHg-myocardial infarction (MI) dose-response function due to studies linking MeHg directly with MI and intermediary toxic effects of MeHg leading to MI. Other recommendations include generating additional epidemiological studies, examining biological mechanisms underlying toxic effects seen in the epidemiological studies, dose-response assessments and examining other cardiovascular endpoints (Roman *et al.*, 2011).

2.5.2 Experimental Evidence and Cardiovascular toxic mechanisms

Although the mechanisms by which MeHg causes cardiovascular effects remains unclear, two main processes are suggested as possible means by which MeHg can induce these effects. These include: oxidative stress, the imbalance between the production of reactive oxygen species (ROS) and the ability to detoxify ROS or repair the damage produced, and lipid peroxidation, the oxidative degradation of phospholipids in the cell membranes resulting in cell damage (do Nascimento *et al*., 2008). MeHg induced oxidative stress has been shown *in vivo* and *in vitro* in myocardial tissues and endothelial cells causing inflammation, mitochondrial dysfunction, disruption of calcium homeostasis and apoptosis (Houston, 2011). Hg binds quite strongly to molecules containing sulfhydryl groups (-SH), which includes the antioxidant protein, glutathione (GSH). GSH is the most prevalent intracellular antioxidant that protects cells against oxidative stress (Clarkson, 2006). The Hg-GSH complex is also the primary form in which Hg is transported and eliminated from the body thus further reducing the cellular oxidant defence (Alissa & Ferns, 2011). Lund *et al.* (1993) demonstrated that the administration of Hg^{2+} resulted

in GSH depletion and increased formation of H_2O_2 and lipid peroxidation in kidney mitochondria in rats (Lund, *et al.*, 1993). Hg^{2+} also serves as a catalyst in Fenton-type reactions generating increased reactive oxygen species, particularly superoxide anion, resulting in damaging tissue effects (Agarwal *et al.,* 2006). Finally, the interaction between Hg and Selenium (Se) may be another mechanism for CVD. Although Hg and Se interactions are beyond the scope of this thesis, it is important to note that Hg has a much higher affinity for Se than sulphur groups and forms insoluble complexes with Se. This reduces the bioavailability of Se as a cofactor for antioxidants such as glutathione peroxidise (GPx), thus promoting lipid peroxidation and subsequent atherosclerosis (Ralston *et al.,* 2008*)*. On the other hand, there has been growing evidence that Se may have protective effects against MeHg toxicity. This may arise from the sequestration of Hg by the Se-Hg bonds and subsequent inactivation of Hg (Heath *et al*., 2010). Consumption of fish and marine mammals is the main source of Hg exposure, yet it is also a rich source of Se which is an essential trace nutrient in the diet. As such, Se has received the most attention as a potential protective nutrient for the effects of MeHg toxicity. Animal studies have shown that co-exposure with Se have decreased the severity, and prolonged the onset of Hg toxic effects (Chapman *et al.,* 2000).

2.5.2.1 Endothelial cell dysfunction

The endothelium is composed of cells that cover the lumen of all blood vessels; this layer of cells has many functions including providing a barrier between the blood and vascular tissue, the maintenance of normal vasculature and permeability, blood pressure and controlling inflammatory responses by releasing regulatory factors (Ringseis & Eder, 2010). Disruption of the endothelial cell layer due to impaired cell function or cell loss from the luminal surface can

lead to cholesterol-rich lipoproteins entering the arterial tissue and subsequent development of atherosclerosis (Hennig *et al*., 2001). Atherosclerosis is the hardening of the arteries caused by chronic accumulation of lipids and other cells (Luis, 2000). Atherosclerosis is the underlying cause for a vast majority of CVD. Atherosclerotic plaques in the arteries can lead to limited blood flow and ischaemic heart disease as well as thrombosis or formation of blood clots in the artery and myocardial infarction (Gonzalez *et al*., 1998). Alteration to the endothelium can be induced by certain lipids, inflammatory cytokines and environmental contaminants. MeHg in endothelial cells has been shown to cause oxidative stress through phospholipase A2 (Mazerik *et al.*, 2007) and phospholipase D (Hagele *et al.*, 2007) activation causing downstream cell damage in bovine pulmonary artery endothelial cells. The production of nitric oxide (NO) by the endothelial nitric oxide synthase (eNOS) plays an important role in maintaining the homeostasis of the blood vessels by regulating the dilation and tone of the vasculature. Inhibition of the eNOS and the decreased production of NO was shown in human umbilical vascular endothelial cells (Kishimoto *et al*., 1995) and in rats that developed hypertension following MeHg exposure (Grotto *et al.*, 2009). Furthermore, Wiggers *et al.* (2008) examined the aorta and the mesenteric resistance arteries (MRA) of rats and found that $HgCl_2$ exposures in the MRA decreased eNOS protein expression and increased total antioxidant status and vascular O_2- (Wiggers *et al.,* 2008).

Interestingly, Jin *et al.* (2011) showed that rats exposed to MeHg with the supplementation of Se and Vitamin E either had a protective or augmentative effect of MeHg toxicity depending on the exposure dose. They examined various cardiovascular markers and found that MeHg decreased serum paraoxonase (PON1) enzyme activity, an anti-atherosclerotic factor and increased ICAM-1 (intercellular adhesion molecule 1), an adhesion molecule involved in cell signalling, inflammation, and is highly activated during the onset of atherosclerosis. These

markers may promote oxidative stress and lipid peroxidation leading to the activation and potential dysfunction of endothelial cells (Jin *et al*., 2011). In summary, MeHg may trigger activation of various factors in the endothelial cells leading to the promotion of the oxidative stress, lipid peroxidation and clinical symptoms such as atherosclerosis and hypertension.

2.6 Cardiomyocyte cell dysfunction

The myocardium of the heart is comprised of fibroblasts, smooth muscle cells and cardiomyocytes. Cardiomyocytes are the fundamental cells responsible for contraction of the heart (Woodcock & Matkovich, 2005). The main function of cardiomyocyte cells (Figure 2.1) is the coordinated contraction which propels blood into and out of the heart. Excitation-contraction (EC) coupling of these cells involves depolarization of the cell membrane causing increased intracellular calcium ions through voltage-sensitive Ca^{2+} channels (L-type calcium channels) in the sarcolemma, the cell membrane of the muscle cell. This Ca^{2+} current triggers further release of Ca^{2+} from intracellular stores in the sarcoplasmic reticulum. Ca^{2+} ions coupled with ATP hydrolysis drives cell shortening and contraction (Walker & Spinale, 1999). Once a cycle of contraction has occurred, several ion channels and pumps are involved in repolarizing the cell and bringing it back to resting state. Removal of Ca^{2+} from the inside of the cell involves the Na^{+}/Ca^{2+} exchanger and the Ca^{2+} ATP-ase on the sarcolemma. The Na^{+}/K^{+} ATP-ase removes Na^{+} from inside of the cell to maintain resting membrane potential (Walker & Spinale, 1999; Woodcock & Matkovich, 2005).

In response to pathological stimuli, such as cardiotoxins, cardiomyocytes may undergo hypertrophy. Clinically, hypertrophy, the enlargening of the muscle cells, involves heightened

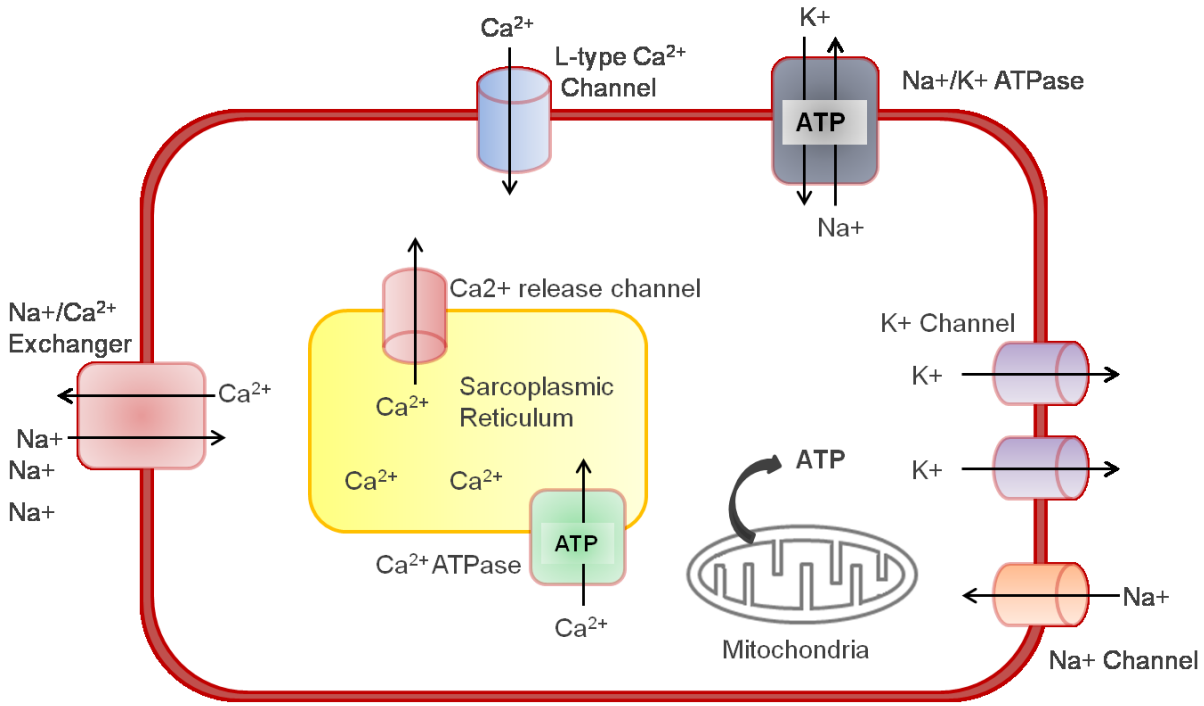

Figure 2.1 Simplified diagram of a cardiomyocyte highlighting the cellular components involved in contraction. Ca^{2+} enters the cell from the L-type Ca^{2+} channels depolarizing the cell membrane and triggering release of intracellular Ca^{2+} from the sarcoplasmic reticulum. Ca^{2+} coupled with ATP drives the contraction by binding to actin filaments and contractile proteins to cause cell shortening. Na^{+}/K^{+} exchanger and the Ca^{2+} ATPase on the sarcoplasmic reticulum are involved in removing intracellular Ca^{2+}, Na^{+}/K^{+} ATPase and the remaining ion channels are involved in bringing the cell back to resting potential.

blood pressure and loss of contractile myocytes from myocardial infarction through apoptosis or necrosis. Hypertrophy occurs to compensate for the loss of the myocytes. If hypertrophy of the cells is sustained heart failure may result from the inability of the cardiomyocytes to generate enough contractile force to sustain cardiac output (Woodcock & Matkovich, 2005)

Some early responses of the myocardium to environmental toxicants include alterations in intracellular calcium concentrations ($[Ca^{2+}]_i$) and energy metabolism resulting in enhanced consumption and decreased production of ATP. Early physiological responses of environmental contaminants in the myocardium include cardiac arrhythmia resulting from changes in $[Ca^{2+}]_i$ where long term exposure to toxicants can cause hypertrophy of the cells, which is considered a protective and adaptive response. Further toxic insult eventually leads to irreversible cardiomyopathy and cell death (Y James Kang, 2001).

Hg exposure can affect contraction of the myocardium as reported by a number of studies. $HgCl_2$ induces a biphasic response and dose-dependent decrease in contractile force of isolated rat papillary muscles, muscles located in the ventricles of the heart. At low concentrations of 1 μM, an initial increase in force and rate of force development was seen, which may be due to Hg inhibiting the Na^+/K^+ ATP-ase activity causing sustained Ca^{2+} ions in the cell thus producing higher force of contraction (Vassallo *et al.,* 1999). However at higher concentrations, contractile depression occurred suggesting possible Ca^{2+} overload as the cause (Oliveira *et al.,* 1994). Furthermore, Hg can reduce the tetanic tension development of the muscles fibres and reduce the myosin ATPase activity (Oliveira *et al*., 1994; Vassallo *et al*.,1999). Together, this reduction of ventricular contractibility may result from both calcium overload and adverse effects on contractile proteins. Similarly, a reduction in isovolumic systolic pressure, ventricular contraction occurring early on in systole, of Langendorff perfused hearts

isolated from rats exposed to acute concentrations (up to 10 mM) and lower concentrations (5 – 20 nM) was seen (Massaroni *et al.*, 2000; Assis *et al.*, 2003). Furthermore, $HgCl_2$ was found to reversibly bind to the ligands of Na^+/K^+ ATPase and inhibit its activity (Anner *et al*., 1992). $HgCl_2$ was also found to block Na^+ channels in cardiomyocytes of guinea pigs by oxidizing cysteinyl residues to form a sulphur-Hg-sulphur linkage potentially altering the permeability of the channel and affecting cellular functions (Hisatome *et al*., 2000; Kurata *et al.*, 1998). Other heavy metals such as cadmium, zinc and lead also have this effect on Na^+ channels, causing downstream effects in the cardiac system (Alissa & Ferns, 2011). Furieri *et al,* (2011) investigated the chronic effects of ventricular function of rats fed low doses (4.6 ug/kg and then subsequent dose of 0.07 ug/kg per day) of $HgCl_2$ for a period of 30 days and isolated perfused hearts from the same group of rats. *In vivo* rats produced increased left ventricle end diastolic pressure but showed no changes in blood pressure or heart rate. Western blot analysis of perfused hearts showed decreased expression of various calcium handling proteins including Na^+/K^+ ATPase, Na^+/Ca^{2+} exchanger and SERCA (the sarcomplasmic reticulum in muscle cells responsible for regulating Ca^{2+}), which may promote changes in contractibility (Furieri *et al*., 2011).

Thus far, effects of inorganic Hg on the myocardium are described, but there seems to be fewer studies examining the effects of MeHg on the heart. Rat primary cardiomyocytes exposed to various concentrations of MeHgCl (5 – 50 μM) for 48 hours was found to cause a significant dose-dependent cell death (Yoon *et al.,*1996). MeHgOH at low doses (0.5 – 2 ppm) induced increased frequency of contraction in isolated rat papillary muscle and left atrial, but was steadily decreased at high concentrations (> 2ppm). The muscles were morphologically examined under the electron microscope and dilation of the sarocplasmic reticulum and swollen mitochondria

with disrupted and loss of cristae were observed, suggesting direct toxic effect on the functions of the muscle tissues (Su & Chen, 1979). Furthermore, MeHgCl was found to induce a positive inotropic effect, increasing muscle contractibility and produce stronger action potentials initially, however at higher concentrations (60 µmol/l) inducing a weaker inotropic effect. This steady decrease following exposures to MeHg and $HgCl_2$ was again explained by the inhibitory effect on the Na^+/K^+ ATP-ase (Halbach *et al.*, 1989). Together these studies observed toxic effects of MeHg on myocardial tissues *in vivo* and with perfused hearts warranting further studies on the underlying mechanisms.

Chapter 3 - The Cytotoxic Effects of Methylmercury on Cardiomyocyte cells

3.0 Abstract

It has been reported that chronic low dose exposures of MeHg is associated with cardiovascular diseases in many populations worldwide. The toxic mechanisms through which these adverse effects occur are currently unknown. The objective of this study was to determine the cytotoxic effect of low and high dose MeHg on AC16 and H9C2 cardiomyocyte cell lines. Both cell lines responded dose-dependently to various endpoints. At 1 μM both cell lines began to exhibit significantly decreased cell viability, increased ROS production and increased $[Ca^{2+}]_i$. Furthermore by examining mitochondrial function parameters, we observed a significantly decreased maximal respiration at 1 μM for both cell lines and lowered reserve capacity. Using positive controls, diamide and menadione, both cell lines exhibited a respiration profile indicative of mitochondrial dysfunction; however differences in the bioenergetic responses between AC16 and H9C2 were noted. AC16 cells show MeHg dose dependant sensitivities with State $_{apparent}$ and ATP production values, but H9C2 cells do not show these trends. It seems as though H9C2 cells may be more resistant to MeHg toxicity than AC16 cells potentially due to higher levels of UCP3 and ANT as reflected in the increases of proton leak and State $_{apparent}$. These results suggest that MeHg has the potential to affect the functioning of cardiomyocytes and induce cytotoxicity, this study also highlighted the differences in respiration of different cell types and how these differences can contribute to altering the toxicity of MeHg or other contaminants.

3.1 Introduction

Mercury (Hg) has become a prevalent global pollutant and a public health concern. Methylmercury (MeHg) is the most toxic form of Hg as it bioaccumulates and biomagifies along the marine food chain. Exposures to methylmercury (MeHg) has been shown to cause severe neurological deficits in both adults and the developing fetus (Clarkson, 1997; Clarkson, 2006). However, in the past decade, epidemiological and experimental data have linked MeHg with the increased risk of developing cardiovascular diseases (CVD) (Houston, 2011). Epidemiological studies show correlations between MeHg exposures and the risks of developing CVD such as, myocardial infarctions, hypertension, arrhythmia and atherosclerosis in diverse populations (Roman *et al.*, 2011; Stern, 2005; Virtanen *et al*., 2007) CVD include all diseases afflicting the cardiovascular system, the heart and blood vessels (veins and arteries) (Heart & Stroke Foundation of Canada, 2013). CVD remain one of the leading causes of death worldwide and the causes are multi-factorial, however exposure to environmental contaminants is a factor that is increasingly being investigated (Alissa & Ferns, 2011). It is important to note that exposures associated with CVD are related to lower concentrations and long term dose exposures than those associated with neurological deficits (Mergler *et al*., 2007; Stern, 2005). Currently, the toxic mechanisms by which MeHg causes these cardiovascular outcomes remains unknown.

MeHg induced-oxidative stress plays a key role in the pathogenesis of MeHg intoxication (Kaur, 2008). MeHg binds strongly to thiol groups in proteins, particularly with the amino acid, cysteine, creating a complex which structurally resembles methionine (Simmons-willis *et al.,* 2002). This mimicry allows MeHg to be transported across the cell membrane onto the large neutral amino acid carrier (Clarkson, 2006). This complex can bind strongly to the antioxidant

protein, glutathione (GSH). GSH is the most prevalent intracellular antioxidant protecting cells against oxidative stress; as a result, the Hg-GSH complex effectively inactivates the function of GSH thus further reducing the cellular oxidant defence (Alissa & Ferns, 2011). Oxidative stress causes many downstream effects ranging from DNA damage to changes in the energy metabolism of cells and is known to be involved in the progression of CVD (Schnabel & Blankenberg, 2007).

Currently, much of the research related to MeHg and CVD has focused on dysfunction of the endothelial cells; cells which comprise the lumen of blood vessels. This has been the focus because environmental contaminants can remain in the blood for long periods of time where these cells are subjected to constant exposure; leading to speculation that the exposures can cause inflammation and plaque formation in the arteries (Jin *et al*., 2011). However, few studies have examined the effect of MeHg exposure on cells in the heart. Cardiomyocytes or cardiac muscle cells are the fundamental cells responsible for the coordinated contraction of the heart. Some early responses of the myocardium to environmental toxicants include alterations in intracellular calcium concentrations ($[Ca^{2+}]_i$) and energy metabolism resulting in enhanced consumption and decreased production of ATP. Early physiologic responses of environmental contaminants in the myocardium include cardiac arrhythmia resulting from changes in $[Ca^{2+}]_i$ and long term exposure to toxicants can cause hypertrophy of the cells. Further toxic insult eventually leads to irreversible cardiomyopathy and cell death (Y James Kang, 2001). Inorganic $HgCl_2$ induces changes in the contractile response of the myocardium in rat papillary muscles (Furieri *et al.*, 2011; Oliveira *et al.*, 1994) generating a biphasic response whereby higher concentrations (5 – 10 μM) of MeHg produced a weaker contractile force as compared to lower concentrations (1 μM) which produced a stronger contractile force. Furthermore, this response was attributed to

Hg irreversibly inhibiting the Na^+/K^+ ATP-ase causing initial sustained Ca^{2+} ions in the cell and eventual Ca^{2+} overload (Vassallo, *et al*., 1999). Other studies have shown that Hg can alter the permeability of Na^+ channels in cardiomyocytes by forming sulphur-Hg-sulphur linkages (Hisatome *et al*., 2000), and an *in vivo* study showed that rats fed $HgCl_2$ showed changes in the diastolic pressure in the ventricle and decreased protein expression of numerous calcium handling proteins including Na+/K+ ATPase, Na+/Ca2+ exchanger and SERCA. Together, these studies highlight potentially damaging effects of mercury on the function of the heart muscle tissues and alterations in contraction warranting further research on the underlying mechanisms.

There are currently few studies examining the effects of organic MeHg on heart function; therefore the objective of this study will use an *in vitro* approach to examine the cytotoxic effects of methylmercury on cardiomyocytes cells by investigating physiological and bioenergetic endpoints which are crucial in the function of these cells. These endpoints include calcium homeostasis, ROS production and mitochondrial function. Not only is $[Ca^{2+}]_i$ involved in contraction, but it plays an important role in regulating cell signalling pathways, and in the mitochondria, it stimulates enzymes crucial for the Kreb's cycle, oxidative phosphorylation, and results in higher respiratory chain activity and higher ATP output (Brookes *et al*., 2004) . Uptake of calcium into the mitochondria is driven by the mitochondrial membrane potential. Furthermore, mitochondrion provide the cell's main source of ROS production with about 1-2% of electrons flowing through the respiratory chain leaking to produce ROS (Yan *et al.,* 2006). MeHg exposures at low micromolar concentrations causes elevation of $[Ca^{2+}]_i$ in cells ranging from neurons, neuroblastoma cells and T-lymphocytes through a number of different pathways (explanation of these pathways are beyond the scope of this thesis) (Roos *et al.,* 2012). An overload of mitochondrial calcium can stimulate cell death pathways, increase generation of

ROS and thereby affect the ATP output. The interplay between ROS production, calcium homeostasis and mitochondrial dysfunction can lead to cytoxicity of cardiomyocytes cells.

We hypothesized that exposure to MeHg will contribute to the cytotoxic impairment of cardiomyocytes by increasing oxidative stress, causing increased intracellular calcium and mitochondrial dysfunction leading to disruption of ATP synthesis. As these cells are highly oxygenized and are active cells with large numbers of mitochondria, mitochondrial function will be analyzed using a bioenergetics approach examining various respiratory states and energetic parameters in the cells to determine whether MeHg has an effect on the cells energy demands.

Primary cells obtained from the myocardium of animal models have proven difficult to maintain and purify due to the heterogeneity of heart tissues and having a finite lifespan where cells will inevitably stop growing and die (Allen *et al.*, 2005). Therefore, a continuously growing cell line possessing the same characteristics of differentiated cardiomyocytes was utilized for these studies. Two different cardiomyocyte cell lines were used in order to compare the results with each cell line; AC16 (Human ventricular cell line) and H9C2 (rat cardiomyoblast cell line). These two cell lines are extensively utilized in drug screening and toxicity studies (Bourgault *et al.*, 2011; Pointon, *et al*., 2011; Liang *et al*., 2010; Zordoky & El-Kadi, 2007; Davidson *et al.*, 2005) They are also increasingly used in a variety of environmental toxicological assessments of contaminants (Aboutabl & El-Kadi, 2007; Allen *et al*., 2005; Sumi *et al*.,2011) High through-put screening of toxicity tests now more commonly use *in vitro* methods. Furthermore, these cell lines and primary cardiomyocytes exhibit similar pathological responses to drug stressors (Davidson *et al*., 2005).

3.2 Methods

3.2.1 Cell culture

The AC16 cell line, originally derived from adult human ventricular cardiomyocytes was purchased from America Tissue Type Collection (ATCC) (Bethesda, MD, USA; patent deposit designation number PTA-1500). The H9C2 cell line, originally derived from embryonic rat ventricle was similarly purchased from ATCC (CRL-1446). Both cell lines were cultured in Dulbecco's modified Eagle's medium (DMEM) (Sigma, D5648) containing 10% fetal bovine serum (FBS) (Fisher Scientific, and 1% antibiotics (100 µg/ml streptomycin and 100U/ml penicillin). Cells were incubated in T75 flasks at 37°C at 5% CO_2 in a humidified incubator. Cells were examined daily for evidence of contamination. Media was changed every 2-3 days and cells were split when they reach 70-80% confluency. Cells from identical passages were used for each experiment (cells from passages 8- 23 were used for all experiments). As these are cell lines, each experiment was repeated either three or four times with different passages of cells and each dosing group consisted of three technical replicates.

3.2.2 MeHg dosing procedure

MeHgCl (standard solution in H_2O; 1000 ppm by AA) was obtained from Alfa Aesar (Wardhill, MA) and dissolved in MilliQ water. Dosing concentrations at 0.01, 0.05, 0.1, 0.5 and 1µM were further diluted in the DMEM.. These concentrations represent sub-lethal and physiologically relevant concentrations. These concentrations were chosen based on prior *in vitro* concentrations (Jin *et al.,* 2008) as well as what was found in various studies of Hg

concentrations in the blood plasma and few studies on the heart (Ayotte et al., 2011; Legrand *et al.,* 2010.). Cells are plated 24 hours prior to treatment for each experiment. In order to ensure concentrations were diluted accurately, a stock concentration of 10 μM of MeHgCl solution was quantified on the MA-3000 Mercury Analyzer.

3.2.3 MTT Cell Viability Assay

Cell viability was determined using an MTT (3-[4,5-dimethylthiazol-2-yl]-2,5 diphenyl tetrazolium bromide) colorimetric enzyme assay. In viable cells, the yellow MTT tetrazolium salt is cleaved by various dehydrogenase enzymes (such as NADPH) in the active mitochondria producing a purple colour which can be quantified using a multi-plate spectrophotometer (Berridge *et al.,*2005; Mosmann, 1983). This reaction only occurs in living cells and therefore is an indicator of the number of viable cells present. MTT (Sigma catalog # M2128) was dissolved in PBS at 5g/L. Cells were plated in a 96 well plate with a density of 10,000 cells per well 24 hours before treatment. Cells were previously optimized for cell density. 0.01, 0.05, 0.1, 0.5, 1, 5, and 10 μM of MeHgCl were added to each well and incubated for 24 hours. Phosphate buffered saline (PBS) was added to the control wells. These concentrations were used in order to ascertain a concentration range that does not cause cell death. Following incubation, MTT solution was added to each well at 5mg/mL and incubated for 4 hours before media from each well was removed and 200 μL of DMSO was added to each well to dissolve the formazan crystal. The plate was then spectrophotometrically read on a SPECTRAmax PLUS 384 microplate reader at an abosorbance of 595 nm with a reference filter at 620 nm. All experiments were repeated four times.

3.2.4 Intracellular Ca2+ Concentrations

Intracellular Ca^{2+} concentrations ($[Ca^{2+}]_i$) changes were determined using Fluo-3 AM (acetoxymethyl ester) (Molecular Probes, F-1242) as modified from June *et al.* (2001) and quantified using the TECAN Infinite F200 PRO plate reader. Ca^{2+} flux as measured by fluorochomes based on the fluorescence intensity after binding to intracellular calcium ions using the following equation:

$$\text{nanomolar}[Ca2+] = K_d \times (F - F_{min}) / (F_{max} - F)$$

K_d represents the effective dissociation constant for calcium-bound Fluo-3. The K_d for both AC16 and H9C2 cell lines were determined using the calcium calibration buffer kits (Molecular probes, Cat no. C-3008MP). F_{max} represents the maximum fluorescence (detergent permeabilized cells; represents intracellular and extracellular Ca^{2+} ions), F_{min} is the fluorescence of the probe in the absence of calcium and F is the fluorescence of the test sample.

2mg/ml of Fluo-3 AM was loaded into cells plated onto 6 well plates at a density of 50,000 cells per well and incubated for 30 minutes at 37°C. Cells were then transferred to a microcentrifuge tube where they were spun for 1 minute at 2000 rpm. The supernatant was discarded and the cells were washed twice with Hank's Balanced Salt Solution (HBSS). The pellet was re-suspended and transferred to a 6 well plate and the fluorescence was quantified using the TECAN plate reader at a wavelength of 525 nm. The fluorescence, F, was recorded initially, afterwards the detergent Triton X-100 (5% stock) was added to the cells to a final concentration at 0.05% (v/v) to permeabilize the cells and F_{max} was recorded at 525 nm. 100mM EGTA and 1 M Tris base was added to the wells and F_{min} was again recorded at the same wavelength (June *et al*., 2001). $[Ca^{2+}]_i$ was then calculated using the above equation and all

experiments were repeated three times.

3.2.5 ROS production by Flow Cytometry

Reactive oxygen species (ROS) production was measured using CM-H_2DCFDA (5-(and-6)-chloromethyl-2',7'-dichlorodihydrofluorescein diacetate, acetyl ester), an intracellular fluorescent probe. It is a general oxidative stress indicator, which detects several ROS species including, hydrogen peroxide, hydroxyl radicals and peroxynitrites. It can passively diffuse into the cell where its acetate groups are cleaved by intracellular esterases and the chloromethyl group reacts with intracellular GSH and other thiols. Oxidation of this molecule by ROS produces florescent DCF (Eruslanov & Kusmartsev, 2010). Flow cytometry allows the measurement of the intracellular fluorescence in culture media and gives quantitative data on the numbers of cells emitting fluorescence. 50 µg of CM-H2DCFDA (Invitrogen, C6827) is dissolved in 100% anhydrous DMSO to a stock concentration of 10 mM. 1.0×10^6 cells were grown in 100 mm culture dishes and treated with the 0, 0.01, 0.1, 1 µM of MeHgCl for 1 hour and 24 hours. Following exposure times, cells were re-suspended and loaded with 5µM of CM-H2DCFDA for 45 minutes at 37°C. Negative controls containing no CM-H2DCFDA were used to determine baseline fluorescence intensity. 50 µM H_2O_2 was used as a positive control. Cells were washed with pre-warmed HBSS prior to flow cytometry measurements in order to remove any remaining probe which had not been oxidized. Fluorescence intensity was measured using an FC500 Flow Cytometer (Beckman Coulter, Mississauga, Ontario). Accumulation of DCF in cells was measured by an increase in fluorescence at an emission wavelength of 530 nm when the sample is excited at 485 nm. A total of 10,000 cells per sample were analyzed. All experiments were repeated three times.

Flow cytometric data was analyzed using FCS Express 4 Research Edition (De Novo Software, Los Angeles, CA), Data were presented as histograms showing the CM-H2DCFDA fluorescence of a population of cells.

3.2.6 Mitochondrial Function Analysis

Mitochondrial respiration and bioenergetics (the study of the flow and transformation of energy in living cells and organisms) was measured using the Seahorse XF24 Extracellular Flux Analyzer (Seahorse Bioscience, North Billerica, MA). The Seahorse XF24 Analyzer is a multi-well based assay platform which allows for real-time measurement of oxygen consumption rates (OCR) which is a useful indicator of mitochondrial respiration (Ferrick *et al.,*, 2008). Cells were treated sequentially with three different compounds that inhibit complexes in the electron transport chain (ETC)– the site of ATP synthesis and oxidative phosphorylation in the mitochondria (Brand & Nicholls, 2011). This allows for the measurement of different mitochondrial bioenergetic parameters, the efficiency of oxidative phosphorylation and the polarity of mitochondrial inner membranes and to predict the ability of the cell to respond to stressors such as MeHg. Further explanation on protocol rationale is in Appendix I.

Assays were optimized to a cell density of 50,000 cells/well prior to experiments. Cells were plated onto 24 well XF24 assay microplates (Seahorse Bioscience, North Billerica, MA) at a density of 50,000 cells/well in DMEM. Once the cells were adhered, the media was removed and the cells were dosed with DMEM media containing 0.01, 0.05, 0.1, 0.5 and 1μM of MeHgCl (dissolved in milliQ H2O) for 24 hours. On the day of the experiment, the exposure media was removed and the cells were washed twice with PBS. Real-time OCR measurements were made in the analyzer by a sensor probe placed 200 microns above the cell monolayer measuring

concentrations of dissolved oxygen every few seconds. Once the measurement has been made, the probes are lifted from the wells in the microplate allowing the media above to mix, permitting cells to return to baseline values until the next measurement (Seahorse Bioscience, 2014). All experiments were conducted four times. Cellular protein is measured using the Bradford protein assay (Bradford, 1976)

Positive controls known to cause mitochondrial toxicity was used, cells were exposed to 100 μM diamide for 1 hour and 10 μM of menadione for 24 hours. Diamide is known to promote S-glutathionylation of proteins and menadione is known to produce superoxide anion in an NADPH dependant manner.

3.2.7 Mitochondrial analysis calculations

To further assess mitochondrial function parameters we used the OCR values obtained from the SeahorseXF24 Analyzer to calculate reserve capacity, O^2 required for ATP production and $State_{apparent}$. See Appendix I for further explanation of these calculations. The reserve capacity or spare respiratory capacity was calculated by taking the difference between FCCP-induced maximal respiration with resting respiration (Hill *et al*., 2010)

The O_2 required for ATP production (Figure 2.1) at resting state was calculated by subtracting the resting respiration with the proton leak (oligmycin induced) respiration.

To determine the state at which the cells are operating (the range between State 3 and State 4 respiration) the $State_{apparamt}$ was calculated using the following equation: $State_{app} = 4 –$ (Basal-Oligo)/(FCCP-Oligo).

3.2.8 Statistical Analyses

Results of all experiments were statistically analyzed where experimental means from all concentrations were compared to control means and between groups using one-way analysis of variance (ANOVA) followed by pair-wise comparisons using the Tukey's post-hoc test. Statistics for flow cytometric data were performed by obtaining the mean value of fluorescence of all histograms. All statistics are expressed as mean ± standard error. All tests were performed on JMP 10 (SAS Institute, USA). Statistical significance in all cases was accepted at $P \leq 0.05$.

3.3 Results

3.3.1 MTT Assay (Cell viability)

24 hour MeHgCl exposure showed a concentration-dependant decrease in percent cell viability in both cell lines (Figure 3.1). No difference in responses to MeHgCl between cell lines was seen. Statistically significant decreases at 1 μM for both AC16 ($F= 28.2$, $df = 7$ and 25, $p<0.001$) and H9C2 ($F = 69.6$, $df = 7$ and 25, $p<0.001$) cell lines was at 60% and 68% cell viability ($p<0.01$), respectively. At 5 and 10 μM, both cell lines decreased to 30-34% cell viability ($p<0.001$) as compared to the control. Following the MTT assays, the concentration range which would and would not induce cell death was determined in order to acertain sub-lethal concentrations to investigate changes in physiological parameters of the cells before cell death. The concentrations I would use for the rest of the experiments range from 0.01 – 5 μM.

3.3.2 Intracellular Calcium Concentration

MeHg has been shown to induce changes in Ca^{2+} homeostasis in various cells types and due to the importance of Ca^{2+} for contraction in cardiomyocyte cells, it is of interest to determine whether changes occur in these cells as well. Intracellular calcium concentrations ($[Ca^{2+}]_i$) measured using Fluo-3 AM, a fluorescent calcium indicator, showed statistically significant increase ($p < 0.05$) at the highest MeHg concentration of 5 µM for AC16 ($F= 20.3$, $df = 6$ and 14, $p< 0.001$) and H9C2 ($F = 83.1$, $df = 6$ and 14, $p<0.001$) as compared to the control (Figure 3.2). Fluorescence intensities were measured immediately following addition of MeHgCl in each well. $[Ca^{2+}]_i$ of AC16 and H9C2 cells based on fluorescence intensity were calculated to be 498 and 463 nM, respectively, as compared to the controls at 283 and 250 nM. In all concentrations, $[Ca^{2+}]_i$ tend to be slightly lower in H9C2 cells than AC16.

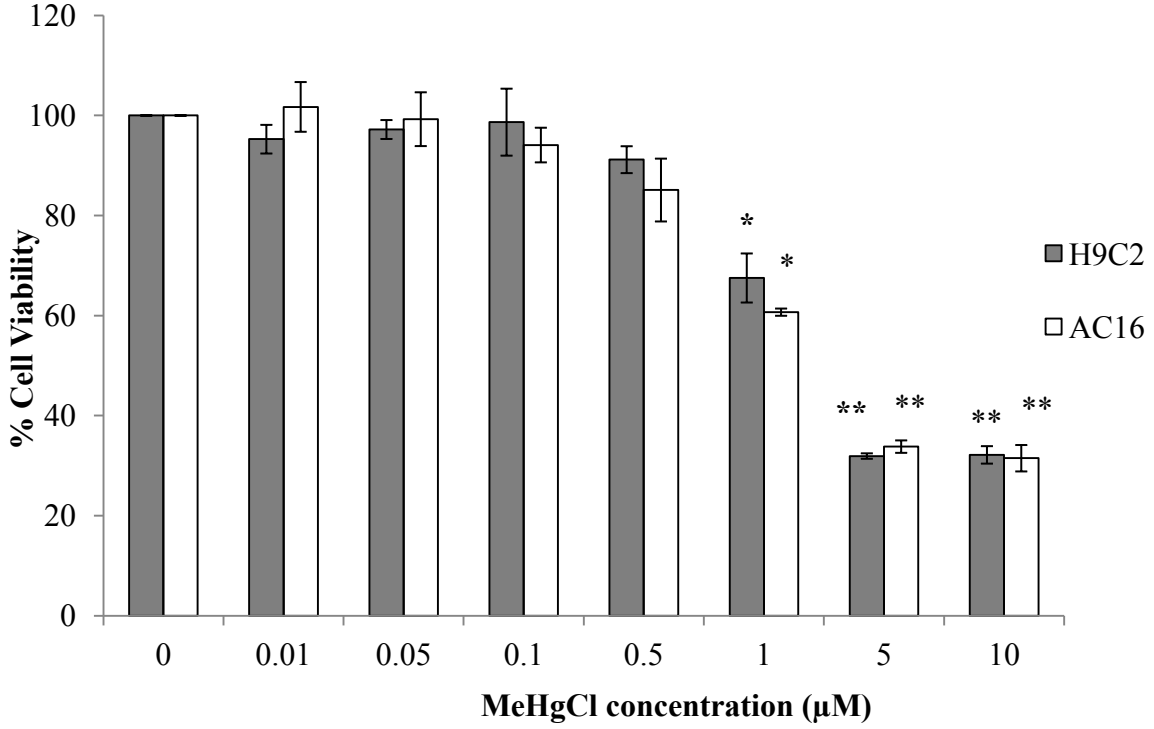

Figure 3.1 % Cell viability of H9C2 and AC16 cells by MTT assay following a 24 hour MeHgCl exposure. Cells are treated with various concentrations (0.01, 0.05, 0.1, 0.5, 1, 5, and 10 µM) of MeHgCl. Data are represented as % mean ± standard error (n=4). Statistical significance of data was analyzed using one-way ANOVAs with post-hoc Tukey's test. No significant difference was found between cell lines. Concentrations marked by "*" and "**" are statistically different at $P< 0.01$ and $P< 0.001$, respectively.

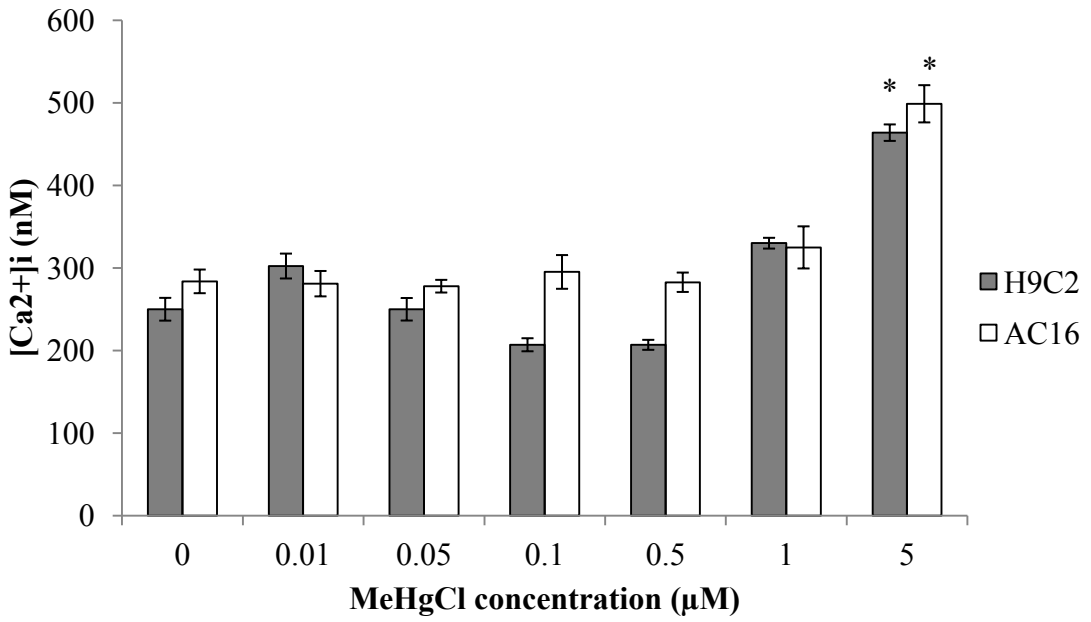

Figure 3.2 Intracellular calcium concentrations measured using the calcium indicator Fluo3-AM of both H9C2 and AC16 cells immediately following exposures with 0-5 µM MeHgCl. Fluorescence values measured immediately after addition of MeHgCl into wells (approximately 1-2 minutes before reading values on fluorometer). Data are represented as mean ± standard error (n=3). Statistical significance of data was analyzed using one-way ANOVAs with post-hoc Tukey's test. No significant difference was found between cell lines. Concentrations marked by "*" are statistically significant at $P < 0.05$.

3.3.3 MeHg-induced ROS production

In order to determine ROS produced immediately after MeHg exposures and for longer exposures, 1 hour exposure and 24 hour exposure was used. Histogram overlays of relative fluorescence from flow cytometry analysis and mean fluorescence obtained from the geometric mean of the relative fluorescence are shown in in bar graphs (Figure 3.3 and 3.4). Only three concentrations (0.01, 0.1 and 1 μM) are presented in the histogram overlays, while all five concentrations are presented in bar graphs. H_2O_2 as the positive control is only present in the histograms for comparison with MeHg treated cells. At 24 hours of exposure, Figure 2.9A and C shows a dose dependant progressive increase in fluorescence and statistical significant change ($p \leq 0.05$) at 1 μM as compared to the controls for AC16 ($F = 19.7$, $df = 5$ and 23, $p < 0.001$) and H9C2 ($F = 2.95$, $df = 5$ and 23, $p = 0.033$) (Figure 3.3 B and D). At 1 hour, the overall relative fluorescence values are much lower than at 24 hours with about a 10-fold difference in relative fluorescence (Figure 3.4 A and C), suggesting that more ROS is being produced as time of exposures increases. At 1 hour exposures, AC16 cells ($F = 6.68$, $df = 5$ and 23, $p = 0.006$) show significant increases at 1 μM, however no changes in the H9C2 cells ($F = 0.787$, $df = 5$ and 23, $p = 0.56$). Similar with 24 hour exposures, at 1 hour there is a progressive increase in relative fluorescence with higher concentrations of MeHg.

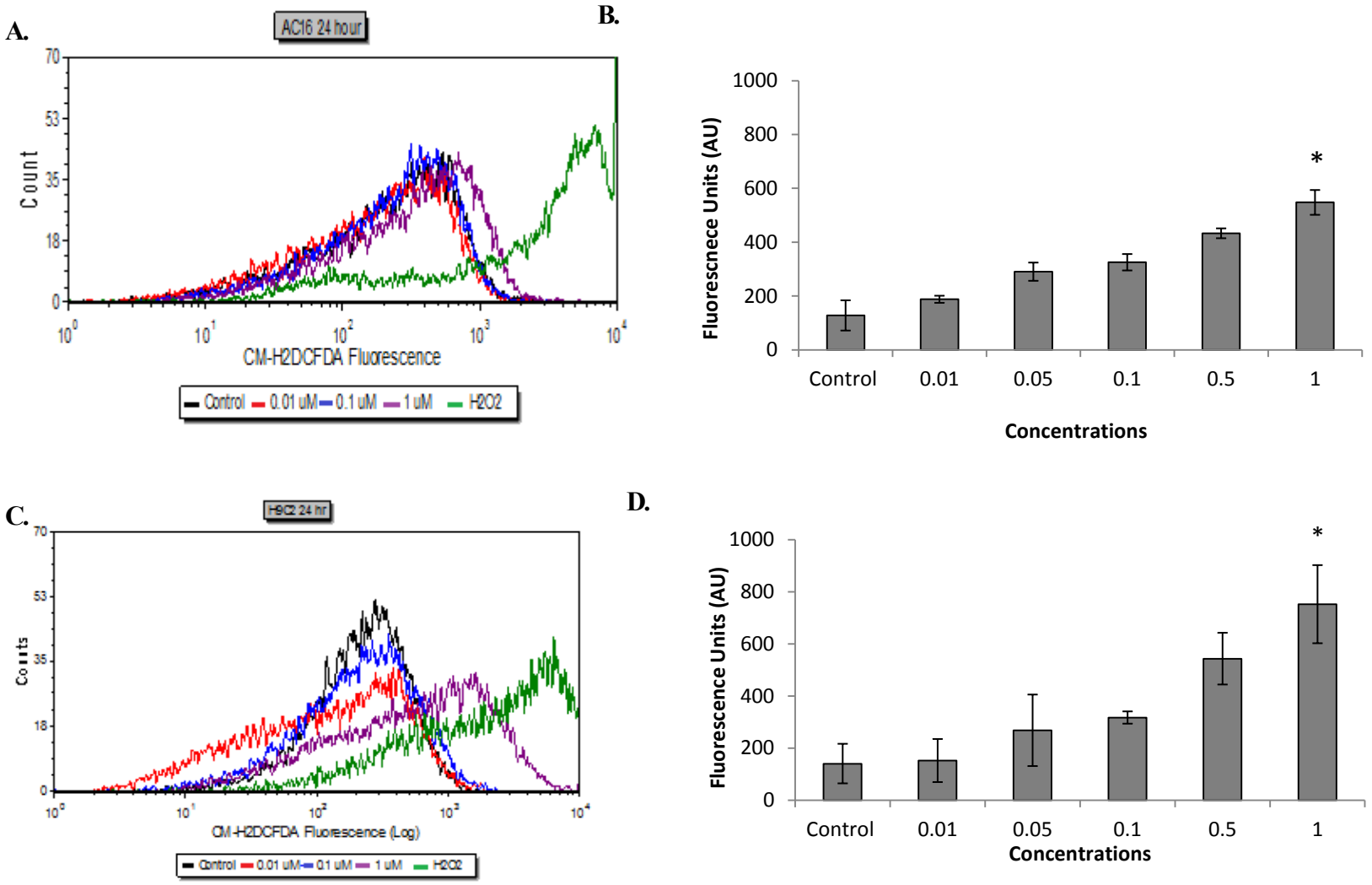

Figure 3.3 Increases in ROS production of AC16 and H9C2 cells exposed to various concentrations of MeHgCl at 24 hours of exposure. (A) (C) Flow cytometric analyses of uptake of CM-H2DCFDA in both cell types as represented by overlay histograms for each exposure concentration. H_2O_2 was used as a positive control. (B) (D) Data in bar graphs represent mean fluorescence units ± standard error taken from geometric means of histograms. (n=3 experiments). Statistical significance analyzed using one-way ANOVA with post-hoc Tukey's test; * represents $p \leq 0.05$.

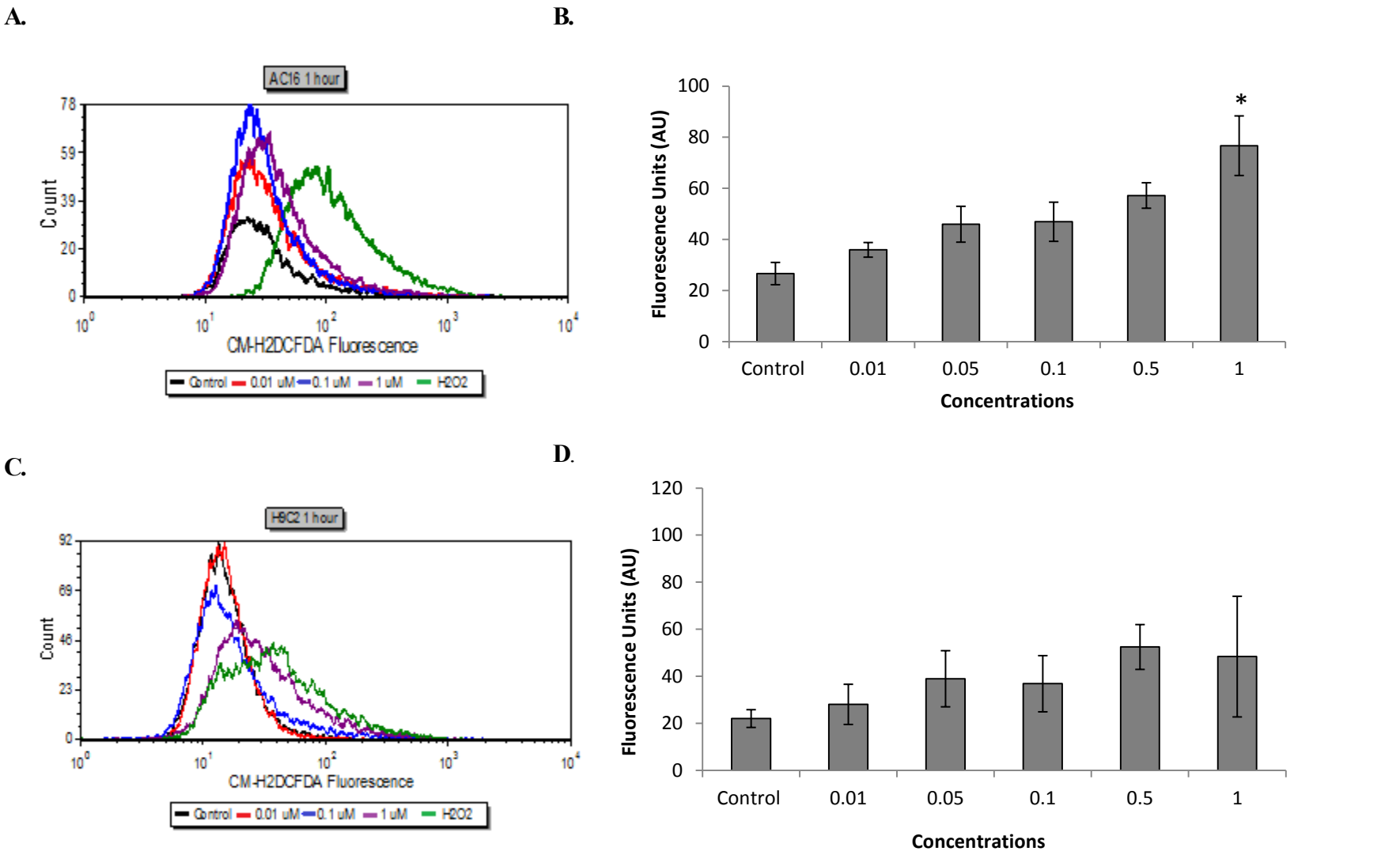

Figure 3.4 Increases in ROS production of AC16 and H9C2 cells exposed to various concentrations of MeHgCl at 1 hour of exposure. (A) (C) Flow cytometric analyses of uptake of CM-H2DCFDA in both cell types as represented by overlay histograms for each exposure concentration. H_2O_2 was used as a positive control. (B) (D) Data in bar graphs represent mean fluorescence units ± standard error taken from geometric means of histograms.(n=3 experiments). Statistical significance analyzed using one-way ANOVA with post-hoc Tukey's test * represents $p \leq 0.05$.

3.3.4 Mitochondrial bioenergetics

The Seahorse XF24 Extracellular Flux Analyzer is an instrument that measures the rate of oxygen consumed by cells, which is a useful indicator of mitochondrial respiration. Cells were metabolically disrupted by the addition of three different compounds which inhibit complexes in the electron transport chain – the site of ATP synthesis and oxidative phosphorylation in the mitochondria. This allows us to determine distinct changes in bioenergetics of the mitochondria and to predict the ability of the cell to respond to stressors. From the oxygen consumption profiles we can take the data points to look at specific respiration states following the injection of each inhibitor compound

Figure 3.5 shows the respiration profile of AC16 and H9C2 cells; there is a much lower oxygen consumption rate (OCR) profile after the addition of the inhibitor compound, FCCP, in the cells exposed to the higher dose group at 1 μM and much higher oxygen consumption profile of cells exposed to 0.01 μM as compared to the controls. Figure 3.6 and 3.7 are bar graph representations of specific respiration states from Figure 3.5 of both cell lines. Generally, OCR of H9C2 cells were lower than AC16 cells which may be due to normal variation of metabolism between cell lines. Resting respiration was measured to establish baseline OCR following 24 hours of MeHgCl exposures. Figure 3.7 A shows no significant differences in H9C2 cells ($F = 1.41$, $df = 5$ and 66, $p = 0.23$), but Figure 3.6 A shows a significant decrease at 1μM in AC16 cells ($F = 3.33$, $df = 5$ and 84, $p = 0.008$). Next, I assessed oligomycin-induced (State 4) respiration which represents proton-leak dependant respiration; it is used to determine the percentage of oxygen consumption devoted to ATP synthesis. Oligomycin blocks the proton channel in the ATP synthase in the ETC. In Figure 3.6 B and Figure 3.7 B there is no statistically

significant difference in proton leak dependant OCR for H9C2 ($F = 1.10$, $df = 5$ and 66, $p = 0.36$) and AC16 ($F = 1.78$, $df = 5$ and 84, $p = 0.12$) as compared to the control. Finally, injection of FCCP disrupts ATP synthesis and stimulates the transport of protons across the mitochondrial membrane instead of through the proton channel of the ATP synthase. This leads to a rapid consumption of energy and oxygen without the generation of ATP thereby simulating the need for increased energy demand in the cells. This increased energy demand allows for the quantification of the maximal respiration (Brennan et al., 2006). Higher concentrations of MeHgCl exposures stimulated significantly lower maximal OCR in both cell lines. AC16 cells (Figure 3.6 C) demonstrated progressively decreased OCR with increasing exposure doses and significant decrease ($F = 5.67$, $df = 5$ and 48, $p = 0.0003$) at 1 μM. Additionally, there was a slight increase in OCR at 0.01 and 0.05 μM which may suggest respiratory compensation for MeHg stress. Similarly, H9C2 cells (Figure 3.7 C) shows statistically significant decrease of OCR at 0.5 and 0.1 μM ($F = 2.83$, $df = 5$ and 84, $p = 0.0021$) as compared to the control. This suggests that low concentrations may cause increase in respiration to compensate for MeHg toxicity and higher concentrations of 1 μM affects both resting respiration and maximal respiration potentially due to the sustained MeHg stress.

Oxygen consumption following MeHgCl exposure is being characterized for the first time in these cells; thus we want to compliment these results with exposures to positive controls which are known to cause mitochondrial dysfunction. Two chemicals, menadione and diamide, were used as positive controls and both these compounds are known to cause mitochondrial dysfunction (Pfefferle et al, 2013). Diamide is known to promote S-glutathionylation of proteins and menadione is known to produce superoxide anion in an NADPH dependant manner (Loor et al., 2010). Low and high concentrations of each chemical were used for exposure doses. Figure

3.8 shows OCR profiles of both cell lines. The resting respiration of AC16 cells (Figure 3.9 A) showed significant decreases in 40 μM menadione ($F = 19.1$, $df = 2$ and 16, $p \leq 0.0001$) and 500 μM diamide ($F = 11.7$, $df = 2$ and 21, $p \leq 0.0001$). Similar decreases at 500 μM diamide ($F = 19.6$, $df = 2$ and 21, $p \leq 0.0001$) for H9C2 cells were observed (Figure 3.10 A), suggesting that these chemicals alter the respiratory capacity of these cells. Exposures in H9C2 cells (Figure 3.10 B), demonstrated an increase in proton leak dependant respiration of cells exposed to the higher concentrations of positive controls ($p \leq 0.05$), potentially due to menadione ($F = 4.49$, $df = 2$ and 21, $p = 0.038$) and diamide ($F = 6.67$, $df = 2$ and 21, $p = 0.012$) mediated oxidative stress in these cells. Alternatively, the effect is not seen in AC16 cells (Figure 3.9 B). Finally, AC16 cells exposed to both concentrations of diamide ($F = 21.6$, $df = 2$ and 17, $p \leq 0.0001$) and menadione ($F = 10.6$, $df = 2$ and 14, $p = 0.0015$) had altered maximal respiration (Figure 3.9 and 3.10 C) as compared to the controls.

Table 3.1 shows the calculated mitochondrial metabolic parameters for both MeHg and positive control cells. Both cells lines exhibit a dose dependant decrease in the reserve capacity with statistical significant change from 0.1 -1 μM ($p \leq 0.0001$), this is also reflected in the positive controls with 500 μM diamide as having the largest effect on lowering the reserve capacity.. Furthermore, AC16 cells show a dose dependant decrease in respiration associated with ATP production and this is again also reflected in the positive controls. However, H9C2 cells do not show a dose dependant decrease following MeHg treatment but did show decreases with positive controls. Similarly, we see a dose dependant increases with $State_{apparent}$ of MeHg treated AC16 cells which are matched by the controls. However MeHg-treated H9C2 cells do not show a statistical increase of the $State_{apparent}$ with dose but positive controls do show an increase with increasing dose.

Positive control responses from the Figure 3.8 do predict trends that may lead to mitochondrial dysfunction from both cell lines and this result is further corroborated with calculations of metabolic parameters in Table 3.1. Therefore, together these results demonstrate the predicted mitochondrial dysfunction response of these chemicals and validate the results from the MeHgCl exposures.

AC16 cells showed dose dependant sensitivities to MeHg as demonstrated by the $State_{apparent}$ and the ATP production calculations (Table 3.1). H9C2 cells do not show the same sensitivities in these parameters and it seems as though H9C2 cells may be more resistant to MeHg toxicity. These trends demonstrate the differences in potential metabolic sensitivities of different cell types to toxicity.

A.

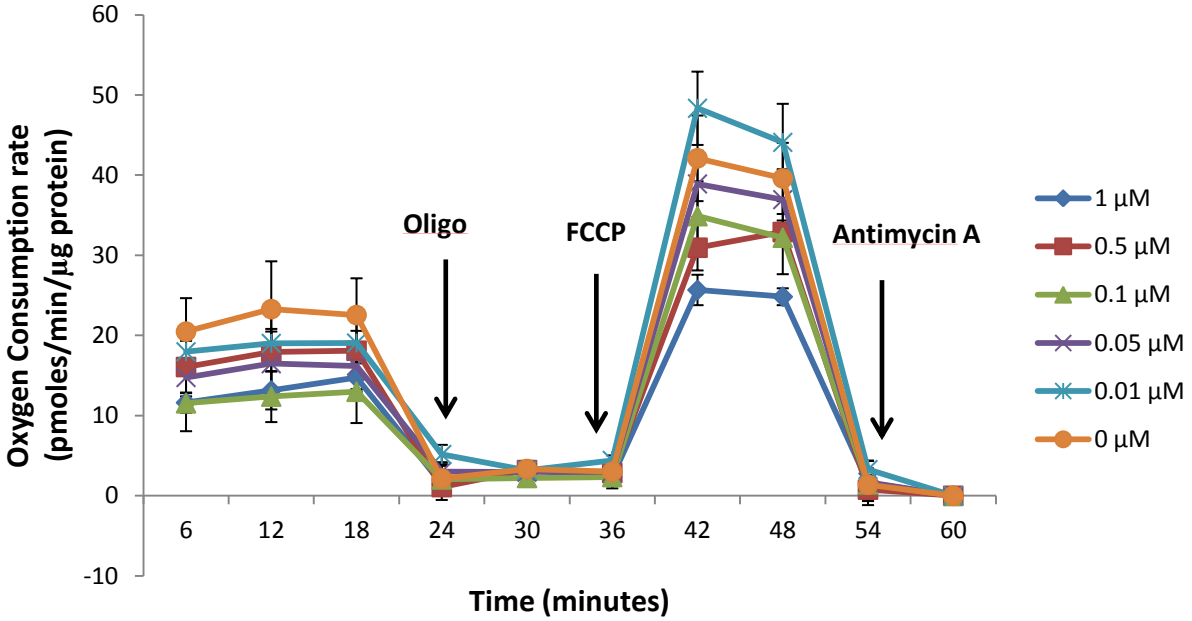

B..

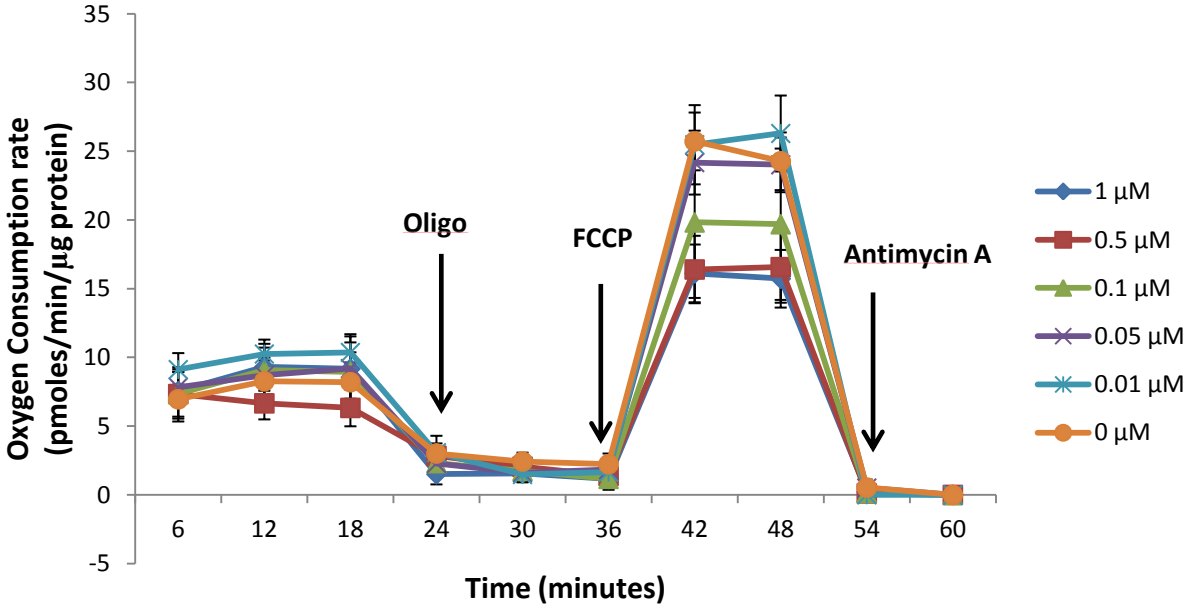

Figure 3.5 Characterization of mitochondrial function following 24 hour exposure to various concentrations of MeHgCl. Cells are attached to welled plates and respiration is analyzed using the XF24 Extracellular Flux Analyzer (A) O_2 consumption rate response of AC16 cells and (B) H9C2 cells for 60 minutes during which oligomycin (1 µg/mL), FCCP (1 µM) and Antimycin A (1 µM) is injected into the cells. Arrows denote times at which the three inhibitors were injected. OCR means ± standard errors are presented. (n=4 separate experiments).

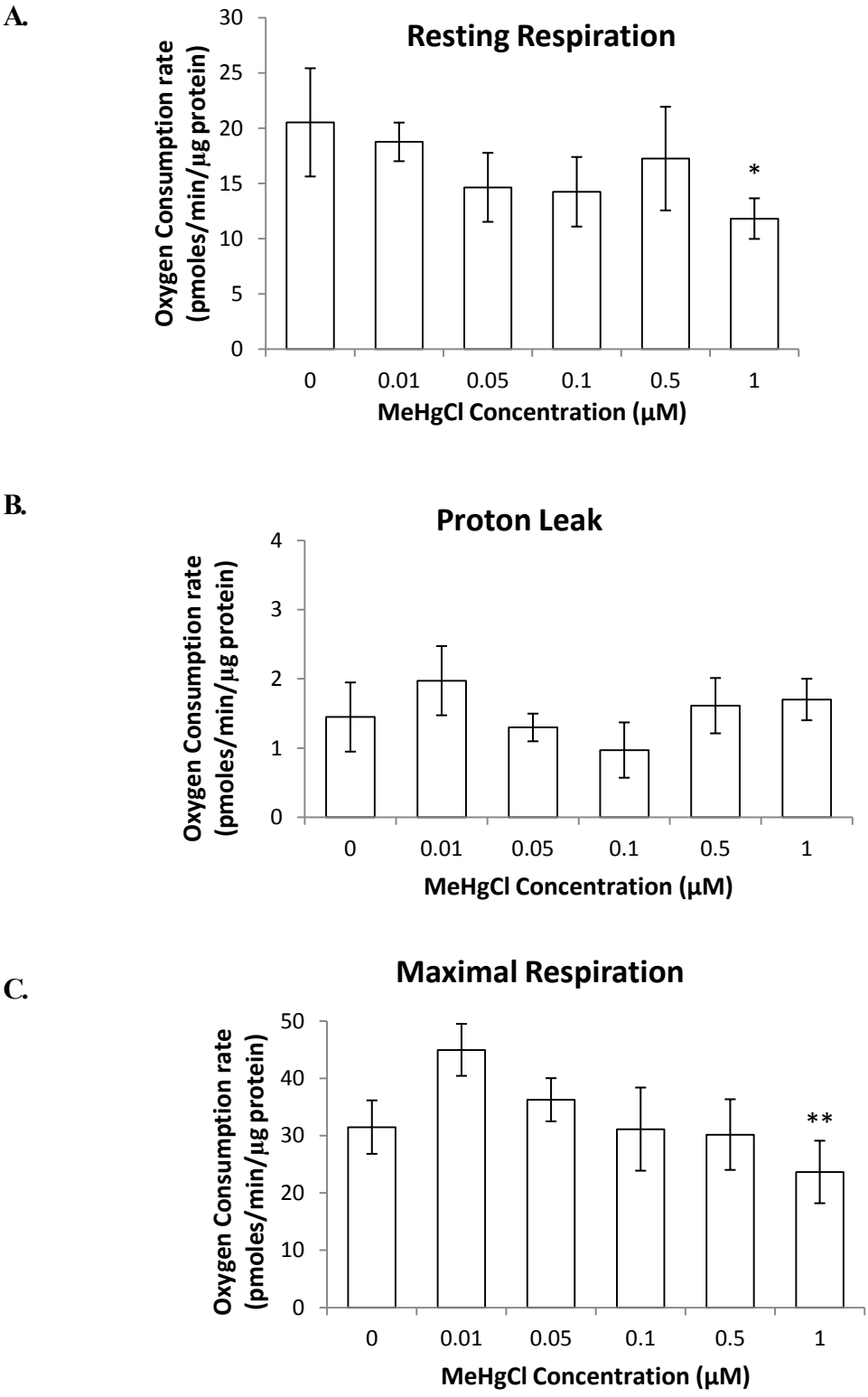

Figure 3.6 Representative bar graphs for three respiration states for AC16 cells following 24 hr MeHgCl exposures. Averages presented are representative of values in Figure 3.5. AC16cells: (A) Resting OCR (B) Proton leak OCR (C) Max respiration OCR (n=4 seperate experiments) Mean OCR ± standard error are shown. All values were corrected to Antimycin A (1 µM). Statistical significance was determined using one-way ANOVA with post-hoc Tukey's test; * represents $p \leq 0.05$, ** represents $p \leq 0.0001$.

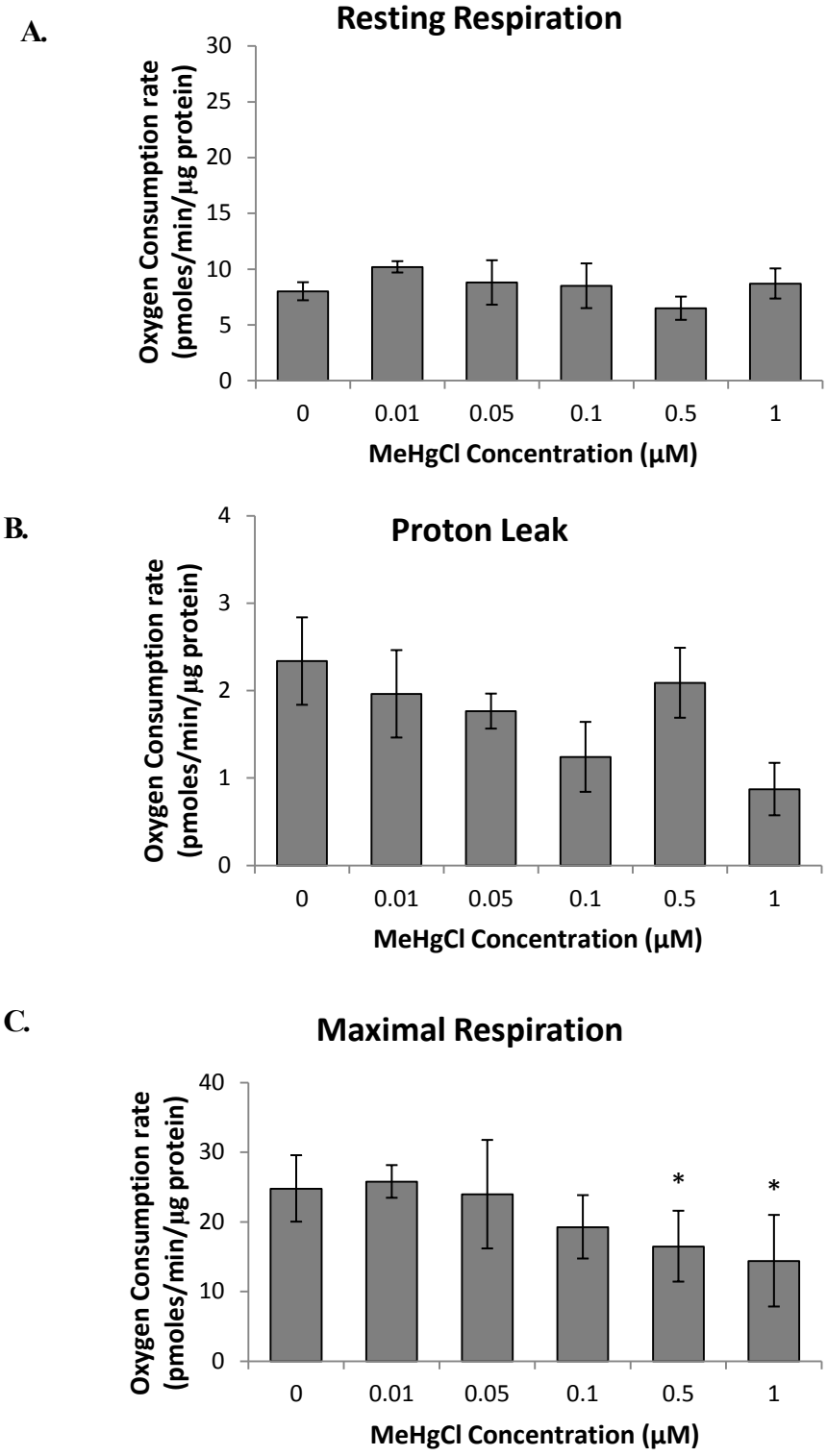

Figure 3.7 Representative bar graphs for three respiration states for H9C2 cells following 24 hr MeHgCl exposures. Averages presented are representative of values in Figure 3.5. (A) Resting OCR (B) Proton leak OCR (C) Max respiration OCR (n=4 separate experiments). Mean OCR ± standard error are shown. All values have been corrected to Antimycin A (1 µM). Statistical significance was determined using one-way ANOVA with post-hoc Tukey's test; * represents $p \leq 0.05$

A.

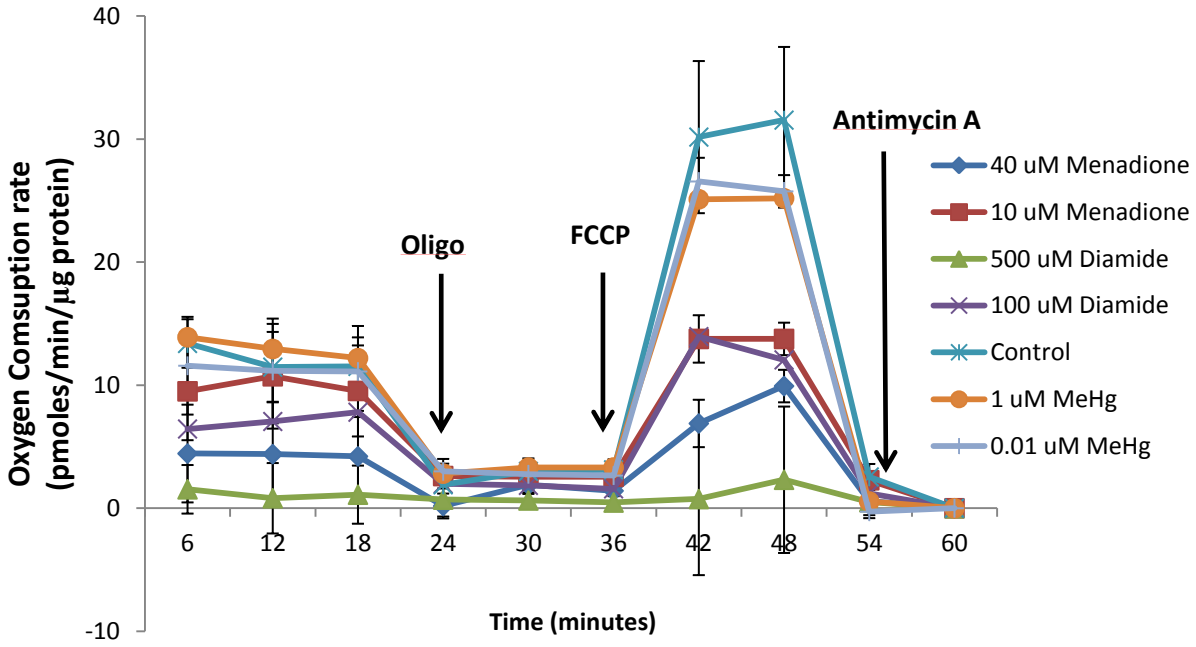

B.

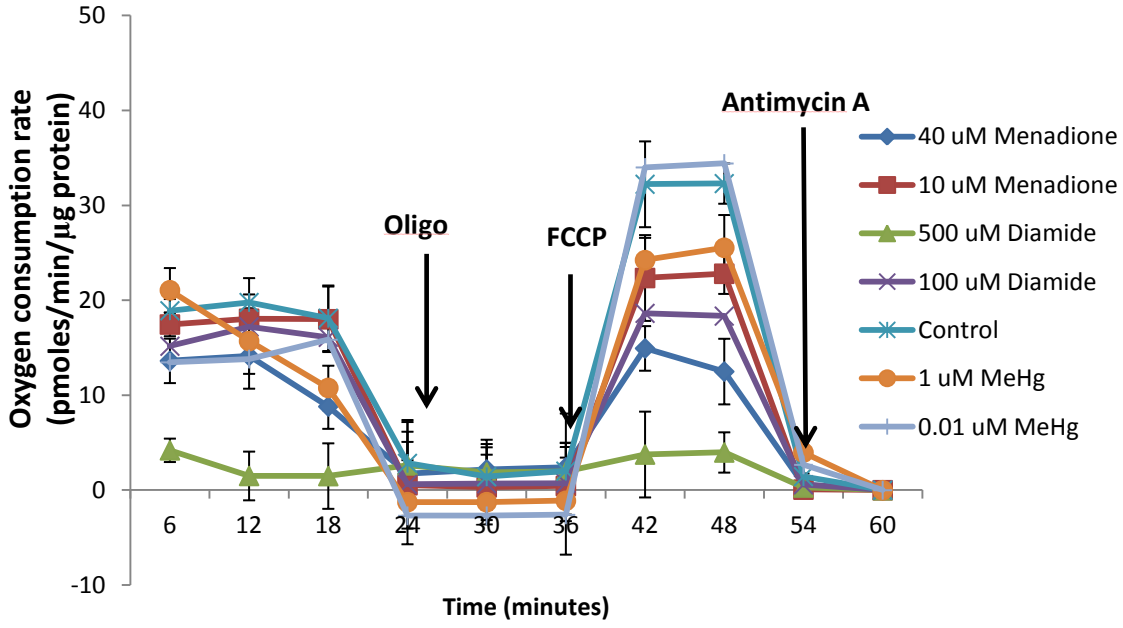

Figure 3.8 Positive control mitochondrial characterizations of AC16 and H9C2 cells. Cells were exposed to two positive controls known to induce mitochondrial dysfunction; menadione and diamide and a high and low concentration of MeHgCl. (A) O_2 consumption rate response of AC16 cells and (B) H9C2 cells for 60 minutes during which oligomycin (1 µg/mL), FCCP (1 µM) and Antimycin A (1 µM) is injected into the cells. Arrows denote times at which the three inhibitors were injected. OCR means ± standard errors are presented. (n=4 separate experiments).

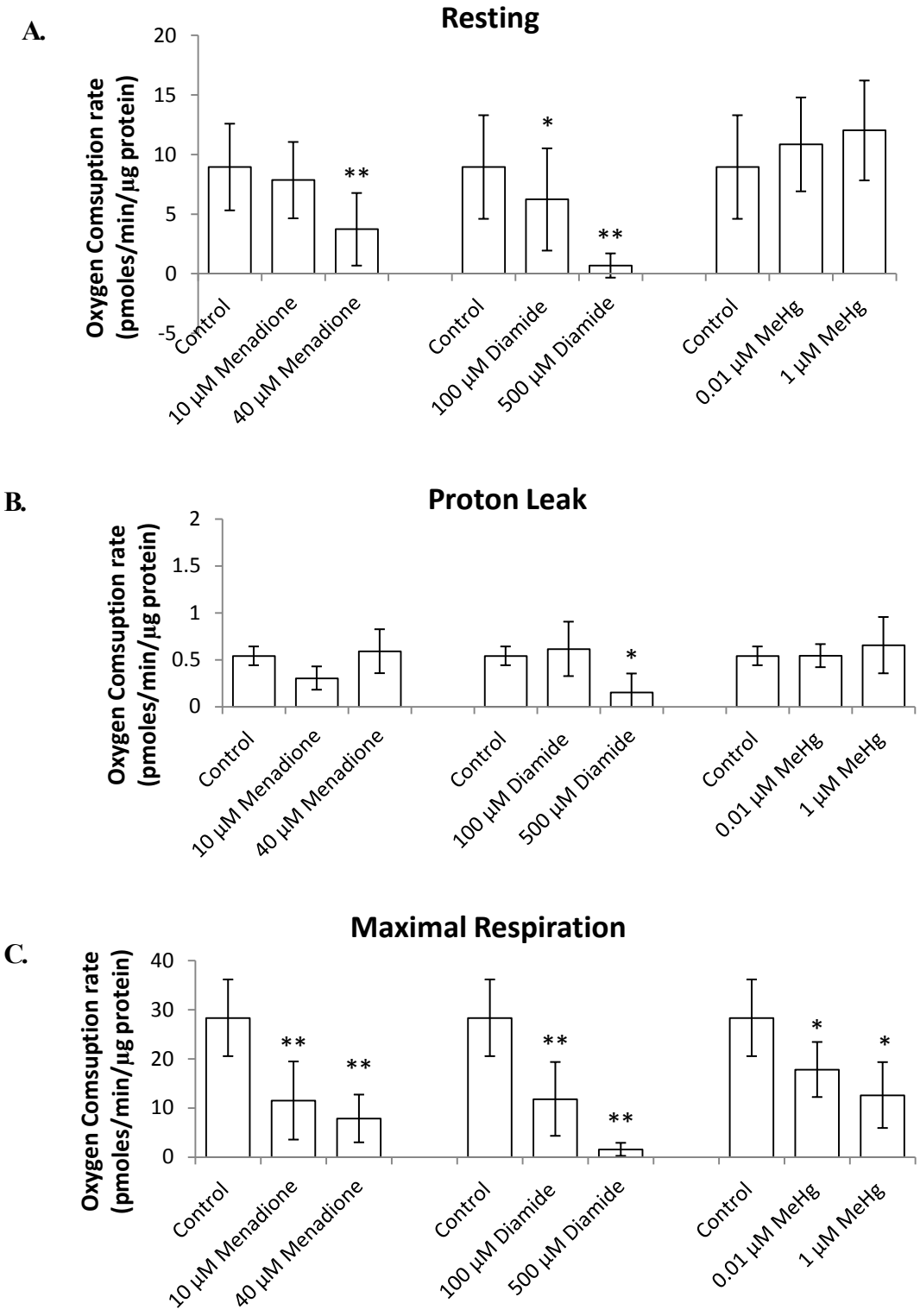

Figure 3.9 Representative bar graphs for three respiration states for AC16 cells following 24 hr positive control exposures. Averages presented are representative of values in Figure 3.8. AC16 cells: (A) Resting OCR (B)Proton leak OCR (C) Max respiration OCR. (n=4 separate experiments) Mean OCR ± standard error are shown. All values have been corrected to Antimycin A (1 µM). Statistical significance for each chemical was determined using one-way ANOVA with post-hoc Tukey's test; * represents $p \leq 0.05$, ** represents $p \leq 0.0001$.

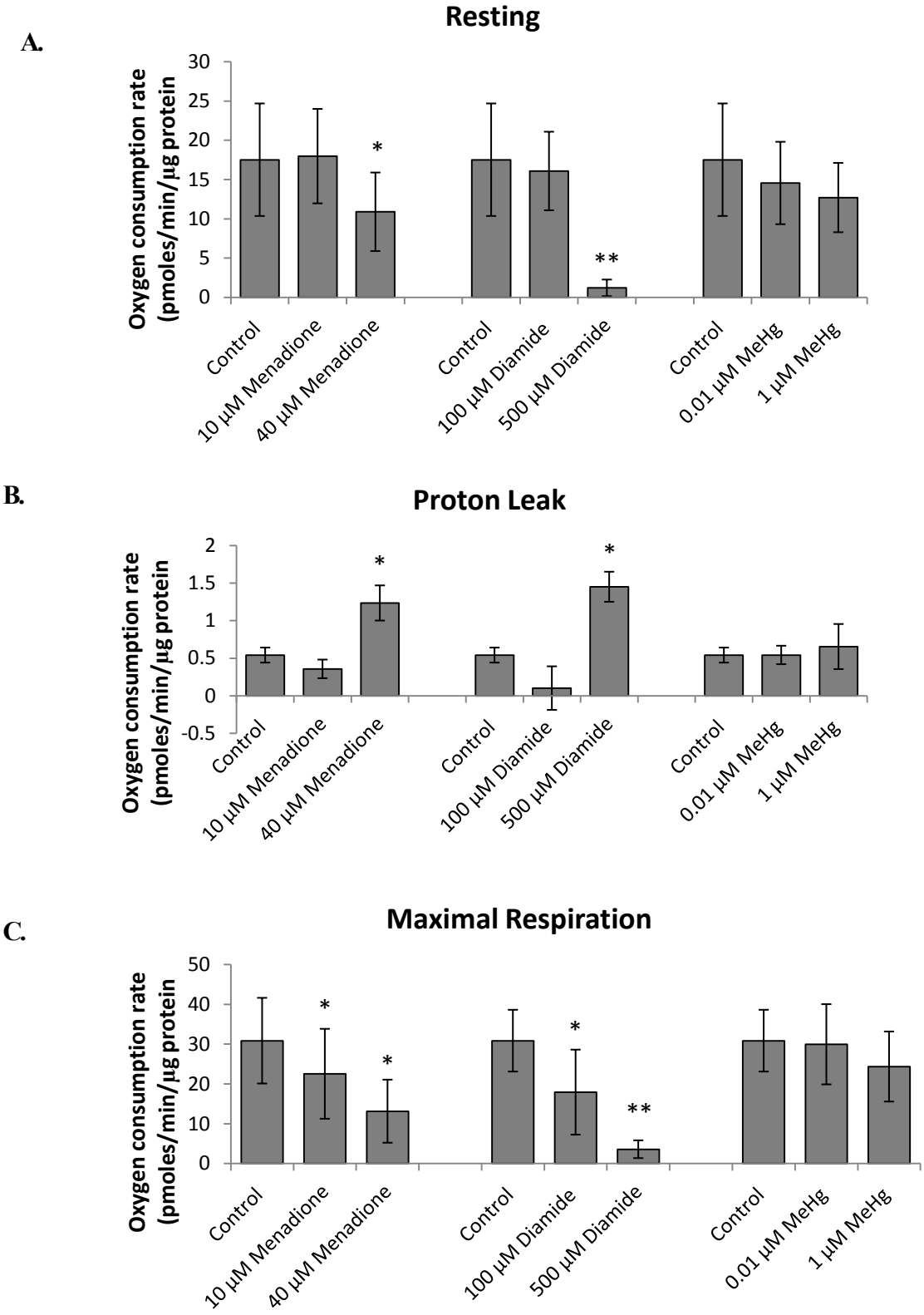

Figure 3.10 Representative bar graphs for three respiration states for H9C2 cells following 24 hr positive control exposures. Averages presented are representative of values in Figure 3.8. H9C2 cells: (A) Resting OCR (B) Proton leak OCR (C) Max respiration OCR. (n=4 separate experiments). Mean OCR ± standard error are shown. All values have been corrected to Antimycin A (1 µM). Statistical significance for each chemical was determined using one-way ANOVA with post-hoc Tukey's test; * represents $p \leq 0.05$, ** represents $p \leq 0.0001$.

Table 3.1 Oxygen consumption rate values for reserve capacity, O_2 consumption required for ATP production at resting state and State apparent for both MeHgCl treated cells and controls. Mean OCR ± standard errors are shown (n=4). Statistical significance was determined using one-way ANOVA using post-hoc Tukey's test, * represents p≤0.0001.

Oxygen consumption rates (pmoles/min/mg protein) (± SE)										
	MeHgCl concentration (µM)						Positive controls			
	Control	**0.01**	**0.05**	**0.1**	**0.5**	**1**	**10 µM Menadione**	**40 µM Mendione**	**100 µM Diamide**	**500 µM Diamide**
AC16										
Reserve capacity[a]	19.9 ±4.90	22.2 ±1.74	21.6 ±3.12	16.9 ±3.15*	12.9 ±4.69*	11.8 ±1.84*	3.63 ±2.34*	4.10 ±2.04*	5.57 ±2.28*	0.860 ±1.45*
ATP production[b]	18.1 ±4.66	16.8 ±4.56	13.3 ±3.77*	13.3 ±5.67*	15.6 ±6.14	10.1 ±5.45*	7.55 ±3.65*	3.14 ±2.12*	5.62 ±1.23*	0.540 ±0.32*
State apparent[c]	3.34 ±0.04	3.60 ±0.07*	3.61 ±0.12*	3.55 ±0.05*	3.45 ±0.04*	3.53 ±0.09*	3.32 ±0.05	3.56 ±0.07*	3.49 ±0.08*	3.61 ±0.06*
H9C2										
Reserve capacity	16.8 ±8.01	15.6 ±10.1	15.1 ±8.79	10.7 ±8.50*	9.98 ±6.44*	5.68 ±5.67*	4.54 ± 1.05*	2.23 ± 2.87*	1.83 ±1.56*	2.37 ± 1.23*
ATP production	5.67 ±2.34	8.23 ±1.95*	7.03 ±5.32*	7.25 ±6.34*	4.39 ±2.34	7.83 ±3.21*	17.6 ± 4.52*	9.65 ±5.43*	15.9 ±5.42*	-0.245 ±1.23*
State apparent	3.74 ±0.05	3.65 ±0.09	3.68 ±0.06*	3.59 ±0.08*	3.69 ±0.10*	3.42 ±0.08*	3.20 ±0.03*	3.18 ±0.06*	3.10 ±0.09*	4.11 ±0.05*

[a] Reserve capacity calculated by subtracting FCCP (maximal respiration) by Basal (resting)respiration
[b] O2 needed for ATP production is calculated by subtracting Basal respiration by Oligo (proton leak)
[c] State apparent is calculated using the following equation: 4-(Basal-Oligo)/(FCCP-Oligo) (Dranka *et al.,* (2010).

3.4 Discussion

Cardiomyocytes are highly oxygenated, containing large numbers of mitochondria as ATP synthesis and calcium intracellular stores are needed for the contractile function of these cells. MeHg mediated toxicity through the production of ROS has been shown to be associated with loss of Ca^{2+} homeostasis triggering cell death pathways (Alissa & Ferns, 2011; Kang, 2001; Roos *et al*., 2012). Furthermore, MeHg has been shown to induce mitochondrial dysfunction in many cell types (hepatocytes, neuronal cells, T-lymphocytes) by accumulating in the mitochondria, increase ROS production, and lowering GSH levels through its high affinity for thiol groups (Houston, 2011), therefore MeHg has the potential to cause adverse effects in cardiomyocytes. In this study, we examine the effects of this toxicant on these parameters in two cardiac cell lines *in vitro* to elucidate underlying mechanisms of the toxicity.

The concentrations of MeHgCl that were utilized in this chapter reflect the concentrations that were obtained in the plasma of the blood. Legrand *et al.,* (2010) compiled the blood total mercury concentrations from Canadian studies published from mid 1990s – 2008, the concentrations range from 0.2 – 10.4 μg/L depending on the populations of the studies (Legrand *et al*., 2010). Furthermore, the current Health Canada MeHg provisional blood guidance values are at 8 μg/L (40 nmol/L) for women of child bearing age and pregnant women. The blood guidance values for females and males of any age are 100 μg/L (500 nmol/L) (Legrand *et al*., 2010).

3.4.1 Cell Viability

Cell viability was affected dose dependently with the most significant effect from 5 μM onwards (Figure 3.3). This is consistent to a study conducted by Yoon *et al.* (1996) who

similarly observed a dose dependant decrease of cell viability in primary neonatal rat myocardial cells exposed to MeHgCl (Yoon *et al.,* 1996). Morphological observations of these primary cells also revealed decreased cell number and disconnection between cultured cells. Although no morphological observations were obtained from this study, results from the MTT assays suggest that decreased cell numbers were evident. The MTT assay is based on quantifying the absorbance of the tetrazolium salt that is cleaved by various dehydrogenase enzymes (such as NADPH) in the active mitochondria producing a purple colour, therefore it also indicates metabolically active cells (Mosmann, 1983). Not only does this indicate that there are non-viable cells at concentrations higher than 1 μM but the metabolism of the cells is also compromised.

3.4.2 Intracellular Calcium and Calcium homeostasis

Disruptions in $[Ca^{2+}]_i$ homeostasis is well documented in *in vitro* experiments on MeHg exposed neuronal cells and astrocytes which caused excitotoxicity followed by calcium uptake in the cells leading to calcium overload, additionally there is evidence that voltage gated Ca^{2+} channels contribute to the increased calcium influx into the cells and tissues (Roos *et al*., 2012). Isolated rat heart papillary muscles exposed to $HgCl_2$ exhibited a biphasic response whereby Hg at low concentrations produced a stronger rate of contraction due to the inhibitions of the Na^+/K^+ ATP-ase by Hg ions causing sustained Ca^{2+} ions in the cell thus producing higher force of contraction. However at higher concentrations, contractile depression occurred suggesting possible Ca^{2+} overload as the cause (Oliveira *et al.,* 1994; Vassallo *et al.*, 1999). Reduced protein expression of various calcium handling proteins such as Na^+/K^+ ATP-ase, Na^+/Ca^{2+} exchanger and SERCA in Hg exposed perfused rat hearts are consistent with the above observations. This study showed statistically significant increases at 5 μM of $[Ca^{2+}]_i$ as compared to the controls for

both cell lines immediately following MeHgCl exposure (Figure 3.4). This elevation may be attributed to overload of calcium in the cells leading to activation of cell death pathways (Shaheen, *et al.*, 2011). As demonstrated with cell viability assays, at 5 μM both cell lines exhibited significant decreases in viable cells (about 30-34%). Similarly, 3 μM MeHg dosed rat cerebellar neurons produced an increased $[Ca^{2+}]_i$ and decreased cell viability dose-dependently (Okazaki *et al.*, 1997; Oyama *et al.*, 1998). Due to the importance of $[Ca^{2+}]_i$ not only for contraction but for cell signalling and its role in maintaining mitochondrial function, MeHgCl exposures have the potential to affect the calcium homeostasis of cardiomyocytes.

3.4.3 ROS production

Oxidative stress and ROS production are known as the main mechanism by which MeHg exerts its toxic effect on cells and tissues. Increasing ROS production and lipid peroxidation has been shown in various cells such as astrocytes and microglial cells (Kaur *et al*., 2011; Ni *et al*., 2010). Hg increases ROS by either binding to thiol containing antioxidants such as GSH, thereby effectively lowering the antioxidant defence of the cell and Hg serves as a fenton catalyst which generates ROS products that act to damages tissue and cells (Alissa & Ferns, 2011). Our study examined ROS production following two exposure time points. The general oxidative stress fluorescent indicator, CM-H2DCFDA has been widely used and measures H_2O_2 and superoxide anion. In order to determine ROS produced immediately after MeHg exposures and for longer exposures, 1 hour exposure and 24 hour exposure was used. One hour exposures showed progressive increases in fluorescence indicative of intracellular H_2O_2 and $\bullet O_2^-$ however, these were not statistically significant. 24 hour exposures exhibited generally higher fluorescence indicating increased production of ROS than following one hour exposures. Shanker *et al.* (2004)

examined ROS production in astrocytes using a time-course experiments with the same fluorescent indicator and found similar progressive increase in ROS produced with five exposure time points using 10 μM MeHg up to 30 minutes (Shanker *et al*. 2004) . Additionally, Kaur *et al.,* (2008) found significant dose dependant increases with ROS following a time course trial from 30 minutes to 4 days in two neuronal cell lines. A similar trend was observed, suggesting that the longer cells were exposed to MeHgCl, the more detectable ROS is produced (Kaur *et al.,* 2008). One note about these studies is that they used much higher concentrations of MeHg (up to 25 μM) and therefore our results reflect low sub-lethal doses.

3.4.4 Mitochondrial Bioenergetics

Approximately, 20% of the cardioymocyte volume is made up of mitochondria and provides all of the energy necessary to sustain the maintenance and contractile function of the cell (Hill, *et al.* 2009). Cardiac pathologies such as ischemia-reperfusion and heart failure is associated with mitochondrial dysfunction. This thesis will be the first to characterize cellular bioenergetics of MeHg exposed cardiomyocytes. Previous studies have found that mitochondria in the rat cerebellum had more susceptibility to MeHg accumulation and oxidative damage than other tissues such as the liver as evidenced by lower GSH levels, higher mitochondrial oxygen consumption levels and higher ROS production (Mori, *et al.*, 2007). MeHg induces the loss of mitochondrial membrane potential in rat neuronal cells through opening of mitochondria transition pore and release of cytochrome c and together with ROS production were shown to produce oxidative damage and induce apoptosis (Polunas *et al.*, 2011; Roos *et al.*, 2011). Furthermore, MeHgCl were shown cause mitochondrial swelling *in vivo,* (Nobuhito, *et al*., 1977).

In the present study, both cells lines exposed to 1 μM MeHg produced significantly lower OCR levels at maximal respiration following FCCP administration, which simulates the need for increased energy demand in the cells. In AC16 cells, there were slight increases in OCR at 0.01 μM. These observations suggest that low concentrations of MeHg may lead to increased mitochondrial respiration to compensate for stress incurred by its toxicity, but at higher concentrations compensation for the stress is no longer possible; thus causing exhaustion and lowering the maximal respiration and resting respiration of the cell (Figure 3.6). Alterations in these mitochondrial parameters of cellular energetic may be due to damaged respiratory chain leading to reduced ATP output. Damages to the respiratory chain have already been demonstrated in rat cerebellar mitochondria, where MeHg exposures demonstrated a decrease in the expression of complex II activity and induced cytochrome c release. These observations were considered to occur in the early stages of MeHg intoxication (Mori, *et al.,* 2011). To further explore this in our study, the reserve capacity and OCR necessary for ATP production was calculated (Table 3.1), we observed a dose dependant decrease in reserve capacity in both MeHg exposed cell lines. The reserve capacity measures the cells capacity to generate ATP during conditions under stress; this is a proxy measure for how much stress a cell can handle. Generally cells exhibiting exhausted reserve capacity leads to failed respiration, lower ATP production and eventual cell death (Readnower *et al.*, 2012). Our results show a decrease in this reserve capacity which may affect the cells ability to produce ATP and handle MeHg toxicity. OCR necessary for ATP production at resting state was calculated to determine whether ATP production was affected; only AC16 cells show dose dependant decreases in ATP production. These observations are in agreement with the hypothesis that MeHg can have a potential impact on energy demand and potential mitochondrial dysfunction of cardiomyocytes.

The $State_{apparent}$ calculations allow us to determine whether these cells are operating in State 3 or 4 respiration (see Appendix I for explanation on respiration states). AC16 cells show a dose dependant increase in $State_{apparent}$ moving closer to State 4 respiration as MeHgCl concentrations increase. This suggests that at higher concentrations of MeHgCl respiration begins to slow as ADP is gradually depleted and proton leak is occurring at much higher levels. Similar to our results, a study conducted in MeHg exposed zebrafish showed no changes to O_2 consumption in state 4 respiration, but significant decreases in state 3 respiration (Bourdineaud *et al*., 2013; Cambier *et al*., 2009). Furthermore, rat liver mitochondria exposed to 10-50 nmol (0.01-0.05 μM) of MeHgCl exposure led to inhibited state 3 respiration (Nobuhito *et al*., 1977). In summary, these mitochondrial parameters exhibit subtle negative effects of MeHg on the bioenergetics of cardiomyocytes leading to lower reserve capacity and decreased ATP production.

The enzymatic reaction of the MTT assay takes place only in functionally intact mitochondria and provides a measure of cell viability as well as another measure of mitochondrial metabolic function (Dreiem *et al.,*, 2005). In terms of mitochondrial metabolic function, Figure 3.1 does show a decrease in the enzymatic activity and a decrease in cell viability at 60 and 68% cell in AC16 and H9C2 cells following 1 μM exposure, respectively. One limitation to take into consideration is that the decreases observed in OCR maximal respiration could be due to the decreased number of viable cells and thereby lowered respiration. Counting of viable and dead cells may need to be conducted in order to investigate whether the decrease in maximal respiration is indeed due to the decrease in the number of cells rather than alterations in cellular bioenergetics.

As this is the first study investigating bioenergetics using the Seahorse XF analyzer

system in these two cell lines, we also examined response following exposures to positive controls that are known to induce mitochondrial dysfunction to compliment our MeHgCl results. We show significant decreases with both menadione and diamide at resting respiration and maximal respiration. Only in H9C2 cells do we observe an increase in proton leak dependant respiration, this increase in proton leak at 100 μM is quite similar to the responses seen by Mailloux *et al.,* (2011) with primary mouse skeletal myotubes attributed to an increase in proton leak to higher numbers of uncoupling protein 3 (UCP3) and adenine nucleotide translocator (ANT) (Mailloux et al., 2011). Furthermore, the respiration profile in these positive controls has a much more pronounced effect on respiration than MeHg, and the effects are indicative of mitochondrial dysfunction. From Table 3.1, both cell lines exhibit dose dependant decreases in reserve capacity, OCR required for ATP production and $State_{apparent.}$ Cells dosed with 500 μM diamide exhibited the most noticeable effect with much lower reserve capacity and ATP OCR values than other chemical and concentrations. Furthermore, diamide exposure produced a much higher $State_{apparent}$ values for both cells line than compared to the controls with H9C2 cells reaching State 4 respiration with a value of 4.11. This suggests that respiration in the cells has been exhausted and there is a higher proton leak-dependant respiration. This higher proton-leak dependant respiration can be attributed to the actions by UCPs and ANT which are shown to leak protons back into the matrix of the mitochondria and acts to decrease mitochondria ROS emissions (Mailloux *et al.,* 2013). Therefore this shift to state 4 respiration and increased proton leak may be a protective effect to decrease the ROS stress mediated by diamide and menadione.

3.4.5 Response comparisons between AC16 and H9C2

This is the first study to compare two cardiomyocyte immortalized cell lines and its responses to various toxins,.. Both cell lines showed a respiration profile indicative of mitochondrial dysfunction with the positive controls; however it also highlights a clear difference in the bioenergetics responses between the AC16 and H9C2 cells. In all experiments, excluding the bioenergetics experiments, both cell lines seem to exhibit similar responses to MeHgCl exposures. However, examining the respiration profile, particularly with the positive controls, we see a clear difference in the bioenergetic signatures of the both cells lines. The trends for both cell lines do not match. Firstly, the general OCR response of H9C2 cells is lower than AC16 cells which may be due to different mitochondrial content in the cells and ATP demands. Both cell lines do exhibit a decrease of maximal respiration with higher MeHgCl exposures (Figure 3.6). From Table 3.1, both cell lines do exhibit a decrease in their reserve capacities with increasing MeHgCl and this is reflected in positive controls. AC16 cells show MeHg dose dependant sensitivities with $State_{apparant}$ and ATP production values, but H9C2 do not show these trends. From these results, it seems as though H9C2 cells are more resistant to MeHg toxicity than AC16 cells and this may be due to higher levels of UCP3 or ANT as reflected in the increases in proton leak and $State_{apparant}$ (Figure 3.8 E and Table 3.1). UCP3 and ANT acts to control the mitochondrial ROS generation by decreasing the proton gradient in the cells thereby lowering the ROS generation from the ETC. To further explore this idea, studies examining the expression of these proteins are necessary.

3.4.6 Conclusion

In summary, AC16 and H9C2 cells, both exhibit similar effects to MeHgCl with the exception of certain bioenergetic responses. From our results, cell death, ROS production, and $[Ca^{2+}]_i$ changes arose at 1 μM MeHg. Maximal respiration in both cell lines also began to decline at this concentrations. Although effects were observed at 1μM, it is important to consider that cell viability decreased at this concentration and therefore the changes in bioenergetics may be attributed to decreased cell numbers leading to a reduction in OCR. Together, these observations contributed to research investigating the cytotoxic effects in cardiomyocytes and attempted to further understand the underlying mechanisms and physiological effects of MeHg in the heart and its potential impact on heart diseases. This study also highlighted the differences in bioenergetic cell responses and how this may impact cells responses to certain contaminant stressors. We have assumed that concentrations used in these experiments are those that are affecting the heart, as these concentrations are those that are found in the blood plasma (Mergler *et al.*, 2007). However, little is known about the distribution of MeHg in the heart during a lifetime of exposure, therefore in the following chapter, we will address the distribution of total mercury and methylmercury in heart tissue samples and how this correlates with total body oxidative stress to compliment the *in vitro* data obtained in this chapter.

Connecting Bridge

The previous chapter explored the toxic mechanisms of MeHg on cardiomyocytes cells *in vitro.* Concentrations in the ranges of the 1 μM and above were found to have effects on cell viability, calcium concentrations and bioenergetic functions. Additionally, a significant increase in the ROS production was found. We examined two separate cell lines in order to make comparable assumptions about the toxic effects seen in different types of cardiomyocytes. While *in vitro* studies allow for simple mechanistic observations, it is still of interest to identify effects on *in vivo* models to determine effects on the whole organism. Furthermore, exposure concentrations used in Chapter 3 were based on concentrations found in the human blood plasma and are concentrations that were used in previous *in vitro* studies (Ayotte *et al*., 2011; Furieri e*t al*., 2011; Yoon *et al*., 1996; Legrand *et al.,* 2010). Distributions of the mercury in the mammalian and human heart are seldom reported. Therefore to compliment *in vitro* cell culture studies, the next chapter examined the distribution of mercury in tissues of the heart and oxidative stress markers from an on-going *in vivo* rat feeding study. This study is part of a larger project supported by Health Canada and the Northern Contaminants Program (NCP).

Chapter 4 - Distribution of total mercury and methylmercury in rat heart tissues and oxidative stress markers

4.0 Abstract

Populations in circumpolar countries are exposed to a mixture of contaminants (Northern Contaminants Mixture – NCM) through the consumption of traditional foods. Increasing evidence suggests that these contaminants may contribute to increased risks for cardiovascular disease, obesity and diabetes. This study is a contribution to a larger *in vivo* animal study examining how and if NCM can affect chronic disease markers while also being exposed to different dietary and lifestyle factors. We determined the distribution of MeHg and THg in rat hearts and found increasing concentrations of Hg levels with dosed rats; % of MeHg was also in the range of what was previously reported. Urinary isoprostane levels, an indicator of oxidative stress, showed significant increases in lean rats dosed with higher levels of contaminants and obese rats showed consistently elevated levels as compared to the control lean rat groups. From these results, it seems as though a high fat and sugar diet in lean and obese rats can contribute to increasing oxidative stress regardless of the level of contaminants. A high fat and sugar diet also did not have any effects on the accumulation of Hg in the heart tissues.

4.1 Introduction

Exposure to environmental contaminants through fish consumption has been associated with various metabolic diseases such as cardiovascular disease, diabetes and obesity (Fillion *et al*., 2006; Goncharov, *et al*, 2011; Valera, *et al.* 2008). One prevalent contaminant is methylmercury (MeHg). Cardiovascular effects mediated by dietary exposures of MeHg are positively associated with hypertension, myocardial infarction, arteriosclerosis and heart rate variability (Houston, 2011). It is important to note that exposures associated with CVD are to lower concentrations and more long term dose exposures of MeHg than those associated with neurological deficits (Mahaffey, 2000).

The arctic is a global sink for contaminants via long-range atmospheric transport and ocean currents (Donaldson et al., 2010; Van Oostdam et al., 2005). Levels of Hg in freshwater and marine organisms of the Canadian Arctic are found to exceed Health Canada's consumer guidelines (Chan *et al.,* 1995; Ostertag *et al.,*2009) This is of particular concern for indigenous peoples living in circumpolar countries who normally rely on traditional foods such as, fish, marine mammals and terrestrial wildlife. These foods contain nutrients which are essential to Inuit health; however with the presence of high levels of contaminants such as MeHg, the health benefits of these foods may be compromised (Chapman & Chan, 2000). Shifts from a protein-rich traditional diet to market foods which contain higher amounts of saturated fats and sugars has been noted as one of the major factors leading to the increase in the number of CVD in these populations. Therefore, with the exposure of MeHg through contaminated traditional foods, the impact on cardiovascular health in these populations has the potential to be quite high.

MeHg has been shown to be accumulated in the heart and it is known that about 80% of that Hg in the heart is in the form of MeHg (Matsuo *et al.*1989).

This study was part of a larger ongoing study with Health Canada (HC) and the Northern Contaminants Program (NCP). The NCP was created in 1991 to address concerns of contaminant exposures from a diet of country or traditional foods (Donaldson *et al*., 2010) Northern Canadian populations are exposed to a mixture of contaminants at levels that are much higher than other populations. Contaminated fish and marine mammals consumed by many northern populations contain elevated levels of heavy metals, polychlorinated biphenyls (PCB), and organochlorines (Ostertag *et al*., 2009; Van Oostdam *et al.,* 2005*)*. A number of epidemiological studies have shown positive correlations between contaminant exposures and chronic diseases. There is very little known about how and if these exposures to northern contaminants are contributing to the development and progression of these diseases and if changes in lifestyles may be a contributing factor. The objective of this Health Canada study was to use an *in vivo* rat model of human metabolic and cardiovascular diseases to investigate the effects of the northern contaminants mixture (NCM), while also being exposed to a high fat and sugar diet or alcohol consumption. Canadian Arctic populations are exposed to a mixture of a variety of environmental contaminants. In a mixture, the presence of one contaminant may interact and alter the effects of another contaminant (Florian *et al.*, 2013). The NCM is a mixture of 22 chemicals that were found in Inuit blood during the 2004 and 2005 Inuit Health Survey (Table 4.1) (Dallaire *et al.,* 2009). An initial study conducted by Florian *et al.* (2013) examined the effects of these contaminant mixtures on human coronary endothelial cells (HCAEC) *in vitro* as endothelial cell dysfunction is a major factor in the development of cardiovascular diseases. They observed alterations in markers of cytotoxicity and endothelial cell dysfunction exposed to NCM with and

without the presence of lipoprotein or ethanol in cell culture media (Florian *et al*., 2013). This *in vivo* study was prompted by the results from the *in vitro* observations to further verify the effects NCM.

We obtained heart tissues and urine samples from this study in order to determine the accumulation of total Hg and MeHg in the heart and whether or not the contaminants mixture affected whole body oxidative stress from urine samples. It is unknown how much MeHg accumulates in the heart and how this may contribute to the development of heart diseases. The findings from this chapter will contribute to a larger collaborative effort to determine effects of NCM on markers of cardiovascular and metabolic diseases.

4.2 Methods

4.2.1 Animals

All rat studies were performed at Health Canada in the laboratory of Dr. Dawn Xiaolei Jin. All experimental procedures adhered to the Canadian Council on Animal Care Guidelines and were approved in advance by Health Canada's Animal Care Committee. 60 male heterozygous and lean (+/?) and homozygous and obese (cp/cp) JCR:LA-cp male rats were obtained from the University of Alberta. The rats were approximately 8 weeks old and weighed from 250-350 grams. The JCR:LA-cp rat displays the autosomal recessive corpulent (cp) gene originally isolated by Koletsky (1975). This strain was chosen because (cp/cp) male rats possess a Tyr763 Stop mutation for the leptin receptor and are severely obese, hyperphagic, hypertriglyceridemic, hyperinsulinemic and markedly insulin resistant. It is unique because it is only one of five major strains with the cp gene to develop atherosclerotic and myocardial lesions from an early age. In addition, these rats exhibit several attributes typical of the metabolic

syndrome, obese/diabetic/hypertensive/dyslipidemic observed in human subjects (Koletsky, 1975). The heterozygous lean rats have normal characteristics and were used as the controls. Rats were acclimatized for 2 weeks and fed on a standardized starch-based AIN93G diet (Table 4.2). Following this acclimation period, one group of rats were fed a modified high fat/sugar AIN93G diet for the duration of the study. Both groups of rats were exposed to the corresponding concentrations of NCM as shown in Table 4.3 by being fed Teddy Graham cookies with the NCM (composition of NCM mixture is shown in Table 4.1) until the 10^{th} week of the experiment where rats are euthanized and tissues are collected for various biochemical endpoints. I received the heart tissues from 5 different rats in the study (n=5) from each treatment group for quantification of total mercury and methylmercury accumulation and the urine samples from 8 different rats (n=8) to determine oxidative stress in the rats.

Table 4.1 Chemical composition of the Northern Contaminants Mixture (NCM) representative of contaminants frequently detected at high concentrations in the Inuit blood samples.

NCM Chemical Composition	Low Dose[1] (µg/L)	High Dose (µg/L)[2]
Heavy Metals (3)		
Cadmium	146.1	730.5
Methylmercury	241.0	1205
Lead	497.3	2486.4
PCBs (12)		
99	4.70	23.5
138	19.0	95
146	6.10	30.5
153	40.0	200
163	6.20	31.00
170	6.18	30.9
180	22.7	113.5
187	9.10	45.5
194	5.10	25.5
201	4.70	23.5
203	2.50	12.5
Organochlorine (4)		
Oxychlordane	16.0	80.00
p,p'-DDE	50.0	250.00
Trans-nonachlor	22.0	110.00
Pentachlorophenol	18.0	90.00
Toxaphene (1)		
Parlar # 50	59.1	29.55
Brominated flame retardants (2)		
PBDE IUPAC #47	2.40	12.00
2,3,4,6-tetrabromophenol	1.39	6.97
Perfluorinated compounds (1)		
PFOS	470.0	2350.00
Total	***1596.4***	***7981.9***

[1] The highest level detected in Inuit plasma samples (Dewailly *et al.,* 2006, Dallaire *et al.,* 2009)
[2] 10X the highest level detected in Inuit plasma samples.

Table 4.2. Diet Composition of rats fed the normal diet and high fat/sugar diet

Diet Ingredients	Normal Diet (AIN93G)		High Fat/Sugar Diet (modified AIN93G)	
Casein	200		100	
L-cysteine	3		1.5	
Corn starch	397.49		87.86	
Maltodextrin	132		100	
Sucrose	100		400	
Lard (pork)	0		130	
Soybean oil	70		70	
Cellulose	50		50	
Mineral Mix (AIN93G-MX)	35		42	
Vitamin Mix (AIN-93-VX)	10		12	
Choline bitartrate	2.5		3	
TBHQ antioxidant	0.014		0.04	
Kcal/g	3.8		4.5	
% weight	**% kcal**		**% weight**	**% kcal**
Protein	17.7	18.8	8.9	7.8
Carbohydrate	60.1	63.9	59.5	52.4
Fat	7.2	17.2	20.1	39.8

Table 4.3 Rat Treatment groups and corresponding doses of NCM mixture

Treatment Groups				
Group	Rat Strain	Diet	NCM dose (mg/kg BW)	Rat #
1	Obese	AIN93G	0	10
2			1.6	10
3			8	10
4		Modified AIN93G (with high fat/sugar)	0	10
5			1.6	10
6			8	10
7	Lean	AIN93G	0	10
8			1.6	10
9			8	10
10		Modified AIN93G (with high fat/sugar)	0	10
11			1.6	10
12			8	10

4.2.2 Total Mercury Quantification

Heart muscle tissue samples were analyzed for total mercury (THg) in ppm using the Nippon MA3000 direct combustion mercury analyzer (Nippon North America, College Station, TX). 10-15 mg wet weight of frozen sample was added to ceramic sample boats. Analytical accuracy and precision were monitored through the use of Standard Reference Materials (SRMs), and intermittent analysis of duplicate samples. SRMs included National Research Council of Canada (NRCC) DOLT-4 (dogfish liver) and DORM-3 (dogfish muscle) yielding recovery ratios of 90-100%. The mercury working standard was made by successive dilution of stock mercury solution of 1000 ppm (Wako Pure Chemical Industries, Ltd. Japan) in 0.001% L-cysteine solution to make a 1 ppm mercury solution.

4.2.3 Methylmercury Extraction and Quantification

10-15 mg of heart muscle tissue was weighed in a 20 ml glass vial. Tissues were chemically digested by addition of 2 ml of 6N KOH to each sample and shaken for 1 hour (Gyrotory Shaker Model G2) at 330 rpm. Thereafter, 6N HCl was added to the vial, followed by 4 ml of a 3:1 ratio of acidic potassium bromide and 1.0 M copper sulfate mixture and 5 ml of dichloromethane (DCM) to extract methylmercury from the aqueous phase. Vials were shaken overnight at 330 rpm. The samples were then centrifuged in a RC-5 Superspeed Refrigerated Centrifuge (Sorvall, Wilmington, DE) for 5 minutes at 5000 rpm. At this point an aqueous phase and organic phase was seen in the vial, approximately 4 ml of the DCM in the organic phase was transferred to a 7 ml glass vial. 1 ml of 0.01M of sodium thiosulfate ($Na_2S_2O_3$) was added to each sample and shaken for 20 minutes and centrifuged for 5 minutes. Approximately 400 µL of

the top aqueous layer ($Na_2S_2O_3$ layer) was transferred to a microcentrifuge tube.

Approximately, 200 µL of the MeHg extract was added to each ceramic sample boat covered in a layer of Additive B (Aluminum oxide) and analyzed using the Nippon MA3000 direct combustion mercury analyzer. SRMs included National Research Council of Canada (NRCC) DOLT-4 (dogfish liver), DORM-4 (dogfish muscle) and TORT-2 (lobster hepatopancreas). MeHg extractions were done on replicates of all three SRMs as a control for extractions.

4.2.4 Urinary isoprostane quantification

Rat urine samples were analyzed for concentrations of urinary isoprostane (UI), specifically 15-isoprostane F_{2t}, a marker of systemic oxidative DNA damage/repair. Isoprostanes are prostaglandin-like compounds that are produced by free radical mediated lipid peroxidation and are useful for assessment of oxidative stress *in vivo* (Morrow, Harris, & Roberts, 1990). Urine samples were analyzed with the Urinary Isoprostane ELISA kit from Oxford Biochemical Research (Cat # EA85, Oxford, Michigan, USA). A portion of excreted isoprostane in urine is conjugated to glucuronic acid, therefore in order to generate a more accurate quantification of urinary isoprostane, all samples were pre-treated with β-glucuronidase (Oxford Biochemical Research, 2012; Morrow et al., 1990). Urine samples were diluted (1:4) and pre-treated with β-glucuronidase prior to experiments. Urine samples were mixed with an enhanced dilution buffer in the kit which eliminates interference due to non-specific binding. The 15-isoprostane F_{2t} in the samples and standards competes with the 15-isoprostane F_{2t} conjugated to horseradish peroxidase (HRP) for binding to the polyclonal antibody specific to 15-isoprostane F_{2t}, coated onto the microplate. A standard curve was generated per plate with duplicates per standard

concentration and per sample. The plate was read at an absorbance of 450 nm using the SPECTRAmax PLUS 384 microplate reader. Sample isoprostane concentrations were extrapolated from the standard curve. All urine samples were normalized to creatinine levels to allow for reasonable sample-to-sample comparison using the colorimetrc Creatinine Assay Kit (Oxford Biochemical Research, Cat # CR01). The amount of creatinine excreted by an organism is considered relatively constant and is therefore used as an index of standardization (Wyss & Kaddurah-Daouk, 2000). Urine samples were diluted at 1:4 and plated in duplicates on a microplate with a standard curve. Picric acid was added to each sample producing an orange colour which is then quantified using the SPECTRAmax PLUS 384 microplate reader at an absorbance of 500 nm. Sample creatinine concentrations were then extrapolated from the generated standard curve and normalized to 15-isoprostane F_{2t} concentrations.

4.2.5 Statistical Analyses

Results from MeHg and THg quantifications and urinary isoprostane results were analyzed using three-way ANOVAs to determine effects between two rat groups, diet groups and dosages, two-way ANOVAs and post-hoc Tukey's test was used to determine differences between diet groups and dosages. Statistical analyses were analyzed using SigmaPlot version 12.5. Statistical significance in all cases was accepted at $P \leq 0.05$.

4.3 Results

4.3.1 Total Hg and MeHg distribution

Total Hg and MeHg distribution of rat heart tissues is shown in Table 4.4. There are differences in mercury levels between the two different rat strains at $p \leq 0.001$. There was no significant difference between diet groups. It is important to note that the levels of Hg detected reflect how much MeHg was ingested. During the animal study, some rats, particularly the lean rats in the high dose groups, did not eat all the treated cookies given.

In all diet groups, we observe differences between NCM groups. In the lean rats group fed the normal diet, there is a significant difference between the vehicle control groups and the low dose ($p \leq 0.05$) and high dose ($p \leq 0.001$) for THg and MeHg. Lean rats fed the HFSD exhibited a similar trend in THg and with MeHg, however with MeHg there was a difference between the high dose group and the low dose group ($p \leq 0.05$). The obese rat groups showed the highest mercury levels in the heart as compared to the lean rats and in all treatment groups.

The obese rat groups fed the normal diet shows the differences in the vehicle group and the low ($p \leq 0.05$) and high dose groups ($p \leq 0.001$) for both THg and MeHg. Furthermore, there were differences between the high and low dose groups ($p \leq 0.001$) for both THg and MeHg. Obese rats fed the high fat diet shows differences between the vehicle control and two dose groups ($p \leq 0.001$). THg in this group also shows differences between high and low dose with at $p \leq 0.05$. As observed with the % MeHg/THg, MeHg makes up the majority of Hg in all groups in the heart. In the obese rat groups, both high dose groups showed about 63-68% MeHg suggesting that some demethylation in the tissues occurred. Overall, MeHg in these tissues underwent very little demethylation except for the high dose in the obese rats.

Table 4.4 THg and MeHg of hearts in rats dosed with a vehicle control, low dose and high dose of northern contaminants mixture means ± standard deviation. (n=5 animals)

	Sample ID[1]	THg (ppm) (± SD)[2]	MeHg (ppm) (±SD)[2]	% (MeHg/THg)
Lean	NV	0.0418 (± 0.029)	0.0519 (± 0.014)	124
	NL	1.44 (± 0.722)	1.41 (± 0.985)*	97.4
	NH	2.02 (± 1.39)**	2.34 (± 0.811)**	115
	HV	0.0266 (± 0.019)	0.0277 (± 0.011)	104
	HL	1.49 (± 0.544)	1.269 (± 0.186)*	81.1
	HH	2.88 (± 1.58)**	3.09 (± 1.48)**x	107
Obese [aa]	NV	0.0274 (± 0.015)	0.0374 (± 0.046)	116
	NL	3.33 (± 0.706)*	2.46 (± 0.781)*	73.8
	NH	10.6 (± 1.54)**y	6.74 (± 2.11)**y	63.4
	HV	0.0739 (± 0.100)	0.0311(± 0.016)	42.1
	HL	3.53 (± 0.590)*	3.87 (± 0.748)**	109
	HH	6.51 (± 2.95)**x	4.46 (± 1.23)**	68.5

[1] N=normal AIN93G(N) diet; H= high fat/sugar diet; V = vehicle control, L = NCM low dose 1.6 mg/kg body weight; H = NCM high dose 8 mg/kg body weight

[2] Two-way ANOVA with post-hoc Tukey's test was used to determine differences in interaction between diet groups, NCM doses and tHg or MeHg.

[aa] Significant difference between rat strains at $p \leq 0.001$, Three way ANOVA was used to examine effects of strains, and diet groups.

* value represents difference between dose groups as compared to the vehicle control at $p \leq 0.05$ within each diet group, ** represents difference at $p \leq 0.001$.

x value represents differences between low dose group and high dose group with $p \leq 0.05$ and y represents difference between low dose group with $p \leq 0.001$.

4.3.2 Urinary Isoprostane – Systemic Oxidative Stress

Urinary Isoprostane (UI) normalized to creatinine levels measured in rat urine from lean and obese rats fed a high fat and sugar diet (HFSD) and a normal diet (ND) with three difference NCM dose groups is shown in Figure 4.1. Overall, a significant difference was found between the lean and the obese rat groups ($p \leq 0.05$). The lowest levels of UI were found in the lean rat groups fed the normal diet and dosed with the vehicle control (0 mg NCM), which serves as our control group. In the lean rats, we observed a significant increase in the UI levels with higher dose groups at $p \leq 0.001$. However we observed no such increase in rats fed with the HFSD. We also observe no significant difference in any groups observed in the obese rats. These results suggest that the high fat and sugar diets in obese and in lean rats increases oxidative stress with and without the influence of NCM mixtures. Lean rats showed increased oxidative stress only when exposed to NCM, however the NCM did not influence the levels of oxidative stress in the dosed rat groups fed the HFSD. A significant difference is observed between both vehicle controls in the lean rat groups at $p \leq 0.05$ suggesting that a HFSD diet may lead to increased oxidative stress further demonstrating that the composition of diets, regardless of NCM dose, can influence oxidative stress.

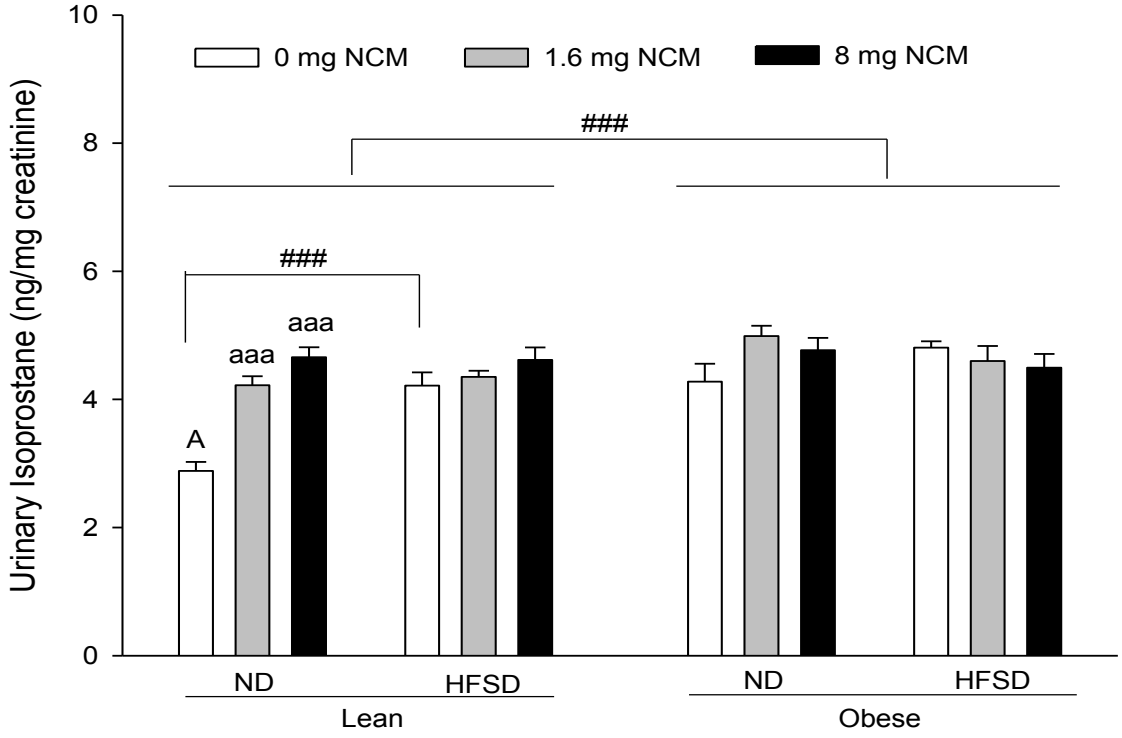

Figure 4.1 Urinary isoprostane levels (ng/mg creatinine) of lean and obese rats fed a normal diet or high fat and sugar diet dosed with three different concentrations of NCM. Data are represented as standard error of the means. ND: normal AIN93G diet, HFSD: high fat and sugar diet. Statistical significance of data was analyzed using three-way ANOVAs with post-hoc Tukey's test to determine difference between two rat strains. Two-way ANOVA with post-hoc Tukey's test was used to determine difference between diet groups and NCM groups. (n=8 animals) $^{###}$ represents difference between two groups at $p \leq 0.05$. "A" is significantly different from "aaa" at $p \leq 0.001$.

4.4 Discussion

The effects of northern contaminants on chronic diseases such as CVD, diabetes and obesity are still unknown. This *in vivo* rat feeding study provides insight into what and how NCM can affect markers of chronic diseases with modulating effects of high fat and sugar diet or alcohol consumption. Results from this chapter contribute to the objectives of this larger study.

4.4.1 Total Hg and MeHg distribution

The distribution of Hg levels in the heart and susceptibility to Hg accumulation is seldom reported. Matsuo *et al.* (1989) determined MeHg, THg and inorganic Hg in human autopsy samples of Japanese subjects who had no known exposures to mercury. In the heart tissue they observed 45 ng/g THg and 33 ng/g MeHg. 80% of the Hg in the heart tissues was in the form of MeHg and suggested that demethylation in organs such as the heart and the brain occurred more slowly than in other organs such as the kidney or spleen (Matsuo *et al.* 1989). Similarly, our results show higher proportions of MeHg to THg (Table 4.4) in the ranges from 63- 97%. Cappon *et al.* (1981) measured tissues obtained from human autopsies from a Canadian Northwestern Ontario aboriginal community who had no acute or chronic mercury poisoning. They observed similar concentrations of THg within the ranges of the low dose groups in this study, however much lower % MeHg in the range of 40% (Cappon & Smith, 1981). From our results, we observed a difference in the levels of Hg between the lean and obese rats. We also observe a significant dose-dependent increase in the distribution of both THg and MeHg in all dosed rat groups. There was no difference between diet groups within each rat strain. It is clear however that obese rats had much higher levels of THg and MeHg in all dosed groups than lean

rats. Similarly, Yamamoto *et al.* (2013) observed increased accumulation of the MeHg in KK-Ay rats, a diabetic rat strain, in blood, cerebrum and liver. The KK-Ay rats accumulated a higher percentage of body fat gained during the experimental conditions than lean rats and low accumulation of MeHg in adipose tissues which may lead to higher MeHg susceptibility (Yamamoto *et al*., 2013). JCR rats used also exhibited increased weight gain during experimental conditions and also exhibited increased susceptibility to MeHg accumulation (unpublished data from this study).

4.4.2 Urinary Isoprostane - systemic oxidative stress

Oxidative stress is associated with numerous pathologies including chronic diseases and cardiovascular disease. Lipid peroxidation is a key feature of oxidative stress and measurement of lipid peroxidation products is a useful indicator of oxidative stress in *in vivo* conditions (Roberts & Morrow, 2000). Urinary Isoprostane (UI), in particular, F_2-isoprostane has been regarded as one of the most reliable and accurate indicators of oxidative stress and were used in *in vivo* animal studies and human studies (Piłacik *et al.,* 2002). The presence of these compounds is also associated with the development of hypercholesterolemia, diabetes, and atherosclerotic lesions (Minuz *et al*., 1998) F_2-isoprostanes are prostaglandin-like compounds produced by peroxidation of arachidonic acid which are produced in detectable quantities in all biological fluids and tissues (Morrow et al., 1990).

In our study, we observed significant differences between lean and obese rat groups with obese rats having overall higher levels of UI providing evidence for oxidative stress in obese rats than in lean rats. In obese rats, the isoprostane levels remained at similar levels regardless of diet groups or NCM groups. There is an association between excess body weight and elevated levels

of F_2-isoprostane in human and animal studies (Piłacik *et al*., 2002). These results have also been reported in obese rat strains (Kaviarasan *et al.,* 2009; Laight *et al.,* 1999). This suggests that regardless of diet, susceptibility to oxidative stress is associated with the predisposition to chronic diseases. In lean rats, however, a HFSD may be linked to increased oxidative stress regardless of NCM group; the lean rat groups observed levels of UI similar to those in obese rats. The effects of the HFSD diet as compared to ND in lean rats is most pronounced in the vehicle controls. Similarly, previous studies also showed elevated isoprostane levels, cerebrocortical oxidative stress, and hearts shows indices of lipid and protein oxidation in *in vivo* studies where the animals were maintained at a high-fat diet (Freeman *et al.*, 2013; Savini *et al.,* 2013; Yuzefovych, *et al.,* 2013). The effects of the NCM were only significantly different in the lean rats fed the ND, in this group we see a dose-dependent increase in the levels of isoprostane. Jin *et al.,* (2008) observed increased urinary F_2-isoprostane with increasing MeHg in exposed rats; the effects of different dietary fats were examined and they found MeHg toxicity may be modulated by certain dietary fats and specifically MeHg peroxidation of polyunsaturated fats may be a source of the UI (Jin *et al.*, 2008) This may explain our observation of the dose-dependent increase of isoprostanes with NCM. Additionally, Jin *et al.,* (2011) further examined MeHg dosed rats with supplementation of nutrients known to have a protective effects of against MeHg toxicity, and found increases of isoprostane levels with MeHg in certain supplement groups suggesting an increased risk of atherosclerosis in those animals (Jin *et al*., 2011).

F_2-isoprostanes are associated with numerous pathologies, it has been found to also be a good indicator and risk factor of coronary heart diseases (CHD). In a case-control study of patients with confirmed CHD, F2-isoprostane 8-iso-prostaglandin and traditional markers of CHD such as HDL, and systolic blood pressure was measured. They found higher isoprostane

levels in patients with greater number of risk factors which placed them at a higher odds ratio for CHD (Schwedhelm *et al*., 2004). Its reported that the increased isoprostanes in the blood and urine for CHD is directly reflected in the increased lipid peroxidation that occurs in blood vessels undergoing atherogenesis (Davies & Roberts, 2011).

This chapter focused primarily on the accumulation and distribution of MeHg in dosed rats, however the objective of the larger ongoing study was to examine the effects of a mixture of contaminants. The NCM contains 22 chemicals which include heavy metals, PCBs and organochlorine (Table 4.3), many of which are linked to an increase in oxidative stress (Hennig et al., 2004; Kishimoto *et al*., 1995; Limaye *et al.,* 1999). Therefore the results shown in Figure 4.1 are the effects of a combination of contaminants where the interaction between one group of chemicals may affect the actions of another. This gives us an overall view of how northern contaminants may affect oxidative stress in populations consuming certain diets.

4.5 Conclusion

In summary, the proportion of MeHg and THg in the low dose groups of the heart samples are similar to those that were previously reported (Cappon & Smith, 1981; Matsuo *et al*., 1989.). There were significant differences found between the lean and obese rats in Hg distribution and UI levels; obese rats accumulated much higher levels of Hg and exhibited elevated UI. No differences were found between diet groups for both experiments, except for UI levels in both vehicle controls which suggest that HFSD may contribute to this increase. NCM showed dose dependant increases in THg and MeHg accumulation in the heart as well as in UI. Together these results contribute to the a larger study examining effects of NCM on chronic disease markers, we demonstrate that the MeHg levels in the NCM can accumulate in heart tissues potentially causing adverse effects, and the NCM levels contribute to elevated levels of UI and oxidative stress in the animals.

Chapter 5 - Conclusions and Future Directions

5.1 Overall Conclusions

The overall objective of this project was to characterize the cytotoxic effects of MeHg on cardiomyocyte cells using two different cell lines, and to determine the distribution of MeHg and THg in the heart and relate those values to oxidative stress markers *in vivo.* I hypothesized that exposures to MeHg at higher concentrations will contribute to the cytotoxic impairment of cardiomyocyte cells. This thesis demonstrated that MeHg at higher concentrations does have the potential to affect certain physiological parameters in cardiomyocytes. Cell viability declined at 1 μM and onwards, intracellular calcium concentrations significantly increased at 5 μM, ROS production significantly increased at 1μM for both 1 hour and 24 hour exposures. ROS production at 24 hours produced a fluorescence that was 10 X that of 1 hour exposures, indicating that the longer the cells are exposed to MeHgCl the increased production of ROS. To our knowledge, this was the first time that cellular bioenergetics using the Seahorse XF analyzer was examined in MeHg exposed cardiomyocytes. Our results revealed that MeHg at low concentrations may lead to increased mitochondrial respiration to compensate for stress incurred by MeHg, but at higher concentrations compensation for the stress is no longer possible; thus causing exhaustion and lowering the maximal respiration and resting respiration of the cell. The reserve capacity of cells exposed to MeHg also decreased dose-dependently, indicating lower ATP production and failed respiration. Alternatively, the observed effects on respiration may be due to the decreased number of cells as demonstrated with the cell viability assays, therefore the alterations in respiration and bioenergetic parameters may be due to a reduction in respiration as a consequence of lower cell numbers following exposures. This is a limitation of this study and

as a future direction, quantifying the number of viable cells after exposures at 1 μM may be needed. Differences in the responses between the two cell lines were also shown indicating that H9C2 cell lines may be more resistant to MeHg exposure that AC16 as reflected in the increases in proton leak and the $State_{apparent}$ calculations which suggest that proteins (uncoupling proteins and ANT) acting to control ROS may be in much higher quantities in these cells than AC16 cells.

In light of these finding it can be concluded that higher concentrations can lead to cell death and changes in physiological parameters, however the effects of MeHg on the vascular system as outline in the Chapter 2 may be a more immediate effect on the vascular system through the progression of atherosclerosis than more direct effects on the heart.

In vivo quantification of mercury in heart rat tissues revealed a dose dependant increase in the accumulation of THg and MeHg and the % of MeHg in these tissues reflect what has been previously reported. The obese rats accumulated more Hg in the tissues than lean rats regardless of diet groups. The urinary isoprostane levels were significantly different between the two rat groups; obese rats seemed to produce higher levels of UI regardless of diet group and NCM dose groups. However, it is interesting to note that in lean rats, the HFSD in the vehicle controls caused an increase in the UI as compared to the controls fed the ND. Additionally, there was a significant difference between the two dose groups and the vehicle control only in the ND lean rats. This suggests that UI levels may increase with either a HFSD or exposures to NCM, and rats that treated with both conditions saw similar threshold levels of UI.

In 2010, the US EPA held a workshop to examine the current science and generate recommendations to address the association between MeHg exposures and cardiovascular endpoints. They recommended generating additional epidemiological studies, conducting

research examining biological mechanisms underlying the toxic effects seen in the epidemiological studies, dose-response assessments and examining other cardiovascular endpoints. Together, this project hopes to contribute to the knowledge base to aid risk assessments on MeHg intakes of at risk populations and to further characterize the underlying mechanisms of adverse effects on the heart.

5.2 Future Directions

Future studies may build on the experiments performed in this project; specifically further examining the energetic differences between AC16 and H9C2 cells by measuring protein expressions of UCP3 and ANT which may explain the energetic differences. We may also want to characterize the intracellular calcium flux of cardiomyocytes exposed to MeHg by using fluorescence microscopy to measure fluorescence instead of solely measuring the intracellular calcium. Additonally, we can test whether the L-type calcium channel is indeed affected by MeHg by adding an L-type calcium channel blocker to characterize the changes. This may allow us to obtain a better picture of the flux and homeostasis of calcium in cardiomyocytes.

There are still some limitations to using cell lines as opposed to primary cell cultures as cell lines are transformed or immortalized. Primary cells are undifferentiated and can be considered a better experimental model for *in vivo* conditions; therefore it may be prudent to examine these parameters with primary cardiomyocytes.

Additionally, to further determine the potential molecular mechanisms by which MeHg can affect the heart, we can utilize molecular biology tools to estimate the gene expression of cardiomyocytes using a PCR array and western blot analysis to determine the expression of various proteins associated with contractile function similar to those analyzed by Furieri *et al.,* (2011) who measured these proteins in rat hearts following $HgCl_2$ exposures. Genes that can be

analyzed using the PCR array can range from those involved in contraction, cell signalling, development, and metabolism.

Consuming marine foods is the primary method of MeHg exposure, it is known that the Inuit traditional diet of fish and marine mammals is rich in nutrients which are essential to Inuit health; however the presence of high levels of contaminants may compromise the benefits of these foods. Nutrient interaction may affect the metabolism, toxicodynamics, absorption and excretion of MeHg (Chapman & Chan, 2000), therefore the effect of various nutrients on MeHg toxicity should be further assessed. Nutrients which are important to examine include selenium, which has shown to have a protective effect against MeHg toxicity and dietary fats. Despite the reported CVD effects associated with MeHg exposure, it is still important to evaluate the risks and benefits of fish consumption. Fish are highly nutritious, containing a high source of proteins, polyunsaturated fatty acids (e.g. omega-3 fatty acids) and selenium which are known to reduce the risks of heart disease. Further studies have suggested that omega-3 fatty acids can modulate the effects of MeHg on cardiovascular health. Jin *et al.* (2008) conducted feeding studies and found a significant increase in MeHg-induced oxidative DNA damage in rats fed a lard diet as compared to rats fed diets containing omega-3 fatty acids (Jin *et al.*, 2008). This suggests that the toxicological effects of MeHg were dependant on the type of dietary fats that were administered; in particular omega-3 fatty acids diets were found to have a protective effect against MeHg. By examining these nutrients in either *in vitro* cardiomyocytes or *in vivo,* particularly in regards to the development of cardiovascular diseases, we can develop methods in order to mitigate the cardiovascular outcomes from MeHg exposures. In addition, the potential effect of nutritional factors in modifying the effect of contaminants may lead to additional considerations in health risk assessments and public health decisions.

References

Aboutabl, M. E., & El-Kadi, A. O. S. (2007). Constitutive expression and inducibility of CYP1A1 in the H9c2 rat cardiomyoblast cells. *Toxicology in Vitro : An International Journal Published in Association with BIBRA*, *21*, 1686–91.

Ahlqwist, M., Bengtsson, C., Lapidus, L., Gergdahl, I. A., & Schütz, A. (1999). Serum mercury concentration in relation to survival, symptoms, and diseases: results from the prospective population study of women in Gothenburg, Sweden. *Acta Odontologica Scandinavica*, *57*, 168–74.

Alissa, E. M., & Ferns, G. a. (2011). Heavy metal poisoning and cardiovascular disease. *Journal of Toxicology*, *2011*, 870125.

Allen, D. D., Caviedes, R., Cárdenas, A. M., Shimahara, T., Segura-Aguilar, J., & Caviedes, P. a. (2005). Cell lines as in vitro models for drug screening and toxicity studies. *Drug Development and Industrial Pharmacy*, *31*, 757–68.

Anner, B. M., Moosmayer, M., & Imesch, E. (1992). Mercury blocks Na-K-ATPase by a ligand-dependent and reversible mechanism. *The American Journal of Physiology*, *262*, F830–6.

Ayotte, P., Carrier, A., Ouellet, N., Boiteau, V., Abdous, B., Sidi, E. A. L., Château-Degat, M.-L., & Dewailly, É. (2011). Relation between methylmercury exposure and plasma paraoxonase activity in inuit adults from Nunavik. *Environmental Health Perspectives*, *119*, 1077–83.

Bakir, F., Damluji, S. F., Amin-Zaki, L., Murtadha, M., Khalidi, A., al-Rawi, N. Y., Tikriti, S., Dahahir, H. I., Clarkson, T. W., Smith, J. C., & Doherty, R. A. (1973). Methylmercury poisoning in Iraq. *Science (New York, N.Y.)*, *181*, 230–41.

Ballatori, N., & Clarkson, T. W. (1985). Biliary secretion of glutathione and of glutathione-metal complexes. *Fundamental and Applied Toxicology : Official Journal of the Society of Toxicology*, *5*, 816–31.

Berridge, M. V, Herst, P. M., & Tan, A. S. (2005). Tetrazolium dyes as tools in cell biology: new insights into their cellular reduction. *Biotechnology Annual Review*, *11*, 127–52.

Boening, D. W. (2000). Ecological effects , transport , and fate of mercury : a general review. *Chemosphere*, *40*, 1335-51.

Bourdineaud, J.-P., Rossignol, R., & Brèthes, D. (2013). Zebrafish: a model animal for analyzing the impact of environmental pollutants on muscle and brain mitochondrial bioenergetics. *The International Journal of Biochemistry & Cell Biology*, *45*, 16–22.

Bourgault, S., Choi, S., Buxbaum, J. N., Kelly, J. W., Price, J. L., & Reixach, N. (2011). Mechanisms of transthyretin cardiomyocyte toxicity inhibition by resveratrol analogs. *Biochemical and Biophysical Research Communications*, *410*, 707–13.

Bradford, M. M. (1976). A rapid and sensitive method for the quantitation of microgram quantities of protein utilizing the principle of protein-dye binding. *Analytical Biochemistry*, *72*, 248–54.

Brand, M. D., & Nicholls, D. G. (2011). Assessing mitochondrial dysfunction in cells. *The Biochemical Journal*, *435*, 297–312.

Brennan, J. P., Southworth, R., Medina, R. A., Davidson, S. M., Duchen, M. R., & Shattock, M. J. (2006). Mitochondrial uncoupling, with low concentration FCCP, induces ROS-dependent cardioprotection independent of KATP channel activation. *Cardiovascular Research*, *72*, 313–21.

Bridges, C. C., & Zalups, R. K. (2010). Transport of inorganic mercury and methylmercury in target tissues and organs. *Journal of Toxicology and Environmental Health. Part B, Critical Reviews*, *13*, 385–410.

Brookes, P. S., Yoon, Y., Robotham, J. L., Anders, M. W., & Sheu, S.-S. (2004). Calcium, ATP, and ROS: a mitochondrial love-hate triangle. *American Journal of Physiology. Cell Physiology*, *287*, C817–33.

Cambier, S., Bénard, G., Mesmer-Dudons, N., Gonzalez, P., Rossignol, R., Brèthes, D., & Bourdineaud, J.-P. (2009). At environmental doses, dietary methylmercury inhibits mitochondrial energy metabolism in skeletal muscles of the zebra fish (Danio rerio). *The International Journal of Biochemistry & Cell Biology*, *41*, 791–9.

Canuel, R., de Grosbois, S. B., Atikessé, L., Lucotte, M., Arp, P., Ritchie, C., Mergler, D., Chan, H. M., Amyot, M., & Anderson, R. (2006). New Evidence on Variations of Human Body Burden of Methylmercury from Fish Consumption. *Environmental Health Perspectives*, *114*, 302–306.

Cappon, C. J., & Smith, J. C. (1981). Mercury and selenium content and chemical form in human and animal tissue. *Journal of Analytical Toxicology*, *5*, 90–8.

Chan, H. M., Kim, C., Khoday, K., Receveur, O., & Kuhnlein, H. V. (1995). Assessment of dietary exposure to trace metals in Baffin Inuit food. *Environmental Health Perspectives*, *103*, 740–6.

Chapman, L., & Chan, H. M. (2000). The influence of nutrition on methyl mercury intoxication. *Environmental Health Perspectives*, *108 Suppl* , 29–56.

Clarkson, T. W. (1997). The toxicology of mercury. *Critical Reviews in Clinical Laboratory Sciences*, *34*, 369–403.

Clarkson, T. W. (2006). The Toxicology of Mercury and Its Chemical Compounds. *Critical Reviews in Toxicology.* 36, 609–662.

Clarkson, T. W., Magos, L., & Myers, G. J. (2003). The toxicology of mercury--current exposures and clinical manifestations. *The New England Journal of Medicine*, *349*, 1731–7.

Clarkson, T. W., Vyas, J. B., & Ballatori, N. (2007). Mechanisms of mercury disposition in the body. *American Journal of Industrial Medicine*, *50*, 757–64.

Dallaire, R., Dewailly, E., Pereg, D., Dery, S., & Ayotte, P. (2009). Thyroid function and plasma concentrations of polyhalogenated compounds in Inuit adults. *Environmental Health Perspectives*, *117*, 1380–6.

Davidson, M. M., Nesti, C., Palenzuela, L., Walker, W. F., Hernandez, E., Protas, L., Hirano, M., & Isaac, N. D. (2005). Novel cell lines derived from adult human ventricular cardiomyocytes. *Journal of Molecular and Cellular Cardiology*, *39*, 133–47.

Davies, S. S., & Roberts, L. J. (2011). F2-isoprostanes as an indicator and risk factor for coronary heart disease. *Free Radical Biology & Medicine*, *50*, 559–66.

Desler, C., Hansen, T. L., Frederiksen, J. B., Marcker, M. L., Singh, K. K., & Juel Rasmussen, L. (2012). Is There a Link between Mitochondrial Reserve Respiratory Capacity and Aging? *Journal of Aging Research*, *2012*, 192503.

Díez, S. (2008). Human Health Effects of Methylmercury. *Reviews of environmental contamination and toxicology*, *198*, 18–26.

Do Nascimento, J. L. M., Oliveira, K. R. M., Crespo-Lopez, M. E., Macchi, B. M., Maués, L. A. L., Pinheiro, M. D. C. N., Silveira, L. C. L., & Herculano, A. M. (2008). Methylmercury neurotoxicity & antioxidant defenses. *The Indian Journal of Medical Research*, *128*, 373–82.

Donaldson, S. G., Van Oostdam, J., Tikhonov, C., Feeley, M., Armstrong, B., Ayotte, P., Boucher, O., Bowers, W., Chan, L., Dallaire, F., Dallaire, R., Dewailly, E., Edwards, J., Egeland, G. M., Fontaine, J., Furgal, C., Leech, T., Loring, E., Muckle, G., Nancarrow, T., Pereg, D., Plusquellec, P., Potyrala, M., Receveur, O. Shearer, R. G. (2010). Environmental contaminants and human health in the Canadian Arctic. *The Science of the Total Environment*, *408*, 5165–234.

Dreiem, A., Gertz, C. C., & Seegal, R. F. (2005). The effects of methylmercury on mitochondrial function and reactive oxygen species formation in rat striatal synaptosomes are age-dependent. *Toxicological Sciences : An Official Journal of the Society of Toxicology*, *87*, 156–62.

Egeland, G. M., & Nutrition, H. (2004). Fish Consumption , Mercury Exposure , and Heart Diseases. *Nutrition review. 62*, 68-72.

Eruslanov, E., & Kusmartsev, S. (2010). Identification of ROS using oxidized DCFDA and flow-cytometry. *Methods in Molecular Biology (Clifton, N.J.)*, *594*, 57–72.

Farina, M., Rocha, J. B. T., & Aschner, M. (2011). Mechanisms of methylmercury-induced neurotoxicity: evidence from experimental studies. *Life Sciences*, *89*, 555–63.

Ferrick, D. A., Neilson, A., & Beeson, C. (2008). Advances in measuring cellular bioenergetics using extracellular flux. *Drug Discovery Today*, *13*, 268–74.

Fillion, M., Mergler, D., José, C., Passos, S., Larribe, F., Lemire, M., Rémy, J., & Guimarães, D. (2006). Environmental Health : A Global A preliminary study of mercury exposure and blood pressure in the Brazilian Amazon. *Blood Pressure*, *9*, 1–9.

Florian, M., Yan, J., Ulhaq, S., Coughlan, M., Laziyan, M., Willmore, W., & Jin, X. (2013). Northern contaminant mixtures induced morphological and functional changes in human coronary artery endothelial cells under culture conditions typifying high fat/sugar diet and ethanol exposure. *Toxicology*, *313*, 103–12.

Freeman, L. R., Zhang, L., Nair, A., Dasuri, K., Francis, J., Fernandez-Kim, S.-O., Bruce-Keller, A. J., & Keller, J. N. (2013). Obesity increases cerebrocortical reactive oxygen species and impairs brain function. *Free Radical Biology & Medicine*, *56*, 226–33.

Furieri, L. B., Fioresi, M., Junior, R. F. R., Bartolomé, M. V., Fernandes, A. A., Cachofeiro, V., Lahera, V., Salaices, M., Stefanon, I., & Vassallo, D. V. (2011). Exposure to low mercury concentration in vivo impairs myocardial contractile function. *Toxicology and Applied Pharmacology*, *255*, 193–9.

Goncharov, A., Pavuk, M., Foushee, H. R., & Carpenter, D. O. (2011). Blood pressure in relation to concentrations of PCB congeners and chlorinated pesticides. *Environmental Health Perspectives*, *119*, 319–25.

Grandjean, P., Budtz-Jørgensen, E., White, R. F., Jørgensen, P. J., Weihe, P., Debes, F., & Keiding, N. (1999). Methylmercury exposure biomarkers as indicators of neurotoxicity in children aged 7 years. *American Journal of Epidemiology*, *150*, 301–5.

Grandjean, P., Satoh, H., Murata, K., & Eto, K. (2010). Adverse effects of methylmercury: environmental health research implications. *Environmental Health Perspectives*, *118*, 1137–45.

Grotto, D., de Castro, M. M., Barcelos, G. R. M., Garcia, S. C., & Barbosa, F. (2009). Low level and sub-chronic exposure to methylmercury induces hypertension in rats: nitric oxide depletion and oxidative damage as possible mechanisms. *Archives of Toxicology*, *83*, 653–62.

Guallar, E., Sanz-Gallardo, M. I., van't Veer, P., Bode, P., Aro, A., Gómez-Aracena, J., Kark, J. D., Riemersma, R. a, Martín-Moreno, J. M., & Kok, F. J. (2002). Mercury, fish oils, and the risk of myocardial infarction. *The New England Journal of Medicine*, *347*, 1747–54.

Hagele, T. J., Mazerik, J. N., Gregory, A., Kaufman, B., Magalang, U., Kuppusamy, M. L., Marsh, C. B., Kuppusamy, P., & Parinandi, N. L. (2007). Mercury activates vascular endothelial cell phospholipase D through thiols and oxidative stress. *International Journal of Toxicology*, *26*, 57–69.

Halbach, S., Schönsteiner, G., & Vierling, W. (1989). The action of organic mercury compounds on the function of isolated mammalian heart muscle. *European Journal of Pharmacology*, *167*, 255–64.

Hallgren, C. G., Hallmans, G., Jansson, J. H., Marklund, S. L., Huhtasaari, F., Schütz, A., Strömberg, U., Vessby, B., & Skerfving, S. (2001). Markers of high fish intake are associated with decreased risk of a first myocardial infarction. *The British Journal of Nutrition*, *86*, 397–404.

Heath, J. C., Banna, K. M., Reed, M. N., Pesek, E. F., Cole, N., Li, J., & Newland, M. C. (2010). Dietary selenium protects against selected signs of aging and methylmercury exposure. *Neurotoxicology*, *31*, 169–79.

Hennig, B., Reiterer, G., Toborek, M., Matveev, S. V., Daugherty, A., Smart, E., & Robertson, L. W. (2004). Dietary Fat Interacts with PCBs to Induce Changes in Lipid Metabolism in Mice Deficient in Low-Density Lipoprotein Receptor. *Environmental Health Perspectives*, *113*, 83–87.

Hennig, B., Toborek, M., & McClain, C. J. (2001). High-energy diets, fatty acids and endothelial cell function: implications for atherosclerosis. *Journal of the American College of Nutrition*, *20*, 97–105.

Hill, B. G., Dranka, B. P., Zou, L., Chatham, J. C., & Darley-Usmar, V. M. (2009). Importance of the bioenergetic reserve capacity in response to cardiomyocyte stress induced by 4-hydroxynonenal. *The Biochemical Journal*, *424*, 99–107.

Hill, B. G., Higdon, A. N., Dranka, B. P., & Darley-Usmar, V. M. (2010). Regulation of vascular smooth muscle cell bioenergetic function by protein glutathiolation. *Biochimica et Biophysica Acta*, *1797*, 285–95.

Hisatome, I., Kurata, Y., Sasaki, N., Morisaki, T., Morisaki, H., Tanaka, Y., Urashima, T., Yatsuhashi, T., Tsuboi, M., Kitamura, F., Miake, J., Takeda, S. i, Taniguchi, S. i, Ogino, K., Igawa, O., Yoshida, A., Sato, R., Maikta, N., Shigemasa, C. (2000). Block of sodium channels by divalent mercury: role of specific cysteinyl residues in the P-loop region. *Biophysical Journal*, *79*, 1336–45.

Houston, M. C. (2011). Role of mercury toxicity in hypertension, cardiovascular disease, and stroke. *Journal of Clinical Hypertension (Greenwich, Conn.)*, *13*, 621–7.

Igata, A. (1993). Epidemiological and clinical features of Minamata disease. *Environmental Research*, *63*, 157–69.

Jin, X., Chan, H. M., Lok, E., Kapal, K., Taylor, M., Kubow, S., & Mehta, R. (2008). Dietary fats modulate methylmercury-mediated systemic oxidative stress and oxidative DNA damage in rats. *Food and Chemical Toxicology : An International Journal Published for the British Industrial Biological Research Association*, *46*, 1706–20.

Jin, X., Hidiroglou, N., Lok, E., Taylor, M., Kapal, K., Ross, N., Sarafin, K., Lau, A., De Souza, A., Chan, H. M., & Mehta, R. (2011). Dietary Selenium (Se) and Vitamin E (V(E)) Supplementation Modulated Methylmercury-Mediated Changes in Markers of Cardiovascular Diseases in Rats. *Cardiovascular Toxicology*, *12*, 10–24.

June, C. H., Abe, R., & Rabinovitch, P. S. (2001). Measurement of intracellular calcium ions by flow cytometry. *Current Protocols in Cytometry / Editorial Board, J. Paul Robinson, Managing Editor ... [et Al.]*, *Chapter 9*, Unit 9.8.

Kang, Y. J. (2001). Molecular and Cellular Mechanisms of Cardiotoxicity to Environmental Toxicants. *Environmental Health*, *109*, 27–34.

Karagas, M. R., Choi, A. L., Oken, E., Horvat, M., Schoeny, R., Kamai, E., Cowell, W., Grandjean, P., & Korrick, S. (2012). Evidence on the human health effects of low-level methylmercury exposure. *Environmental health perspectives*. 120:799-806.

Kaur, P., Aschner, M., & Syversen, T. (2011). Biochemical factors modulating cellular neurotoxicity of methylmercury. *Journal of Toxicology*, *2011*, 721987.

Kaur, P., Schulz, K., Heggland, I., Aschner, M., & Syversen, T. (2008). The use of fluorescence for detecting MeHg-induced ROS in cell cultures. *Toxicology in Vitro : An International Journal Published in Association with BIBRA*, *22*, 1392–8.

Kaviarasan, S., Muniandy, S., Qvist, R., & Ismail, I. S. (2009). F(2)-isoprostanes as novel biomarkers for type 2 diabetes: a review. *Journal of Clinical Biochemistry and Nutrition*, *45*, 1–8.

Kishimoto, T., Oguri, T., & Tada, M. (1995). Effect of methylmercury (CH3HgCl) injury on nitric oxide synthase (NOS) activity in cultured human umbilical vascular endothelial cells. *Toxicology*, *103*, 1–7.

Koletsky, S. (1975). Pathologic findings and laboratory data in a new strain of obese hypertensive rats. *The American Journal of Pathology*, *80*, 129–42.

Kurata, Y., Hisatome, I., Tsuboi, M., Uenishi, H., Zhang, G., Oyaizu, M., Sato, R., & Imanishi, S. (1998). Effect of sulfhydryl oxidoreduction on permeability of cardiac tetrodotoxin-insensitive sodium channel. *Life Sciences*, *63*, 1023–1035.

Laight, D. W., Desai, K. M., Gopaul, N. K., Änggård, E. E., & Carrier, M. J. (1999). F2-isoprostane evidence of oxidant stress in the insulin resistant, obese Zucker rat: effects of vitamin E. *European Journal of Pharmacology*, *377*, 89–92.

Lawes, C. M. M., Vander Hoorn, S., & Rodgers, A. (2008). Global burden of blood-pressure-related disease, 2001. *Lancet*, *371*, 1513–8.

Legrand, M., Feeley, M., Tikhonov, C., Schoen, D., & Li-Muller, A. (2010). Methylmercury blood guidance values for Canada. *Canadian Journal of Public Health. 101*, 28–31.

Liang, J.-L., Xiao, D.-Z., Liu, X.-Y., Lin, Q.-X., Shan, Z.-X., Zhu, J.-N., Lin, S.-G., & Yu, X.-Y. (2010). High glucose induces apoptosis in AC16 human cardiomyocytes via macrophage migration inhibitory factor and c-Jun N-terminal kinase. *Clinical and Experimental Pharmacology & Physiology*, *37*, 969–73.

Limaye, D. A., Shaikh, Z. A., Limaye, C., & Pharmacol, T. A. (1999). Cytotoxicity of Cadmium and Characteristics of Its Transport in Cardiomyocytes 1 , 2 Cytotoxicity of Cadmium and Characteristics of Its Transport. *Toxicology and Applied Pharmacology*, *66*, 59–66.

Loor, G., Kondapalli, J., Schriewer, J. M., Chandel, N. S., Vanden Hoek, T. L., & Schumacker, P. T. (2010). Menadione triggers cell death through ROS-dependent mechanisms involving PARP activation without requiring apoptosis. *Free Radical Biology & Medicine*, *49*, 1925–36.

Lund, B. O., Miller, D. M., & Woods, J. S. (1993). Studies on Hg(II)-induced H2O2 formation and oxidative stress in vivo and in vitro in rat kidney mitochondria. *Biochemical Pharmacology*, *45*, 2017–24.

Mahaffey, K. R. (2000). Recent advances in recognition of low-level methylmercury poisoning. *Current Opinion in Neurology*, *13*, 699–707.

Mailloux, R. J., McBride, S. L., & Harper, M.-E. (2013). Unearthing the secrets of mitochondrial ROS and glutathione in bioenergetics. *Trends in Biochemical Sciences*, *38*, 592–602.

Mailloux, R. J., Seifert, E. L., Bouillaud, F., Aguer, C., Collins, S., & Harper, M.-E. (2011). Glutathionylation acts as a control switch for uncoupling proteins UCP2 and UCP3. *The Journal of Biological Chemistry*, *286*, 21865–75.

Massaroni, L., Rossoni, L. V, Amaral, S. M., Stefanon, I., Oliveira, E. M., & Vassallo, D. V. (1995). Haemodynamic and electrophysiological acute toxic effects of mercury in anaesthetized rats and in langendorff perfused rat hearts. *Pharmacological Research : The Official Journal of the Italian Pharmacological Society*, *32*, 27–36.

Matsuo, N., Suzuki, T., & Akagi, H. (n.d.). Mercury concentration in organs of contemporary Japanese. *Archives of Environmental Health*, *44*, 298–303.

Mazerik, J. N., Hagele, T., Sherwani, S., Ciapala, V., Butler, S., Kuppusamy, M. L., Hunter, M., Kuppusamy, P., Marsh, C. B., & Parinandi, N. L. (2007). Phospholipase A2 activation regulates cytotoxicity of methylmercury in vascular endothelial cells. *International Journal of Toxicology*, *26*, 553–69.

Mergler, D., Anderson, H. A., Chan, L. H. M., Mahaffey, K. R., Murray, M., Sakamoto, M., Stern, A. H., Hing, L., & Chan, M. (2007). Methylmercury exposure and health effects in humans: a worldwide concern. *Ambio*, *36*, 3–11.

Minuz, P., Andrioli, G., Degan, M., Gaino, S., Ortolani, R., Tommasoli, R., Zuliani, V., Lechi, A., & Lechi, C. (1998). The F2-Isoprostane 8-Epiprostaglandin F2 Increases Platelet Adhesion and Reduces the Antiadhesive and Antiaggregatory Effects of NO. *Arteriosclerosis, Thrombosis, and Vascular Biology*, *18*, 1248–1256.

Mori, N., Yasutake, a, & Hirayama, K. (2007). Comparative study of activities in reactive oxygen species production/defense system in mitochondria of rat brain and liver, and their susceptibility to methylmercury toxicity. *Archives of Toxicology*, *81*, 769–76.

Mori, N., Yasutake, A., Marumoto, M., & Hirayama, K. (2011). Methylmercury inhibits electron transport chain activity and induces cytochrome c release in cerebellum mitochondria. *The Journal of Toxicological Sciences*, *36*, 253–9.

Morrow, J. D., Harris, T. M., & Roberts, L. J. (1990). Noncyclooxygenase oxidative formation of a series of novel prostaglandins: analytical ramifications for measurement of eicosanoids. *Analytical Biochemistry*, *184*, 1–10.

Mosmann, T. (1983). Rapid colorimetric assay for cellular growth and survival: application to proliferation and cytotoxicity assays. *Journal of Immunological Methods*, *65*, 55–63.

Myers, G. J., & Davidson, P. W. (1998). Prenatal methylmercury exposure and children: neurologic, developmental, and behavioral research. *Environmental Health Perspectives*, *106 Suppl* , 841–7.

Ni, M., Li, X., Yin, Z., Jiang, H., Sidoryk-Wegrzynowicz, M., Milatovic, D., Cai, J., & Aschner, M. (2010). Methylmercury induces acute oxidative stress, altering Nrf2 protein level in primary microglial cells. *Toxicological Sciences : An Official Journal of the Society of Toxicology*, *116*, 590–603.

Nobuhito, S., Larsstuvold, M., & Kagawa, Y. (1977). Effect of Methyl Mercury on Phosphorylation, Transport, and Oxidation in Mammalian Mitochondria. *Journal of Biochemistry*, *82*, 859–868.

Okazaki, E., Oyama, Y., Chikahisa, L., Nagano, T., Katayama, N., & Sakamoto, M. (1997). Fluorescent estimation on cytotoxicity of methylmercury in dissociated rat cerebellar neurons: its comparison with ionomycin. *Environmental Toxicology and Pharmacology*, *3*, 237–44.

Oliveira, E. M., Vassallo, D. V, Sarkis, J. J., & Mill, J. G. (1994). Mercury effects on the contractile activity of isolated heart muscle. *Toxicology and Applied Pharmacology*, *128*, 86–91.

Ostertag, S. K., Chan, H. M., Moisey, J., Dabeka, R., & Tittlemier, S. a. (2009). Historic dietary exposure to perfluorooctane sulfonate, perfluorinated carboxylates, and fluorotelomer unsaturated carboxylates from the consumption of store-bought and restaurant foods for the Canadian population. *Journal of Agricultural and Food Chemistry*, *57*, 8534–44.

Oyama, Y., Nakata, M., Sakamoto, M., Chikahisa, L., Miyoshi, N., & Satoh, M. (1998). Methylmercury toxicity in dissociated rat brain neurons: modification by l-cysteine and trimethylbenzylmercaptan and comparison with dimethylmercury and N-ethylmaleimide. *Environmental Toxicology and Pharmacology*, *6*, 221–7.

Pfefferle, A., Mailloux, R. J., Adjeitey, C. N.-K., & Harper, M.-E. (2013). Glutathionylation of UCP2 sensitizes drug resistant leukemia cells to chemotherapeutics. *Biochimica et Biophysica Acta*, *1833*, 80–9.

Piłacik, B., Nofer, T. W., & Wasowicz, W. (2002). F2-isoprostanes biomarkers of lipid peroxidation: their utility in evaluation of oxidative stress induced by toxic agents. *International Journal of Occupational Medicine and Environmental Health*, *15*, 19–27.

Pointon, A. V., Dawson, S., Gerges, N. A., Pollard, C. E., & Sidaway, J. E. (2011). In vitro detection of cardiotoxicity using the rat-derived H9c2 cardiomyocyte cell line. *Journal of Pharmacological and Toxicological Methods*, *64*, e13–e14.

Polunas, M., Halladay, A., Tjalkens, R. B., Philbert, M. A., Lowndes, H., & Reuhl, K. (2011). Role of oxidative stress and the mitochondrial permeability transition in methylmercury cytotoxicity. *Neurotoxicology*, *32*, 526–34.

Ralston, N. V. C., Ralston, C. R., Blackwell, J. L., & Raymond, L. J. (2008). Dietary and tissue selenium in relation to methylmercury toxicity. *Neurotoxicology*, *29*, 802–11.

Readnower, R. D., Brainard, R. E., Hill, B. G., & Jones, S. P. (2012). Standardized bioenergetic profiling of adult mouse cardiomyocytes. *Physiological Genomics*, *44*, 1208–13.

Rice, G. E., Hammitt, J. K., & Evans, J. S. (2010). A probabilistic characterization of the health benefits of reducing methyl mercury intake in the United States. *Environmental Science & Technology*, *44*, 5216–24.

Ringseis, R., & Eder, K. (2010). Fatty acids and signalling in endothelial cells. *Prostaglandins, Leukotrienes, and Essential Fatty Acids*, *82*, 189–98.

Rissanen, T., Voutilainen, S., Nyyssönen, K., Lakka, T. A., & Salonen, J. T. (2000). Fish oil-derived fatty acids, docosahexaenoic acid and docosapentaenoic acid, and the risk of acute coronary events: the Kuopio ischaemic heart disease risk factor study. *Circulation*, *102*, 2677–9.

Roberts, L. J., & Morrow, J. D. (2000). Measurement of F(2)-isoprostanes as an index of oxidative stress in vivo. *Free Radical Biology & Medicine*, *28*, 505–13.

Roman, H. a, Walsh, T. L., Coull, B. a, Dewailly, É., Guallar, E., Hattis, D., Mariën, K., Schwartz, J., Stern, A. H., Virtanen, J. K., & Rice, G. (2011). Evaluation of the cardiovascular effects of methylmercury exposures: current evidence supports development of a dose-response function for regulatory benefits analysis. *Environmental Health Perspectives*, *119*, 607–14.

Rooney, J. P. K. (2007). The role of thiols, dithiols, nutritional factors and interacting ligands in the toxicology of mercury. *Toxicology*, *234*, 145–56.

Roos, D. H., Puntel, R. L., Farina, M., Aschner, M., Bohrer, D., Rocha, J. B. T., & de Vargas Barbosa, N. B. (2011). Modulation of methylmercury uptake by methionine: prevention of mitochondrial dysfunction in rat liver slices by a mimicry mechanism. *Toxicology and Applied Pharmacology*, *252*, 28–35.

Roos, D., Seeger, R., Puntel, R., & Vargas Barbosa, N. (2012). Role of calcium and mitochondria in MeHg-mediated cytotoxicity. *Journal of Biomedicine & Biotechnology*, *2012*, 248764.

Rowland, I. R. (1988). Interactions of the gut microflora and the host in toxicology. *Toxicologic Pathology*, *16*, 147–53.

Salonen, J. T., Seppänen, K., Nyyssönen, K., Korpela, H., Kauhanen, J., Kantola, M., Tuomilehto, J., Esterbauer, H., Tatzber, F., & Salonen, R. (1995). Intake of mercury from fish, lipid peroxidation, and the risk of myocardial infarction and coronary, cardiovascular, and any death in eastern Finnish men. *Circulation*, *91*, 645–55.

Savini, I., Catani, M. V., Evangelista, D., Gasperi, V., & Avigliano, L. (2013). Obesity-associated oxidative stress: strategies finalized to improve redox state. *International Journal of Molecular Sciences*, *14*, 10497–538.

Schnabel, R., & Blankenberg, S. (2007). Oxidative stress in cardiovascular disease: successful translation from bench to bedside? *Circulation*, *116*, 1338–40.

Schwedhelm, E., Bartling, A., Lenzen, H., Tsikas, D., Maas, R., Brümmer, J., Gutzki, F.-M., Berger, J., Frölich, J. C., & Böger, R. H. (2004). Urinary 8-iso-prostaglandin F2alpha as a

risk marker in patients with coronary heart disease: a matched case-control study. *Circulation*, *109*, 843–8.

Shaheen, M., Cheema, Y., Shahbaz, A. U., Bhattacharya, S. K., & Weber, K. T. (2011). Intracellular calcium overloading and oxidative stress in cardiomyocyte necrosis via a mitochondriocentric. *Clinical Cardiology*, *16*, 109–115.

Shanker, G., Aschner, J. L., Syversen, T., & Aschner, M. (2004). Free radical formation in cerebral cortical astrocytes in culture induced by methylmercury. *Brain Research. Molecular Brain Research*, *128*, 48–57.

Shchepina, L. A., Pletjushkina, O. Y., Avetisyan, A. V, Bakeeva, L. E., Fetisova, E. K., Izyumov, D. S., Saprunova, V. B., Vyssokikh, M. Y., Chernyak, B. V, & Skulachev, V. P. (2002). Oligomycin, inhibitor of the F0 part of H+-ATP-synthase, suppresses the TNF-induced apoptosis. *Oncogene*, *21*, 8149–57.

Simmons-willis, T. A., Koh, A. S., Clarkson, T. W., & Ballatori, N. (2002). large neutral amino acid transporter (LAT) 1 and LAT2, *246*, 239–246.

Souza de Assis, G. P., Cunha Silva, C. E., Stefanon, I., & Vassallo, D. V. (2003). Effects of small concentrations of mercury on the contractile activity of the rat ventricular myocardium. *Comparative Biochemistry and Physiology Part C: Toxicology & Pharmacology*, *134*, 375–383.

Stern, A. H. (2005). A review of the studies of the cardiovascular health effects of methylmercury with consideration of their suitability for risk assessment. *Environmental Research*, *98*, 133–42.

Stuart, J. A., Brindle, K. M., Harper, J. A., & Brand, M. D. (1999). Mitochondrial proton leak and the uncoupling proteins. *Journal of Bioenergetics and Biomembranes*, *31*, 517–25.

Su, J. Y., & Chen, W. (1979). The Effects of Methylmercury on Isolated Cardiac Tissues. *The American Journal of Pathology.* 95,753-64.

Sumi, D., Sasaki, T., Miyataka, H., & Himeno, S. (2011). Rat H9c2 cardiac myocytes are sensitive to arsenite due to a modest activation of transcription factor Nrf2. *Archives of Toxicology*, *85*, 1509–16.

Valera, B., Dewailly, E., & Poirier, P. (2008). Cardiac autonomic activity and blood pressure among Nunavik Inuit adults exposed to environmental mercury : a cross-sectional study. *Environmental Health*, *11*, 1–11.

Van Oostdam, J., Donaldson, S. G., Feeley, M., Arnold, D., Ayotte, P., Bondy, G., Chan, L., Dewaily, E., Furgal, C. M., Kuhnlein, H., Loring, E., Muckle, G., Myles, E., Receveur, O., Tracy, B., Gill, U., & Kalhok, S. (2005). Human health implications of environmental

contaminants in Arctic Canada: A review. *The Science of the Total Environment*, *351-352*, 165–246.

Vassallo, D. V, Moreira, C. M., Oliveira, E. M., Bertollo, D. M., & Veloso, T. C. (1999). Effects of mercury on the isolated heart muscle are prevented by DTT and cysteine. *Toxicology and Applied Pharmacology*, *156*, 113–8.

Virtanen, J. K., Rissanen, T. H., Voutilainen, S., & Tuomainen, T.-P. (2007). Mercury as a risk factor for cardiovascular diseases. *The Journal of Nutritional Biochemistry*, *18*, 75–85.

Walker, C. A., & Spinale, F. G. (1999). The structure and function of the cardiac myocyte: a review of fundamental concepts. *The Journal of Thoracic and Cardiovascular Surgery*, *118*, 375–82.

Woodcock, E. a, & Matkovich, S. J. (2005). Cardiomyocytes structure, function and associated pathologies. *The International Journal of Biochemistry & Cell Biology*, *37*, 1746–51.

Wyss, M., & Kaddurah-Daouk, R. (2000). Creatine and creatinine metabolism. *Physiological Reviews*, *80*, 1107–213.

Yamaguchi, S., Matsumoto, H., Kaku, S., Tateishi, M., & Shiramizu, M. (1975). Factors affecting the amount of mercury in human scalp hair. *American Journal of Public Health*, *65*, 484–8.

Yamamoto, M., Yanagisawa, R., Motomura, E., Nakamura, M., Sakamoto, M., Takeya, M., & Eto, K. (2013). Increased methylmercury toxicity related to obesity in diabetic KK-Ay mice. *Journal of Applied Toxicology :JAT*. 34, 914-23.

Yan, Y., Wei, C., Zhang, W., Cheng, H., & Liu, J. (2006). Cross-talk between calcium and reactive oxygen species signaling. *Acta Pharmacologica Sinica*, *27*, 821–6.

Yoshizawa, K., Rimm, E. B., Morris, J. S., Spate, V. L., Hsieh, C., Spiegelman, D., Stampfer, M. J., & Willett, W. C. (2002). Mercury and the risk of coronary heart disease in men. *The New England Journal of Medicine*, *347*, 1755–60.

Yuzefovych, L. V., Musiyenko, S. I., Wilson, G. L., & Rachek, L. I. (2013). Mitochondrial DNA Damage and Dysfunction, and Oxidative Stress Are Associated with Endoplasmic Reticulum Stress, Protein Degradation and Apoptosis in High Fat Diet-Induced Insulin Resistance Mice. *PLoS ONE*, *8*, e54059.

Zahir, F., Rizwi, S. J., Haq, S. K., & Khan, R. H. (2005). Low dose mercury toxicity and human health. *Environmental Toxicology and Pharmacology*. 20, 351-60.

Zordoky, B. N. M., & El-Kadi, A. O. S. (2007). H9c2 cell line is a valuable in vitro model to study the drug metabolizing enzymes in the heart. *Journal of Pharmacological and Toxicological Methods*, *56*, 317–22.

Appendix I
Background and protocol rationale for Seahorse XF-24 Analyzer

Mitochondrial Function Analysis

Mitochondrial bioenergetic parameters were ascertained by measuring resting respiration, a proxy measure for the amount of O_2 consumed to produce ATP for the maintenance of basic cellular functions (ion transport, gene expression etc.), followed by injection of oligomycin, FCCP, and antimycin A, respectively. Resting OCR was read over the course of 3 measurement cycles. Each measurement cycle consists of 2 minutes of mixing, 2 minutes of incubation and 2 minutes of measurements. To measure proton leak dependant OCR (state 4) respiration, 1 µg/ml oligomycin is injected to the wells and 3 measurements are again made. Oligomycin, inhibits the ATP synthase of the electron transport chain and blocks ATP synthesis allowing the measurement of the contribution of proton leaks to cellular oxygen consumption (Shchepina et al., 2002). Maximal mitochondrial phosphorylation capacity was measured by injections of 1uM carbonyl cyanide p-trifluoro methoxyphenylhydrazone (FCCP) and 3 measurements are made. FCCP is a proton ionophore which uncouples the electron transport chain from phosphorylation by dissolving phospholipid bilayers and enormously increases their ionic permeability and the proton permeability to disconnect the electron transport chain from the formation of ATP (Brennan *et al*., 2006). Lastly, 1 µM Antimycin A, an inhibitor of complex III in the ETC, was injected into the wells to inhibit electron transport to O_2. This allows us to measure non-mitochondrial oxygen consumption, the remaining oxygen consumption that is extra-

mitochondrial. OCR was normalized to cellular protein/well and corrected for extramitochondrial O_2 consumption.

Mitochondrial analysis calculations

Spare respiratory capacity or reserve capacity (Figure 2.1) is the amount of extra ATP produced by oxidative phosphorylation in case of sudden increase in energy demand, if the reserve capacity is not sufficient to provide the required ATP or if it is depleted then the cells risk cell death. This depletion is associated with numerous pathologies including heart diseases (Desler *et al*., 2012).

Lastly, bioenergetics and cell biology research have described various metabolic respiratory states of isolated mitochondria which was first described by Chance and Williams (1955). State 3 respiration is described as the state at which the cells have a high levels of ADP and substrate (electron donors such as NADH and $FADH_2$ for the electron transport chain) allowing for rapid and maximal respiration and more ATP is produced. State 4 respiration occurs when all ADP is gradually depleted because it is converted to ATP and the respiration slows, at this point, consumption of oxygen is due primarily to proton leak. It is known that ATP synthase is not the only route where the proton gradient (formed by the ETC) is dissipated, when the ATP synthase is not working either in the absence of ADP or in the presence of an inhibitor such as oligomycin, protons can be pumped back into the mitochondria through other channels such as mitochondrial uncoupling proteins, this process is called “proton leak”. The respiration required to maintain the proton gradient against this proton leak is represented by state 4 respiration (Stuart *et al.* 1999).

These respiration states are mainly used to describe isolated mitochondria as it is unlikely

that either extremes exist for mitochondria for intact cells. Dranka *et al.* (2010) suggests that it is more likely that cells exist in an intermediate state, assigned as State 3.5 (the $State_{apparamt}$).

To determine the state at which the cells are operating (the range between State 3 and State 4 respiration) we will be calculating the $State_{apparamt}$ using the following equation: $State_{app}$ = 4 – (Basal-Oligo)/(FCCP-Oligo)

The assumption based on this equation is that State 3 respiration is equivalent to the OCR after the addition of FCCP (the maximal respiration) and State 4 is assumed to be the rate measured after addition of oligomycin (proton leak). When demand for ATP is high, the cells approach state 3 but when ATP/ADP ratios are high and little respiration is needed, cells approach state 4. The $State_{apparamt}$ value allows us to determine where the cells fall on the scale between state 3 and 4 respiration (Hill *et al*., 2010).

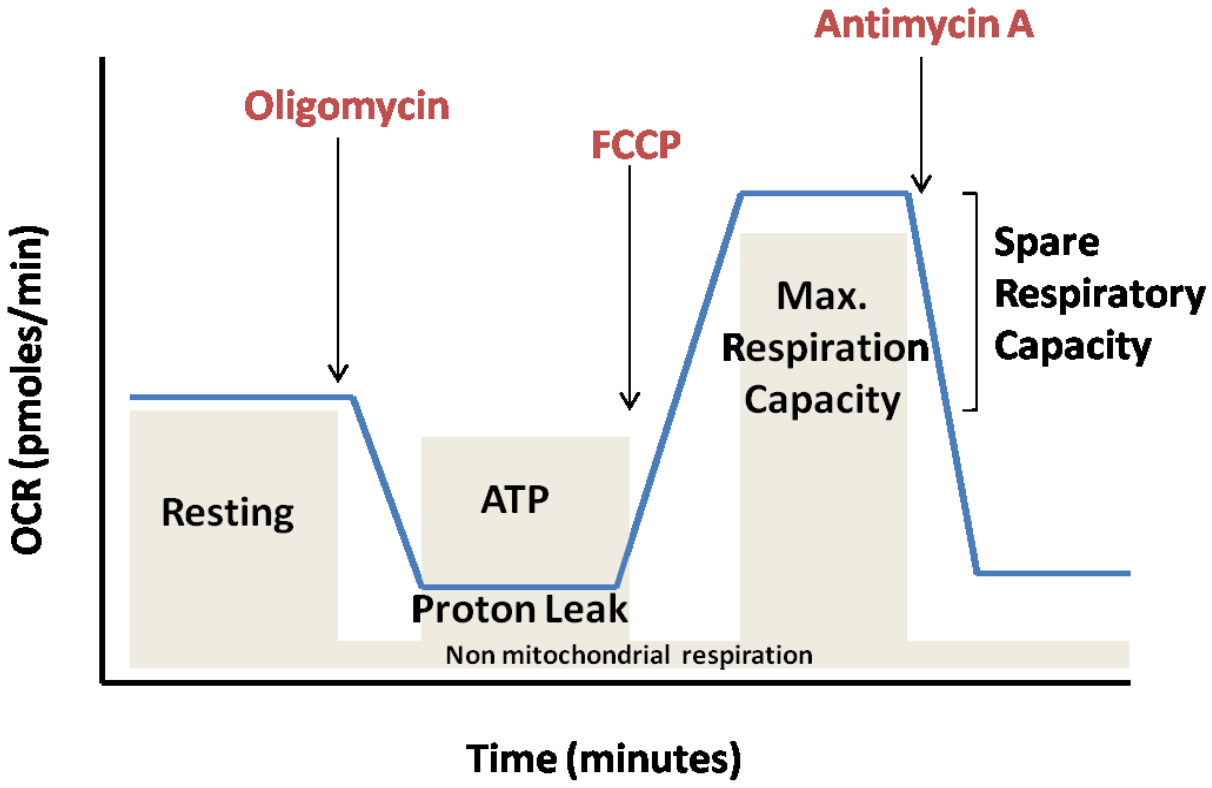

Figure I-1. Typical Seahorse oxygen consumption schematic with corresponding respiratory states that can be analyzed. Image re-adaped from Seahorse Bioscience, 2013. Real-time oxygen consumption rate (OCR) measurements were made in the analyzer by a sensor probe placed 200 microns above the cell monolayer measuring concentrations of dissolved oxygen every few seconds. Three baseline (Resting) measurements are made. Oligomycin is injected into the wells to measure proton leak dependant OCR (state 4 respiration) for another three measurements. Afterwards, FCCP is injected to the wells and three OCR measurements representing the maximal respiration of the cells is recorded. Finally, Antimycin A is injected and OCR measurements which represent oxygen consumption not associated with the mitochondria (non-mitochondrial respiration) are recorded

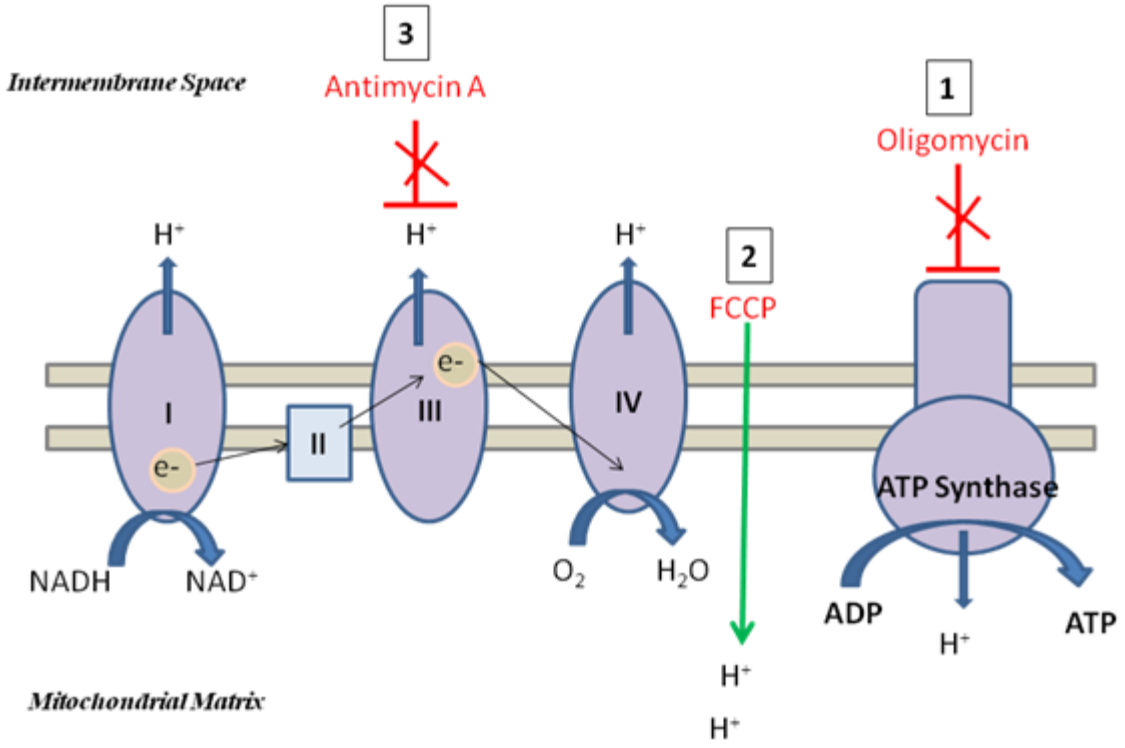

Figure I-2 Simple schematic of the electron transport chain (ETC) in mitochondria and the effects of various inhibitors. The ETC of the mitochondria is fueled by electrons from the Krebs cycle crossing the electron transport chain creating a proton (H^+) gradient which allows the phosphorylation of ADP to ATP by the ATP synthase. Oxidative phosphorylation is the combination of oxidation of ETC and the phosphorylation of the ATP-ase, both of which are reliant on the proton gradient formed. Mitochondria that show high rates of respiration with no ATP production are considered uncoupled respiration. Inhibitors produce this uncoupled effect. Oligomycin inhibits the ATP synthase complex preventing ATP formation, FCCP is a proton ionophore shuttling more protons into the mitochondrial matrix which effectively disconnects the ETC from the formation of ATP and the mitochondria are consuming oxygen at its maximal rate. Lastly, Antimycin A inhibits Complex III stopping the ETC and allows for measurement of non-mitochondrial respiration. Numbers coincide with the order of injection in the wells of each inhibitor.